THESIS FOR THE DEGREE OF LICENTIATE OF ENGINEERING

Thermokinetic Uncertainty Relations and Dynamical Activities in Quantum Systems

Didrik Palmqvist

Department of Microtechnology and Nanoscience (MC2)
Applied Quantum Physics Laboratory
Chalmers University of Technology
Gothenburg, Sweden, 2026

Thermokinetic Uncertainty Relations and Dynamical Activities in Quantum Systems

Didrik Palmqvist

Technical Report MC2-479
ISSN 1652-0769

Applied Quantum Physics Laboratory
Department of Microtechnology and Nanoscience (MC2)
Chalmers University of Technology
SE-412 96 Gothenburg, Sweden
Phone: +46 (0)31-772 10 00
www.chalmers.se

Cover: Sketch of a quantum system interacting with its environment by exchanging particles and energy. The strength of the coupling to one of the reservoirs is controlled by a parameter θ.

Printed by Chalmers Digitaltryck
Gothenburg, Sweden, 2026

Abstract

At the nanoscale, thermodynamics is strongly influenced by fluctuations, quantum effects, and nonequilibrium resources. Consequently, precision becomes an important aspect of performance: even when a device operates efficiently on average, fluctuations in currents, heat flows, or delivered power may hinder it from reliably performing its intended task. This is especially relevant for quantum technologies, which rely on quantum coherence that is sensitive to noise.

This thesis investigates how fluctuations constrain the thermodynamic performance in quantum systems, with a focus on thermodynamic and kinetic uncertainty relations. These relations, originally discovered for classical stochastic systems, limit precision in terms of entropy production and dynamical activity. Extending these bounds to quantum systems is nontrivial, both because the classical bounds may be violated due to quantum effects and because the definition of dynamical activity becomes conceptually subtle.

We tackle these questions by deriving bounds on current noise for coherent quantum transport in the spirit of thermodynamic and kinetic uncertainty relations, together with inference bounds for entropy production relying on current and noise measurements. Moreover, a *partial dynamical activity* is introduced to clarify the relation between different definitions of dynamical activity. In addition, a pragmatic approach is presented where useful parts of the activity are estimated from particle-current noise.

Keywords: Quantum thermodynamics, quantum transport, thermodynamic uncertainty relation, kinetic uncertainty relation, current noise, fluctuations, nonequilibrium, dynamical activity, precision bounds.

Acknowledgments

To begin with, I extend my gratitude to my supervisor, Janine Splettstößer, for giving me the opportunity to pursue a PhD in her group, her guidance and enthusiasm, and for enduring my foolish ideas.

I want to thank all the members of the group I am a part of for creating a warm environment with lots of interesting discussions. In particular, I want to thank Nicolás Torres Domínguez and Henning Kirchberg for many engaging conversations over lunch and coffee.

Furthermore, I thank all collaborators on papers published and in preparation. In particular, I want to thank Juliette Monsel and Luca Magazzù. Lastly, I want to thank Ludovico Tesser for being a great mentor, providing many useful comments on this thesis, and teaching me how to set boundaries.

"This discussion is being currently held in a relatively niche subcommunity interested also in quantum thermodynamics." — Referee

List of Publications

This thesis presents introductions, summary and extensions to the following appended papers:

[A] **Didrik Palmqvist**, Ludovico Tesser, Janine Splettstoesser, "Kinetic Uncertainty Relations for Quantum Transport". Published in Phys. Rev. Lett. Oct. 2025.

[B] **Didrik Palmqvist**, Ludovico Tesser, Janine Splettstoesser, "Combining kinetic and thermodynamic uncertainty relations in quantum transport". Published in Quantum Sci. Technol, Jul. 2025.

[C] Juliette Monsel, Matteo Acciai, **Didrik Palmqvist**, Nicolas Chiabrando, Rafael Sánchez, Janine Splettstoesser, "Precision of an autonomous demon exploiting non-thermal resources and information". ArXiv (2025) arXiv:2510.14578.

Acronyms

CFI:	Classical Fisher Information
CTMP:	Continuous-Time Markov Process
CPTP:	Completely Positive and Trace Preserving
GKSL:	Gorini–Kossakowski–Sudarshan–Lindblad
KUR:	Kinetic Uncertainty Relation
LDB:	Local Detailed Balance
NEGF:	Nonequilibrium Green's Function
PDA:	Partial Dynamical Activity
QCRB:	Quantum Cramér–Rao Bound
QFI:	Quantum Fisher Information
SLD:	Symmetric Logarithmic Derivative
TDA:	Total Dynamical Activity
TKUR:	Thermodynamic-Kinetic Uncertainty Relation
TRS:	Time-Reversal Symmetry
TUR:	Thermodynamic Uncertainty Relation

Contents

CHAPTER 1

Introduction

1.1 Quantum thermodynamics and fluctuations

The traditional theory of thermodynamics was developed from the efforts to understand and improve the performance of technologies such as engines during the Industrial Revolution. A key focus of thermodynamics since its inception has been the study of the trade-offs between different performance quantifiers, such as power, efficiency, and dissipation. This is exemplified by Carnot's theorem, which bounds the maximum efficiency of a heat engine independent of its microscopic details. By developing such universal bounds on performance, we uncover both fundamental principles describing physical systems and practical knowledge applicable to technologies.

Traditional thermodynamics governs the behaviour of macroscopic systems consisting of many degrees of freedom. However, nowadays, nanoscale and quantum devices are a focus of both research and technological development. Still, we are interested in understanding performance trade-offs between e.g., energy consumption and efficiency. This is, for example, relevant when we intend to scale up the size of quantum computers. Moreover, small-scale systems that are capable of performing useful thermodynamic tasks have already been realized in experiments, such as highly efficient quantum dot heat engines [1] and superconducting circuits refrigerating qubits [2, 3].

There are, however, important new features that we need to understand when dealing with the thermodynamics of small-scale systems. These systems can display quantum effects such as coherence, superpositions, and entanglement, which

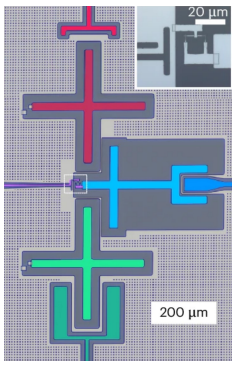

(a) On-chip absorption fridge used for resetting qubits, implemented using superconducting circuits and sources of thermal photons [2].

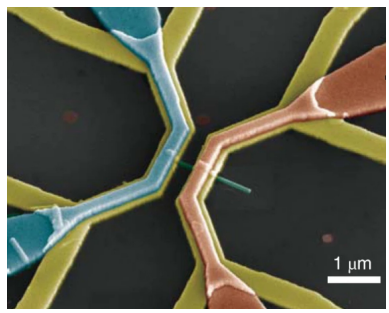

(b) Heat engine consisting of a quantum dot set in a nanowire, connected to cold and hot metallic contacts producing electrical power [1].

Figure 1.1: Examples of small-scale devices where transport through a central region enables tasks such as cooling and power production using nonequilibrium boundary conditions.

are important to manage and can sometimes even lead to thermodynamic advantages [4, 5]. Another key difference is the prevalence of fluctuations and noise. In macroscopic systems, fluctuations are averaged out by the large number of degrees of freedom. The opposite is true in small-scale systems, where the fluctuations and average can be of the same order of magnitude. As a result, the precision in the output of a nanoscale thermodynamic device becomes an important measure of performance. For instance, a refrigerator that fluctuates between cooling and heating a working substance is of limited practical use when high precision is required. This concern becomes even more crucial in quantum devices, which rely on quantum coherence that is sensitive to noise and external disturbances. An important question arises: *How can we formulate trade-off relations between performance quantifiers such as energetic cost, dissipation, and precision, with relevance for quantum technologies?*

Fluctuations are, however, not always detrimental, as noise can power thermodynamic devices [3]. Moreover, fluctuations are often a key part of the physics, and studying them can reveal important insights. A few examples are: The study of the fluctuating position of a Brownian particle, which resulted in strong evidence for the atomic hypothesis [6]. Correlations and fluctuations play an important role in critical phenomena. For example, critical opalescence is caused by large density fluctuations. Shot noise measurements allow for the detection of fractional charge carriers [7, 8]. The fluctuation-dissipation theorem, which determines susceptibilities and linear response to external stimuli through fluctuations [9–11], can also be utilized to perform temperature measurements using Johnson-Nyquist noise [12,

13]. While the fluctuation-dissipation theorem applies broadly, it is fundamentally limited to equilibrium with some exceptions [14, 15]. However, when we want to use a device to perform a thermodynamic task, we must operate it in a nonequilibrium setting.

Out of equilibrium, the possible behaviour of a system is much more diverse compared to equilibrium, and microscopic details are often important. Despite this, classical stochastic thermodynamics has uncovered relations constraining fluctuations even far from equilibrium. A central example are the fluctuation theorems, which have given insight into thermodynamics and the second law on a fluctuating level relevant to, for instance, biomolecular processes [16–24]. While these results are of immense theoretical importance, they are not easily applied to practical situations, since they typically rely upon knowledge of the full probability distribution of e.g. work or entropy production.

More recently, it has been found that the precision of a nonequilibrium process is constrained by entropy production via the Thermodynamic Uncertainty Relation (TUR) [25–28] and by the so-called dynamical activity through the Kinetic Uncertainty Relation (KUR) [29–33]. In addition, combinations of these have been developed [34, 35]. These relations are more easily applied in an experimental setting than the fluctuation relations since they rely on integrated currents, fluctuations, and average entropy production and dynamical activity. However, these bounds do not, in general, continue to hold for quantum systems, with their violations indicating possible quantum advantages in achieving precision [4, 36–40]. The extension of the thermodynamic and kinetic uncertainty relations to quantum systems is an ongoing research topic [40–49].

The generalization of these bounds to quantum systems is a main focus of the appended Papers A and B. Moreover, in Paper C, where the performance of an autonomous demon performing refrigeration is studied, they are used as performance quantifiers. However, a complication arises for the kinetic uncertainty relations as the notion of dynamical activity, while intuitive in classical stochastic dynamics, becomes more subtle in quantum systems [44, 46, 50]. Comparing and connecting different notions of dynamical activity is another key goal of this thesis.

1.2 Organization of thesis

We now outline the structure of the remaining parts of this thesis. Chapter 2 is dedicated to introducing quantum transport and its relevance for quantum thermodynamics. After presenting the general statement of the transport problem as related to thermodynamics, we recap scattering theory, the nonequilibrium Green's function method, Gorini–Kossakowski–Sudarshan–Lindblad master equation, and full counting statistics.

In Chapter 3, we give a detailed introduction to the thermodynamic and ki-

netic uncertainty relations in the context of continuous-time Markov processes. Moreover, Chapter 3 also contains detailed discussions on the different notions of dynamical activity that are used for quantum systems, together with associated bounds on precision. In particular, in Sec. 3.2.3.2 we introduce a *partial dynamical activity* based on information geometry that casts light on the relation between previous definitions [44, 46, 50]. In Sec. 3.2.4 we discuss some of the subtleties of defining dynamical activity in quantum systems with time-dependent Hamiltonians and introduce a definition based on the speed of a protocol.

In Chapter 4, we summarize the results of the appended papers, and in Chapter 5, we give some conclusions and an outlook.

CHAPTER 2

Quantum transport and thermodynamics

This chapter introduces the transport methods used throughout this thesis and explains their relevance for quantum thermodynamics. In section Sec. 2.1 we discuss the first and second law of quantum thermodynamics following Refs. [51, 52]. In Sec. 2.2 we present the general formulation of the quantum transport problem and introduce currents and their associated fluctuations. We then move on to reviewing scattering theory [Sec. 2.3], the nonequilibrium Green's function method [Sec. 2.4], the Gorini–Kossakowski–Sudarshan–Lindblad master equation [Sec. 2.5], and full counting statistics [Sec. 2.6].

2.1 The first and second law of quantum thermodynamics

To formulate the first and second laws of quantum thermodynamics, we consider a system S exchanging energy and particles with an environment consisting of reservoirs labeled by α,

$$\hat{H}(t) = \hat{H}_{\mathrm{S}}(t) + \sum_{\alpha} (\hat{H}_{\alpha} + \hat{V}_{\alpha}), \tag{2.1}$$

where $\hat{H}_{\mathrm{S}}(t)$ is the Hamiltonian of the system which may depend on time explicitly due to external driving, $\hat{H}_{\alpha}$ is the Hamiltonian of reservoir α, and $\hat{V}_{\alpha}$ describes the coupling between S and α. The state of the system and environment at time t is given by the density operator $\hat{\rho}(t)$, which evolves according to the von Neumann

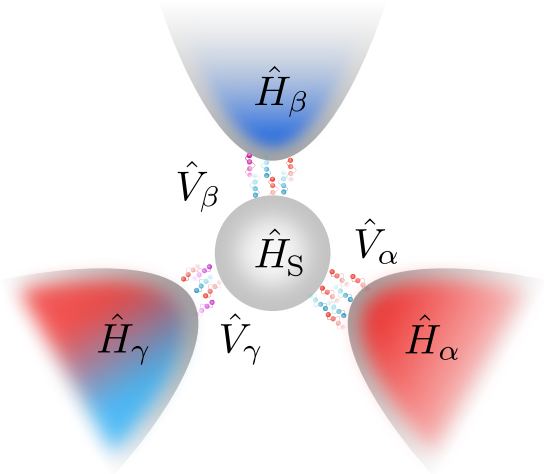

Figure 2.1: A quantum system S exchanging particles and energy with reservoirs.

equation

$$\partial_t \hat{\rho}(t) = -\frac{i}{\hbar}[\hat{H}(t), \hat{\rho}(t)] = -\frac{i}{\hbar}(\hat{H}(t)\hat{\rho}(t) - \hat{\rho}(t)\hat{H}(t)). \tag{2.2}$$

Specifying an initial condition $\hat{\rho}(t_0)$, the formal solution to Eq. (2.2) is $\hat{\rho}(t) = \hat{U}(t, t_0)\hat{\rho}(t_0)\hat{U}^\dagger(t, t_0)$ using the time evolution operator

$$\hat{U}(t, t_0) = T_+ \exp\left\{-\frac{i}{\hbar}\int_{t_0}^{t} dt' \hat{H}(t')\right\}, \quad t \geq t_0. \tag{2.3}$$

Here T_+ is the time-ordering operator, which should be applied to the exponential expanded as a power series in $\hat{H}(t')$. If $t \leq t_0$, one should instead replace the time ordering operator with the anti-time ordering operator. We are, however, not able to describe the full state $\hat{\rho}(t)$ in general, nor control all environmental degrees of freedom in an experiment. A common effective description is to model the reduced system state $\hat{\rho}_\mathrm{S}(t) := \mathrm{tr}_\mathrm{E}\{\hat{\rho}(t)\}$, where the trace is carried out over the environment degrees of freedom and approximate the reservoirs states by fixed thermal states

$$\hat{\rho}_\alpha = \frac{e^{-(\hat{H}_\alpha - \mu_\alpha \hat{N}_\alpha)/k_\mathrm{B}T_\alpha}}{Z_\alpha}, \quad Z_\alpha = \mathrm{tr}\left\{e^{-(\hat{H}_\alpha - \mu_\alpha \hat{N}_\alpha)/k_\mathrm{B}T_\alpha}\right\}. \tag{2.4}$$

Here $\hat{N}_\alpha$ is the number operator, μ_α is the chemical potential, and T_α is the temperature of reservoir α. With the effective description, we approximate $\hat{\rho}(t) \approx \hat{\rho}_\mathrm{S}(t) \bigotimes_\alpha \hat{\rho}_\alpha$, and neglect system-bath correlations and the detailed state of the

environment. Notice that when the system and baths are entangled, we are also neglecting details about the true state of the system. We can expect the effective description to be close to the true one when the system and baths are coupled weakly, and the baths are large. The expectation value of an operator $\hat{X}$ at time t is given $X(t) = \langle \hat{X} \rangle = \mathrm{tr}\{\hat{X}\hat{\rho}(t)\}$. With the preliminaries in place, we now move on to discussing the first and second laws of quantum thermodynamics.

The first law of thermodynamics states that energy is conserved and is formulated as [51, 52]

$$\partial_t \langle \hat{H}_{\mathrm{S}}(t) \rangle = \partial_t W_{\mathrm{S}}(t) - \sum_\alpha (I_\alpha^{(Q)}(t) + \mu_\alpha I_\alpha^{(N)}(t)) - \sum_\alpha \partial_t \langle \hat{V}_\alpha \rangle. \tag{2.5}$$

The first term is the time derivative of the work performed on the system, $\partial_t W(t) = \langle \partial_t \hat{H}_{\mathrm{S}}(t) \rangle$, $I_\alpha^{(Q)}(t) = \partial_t \langle \hat{H}_\alpha - \mu_\alpha \hat{N}_\alpha \rangle$ is the heat current into α, $I_\alpha^{(N)}(t) = \partial_t \langle \hat{N}_\alpha \rangle$ is the particle current into α and $\langle \hat{V}_\alpha \rangle$ is the energy stored in the coupling. We use the convention that the heat and particle currents are positive when flowing into the reservoirs. Eq. (2.5) states that the change in energy of the system is given by the work received through driving minus the heat and chemical work absorbed by the environment, and the change in the coupling energies. While the last term is often neglected, it can play an important role at strong coupling between system and bath [53–57].

The heat and particle currents are not only important for considerations of energy balance, but they also enter the entropy production. The von Neumann entropy of a state is defined as $S_{\mathrm{vN}}(\hat{\rho}) = -k_{\mathrm{B}} \,\mathrm{tr}\{\hat{\rho} \ln \hat{\rho}\}$ and is invariant under a unitary transformation $\hat{U}$, $S_{\mathrm{vN}}(\hat{\rho}) = S_{\mathrm{vN}}(\hat{U}\hat{\rho}\hat{U}^\dagger)$. It is thus conserved in a closed quantum system. However, in our effective description, we neglect the correlations between the system and the environment. The loss of information about system-environment correlations appears as the entropy production rate $\sigma(t)$, which can be expressed using the relative entropy $D(\hat{\rho}_1 || \hat{\rho}_2) = \mathrm{tr}\{\hat{\rho}_1 \ln \hat{\rho}_1\} - \mathrm{tr}\{\hat{\rho}_1 \ln \hat{\rho}_2\} \geq 0$, [51, 52]

$$\begin{aligned} \sigma(t) &= k_{\mathrm{B}} \partial_t D(\hat{U}(t,t_0)\hat{\rho}(t_0)\hat{U}^\dagger(t,t_0) || \hat{\rho}_{\mathrm{S}}(t) \otimes_\alpha \hat{\rho}_\alpha) \\ &= \partial_t S_{\mathrm{vN}}(\hat{\rho}_{\mathrm{S}}(t)) + \sum_\alpha \frac{I_\alpha^{(Q)}}{T_\alpha}. \end{aligned} \tag{2.6}$$

If we assume that initially the system and environment are in a product state $\hat{\rho}(t_0) = \hat{\rho}_{\mathrm{S}}(t_0) \bigotimes_\alpha \hat{\rho}_\alpha$, the second law of thermodynamics is formulated as [51, 52]

$$\Sigma(t) = \int_{t_0}^{t} dt' \sigma(t') = S_{\mathrm{vN}}(\hat{\rho}_{\mathrm{S}}(t)) - S_{\mathrm{vN}}(\hat{\rho}_{\mathrm{S}}(t_0)) + \sum_\alpha \frac{\Delta Q_\alpha}{T_\alpha} \geq 0, \tag{2.7}$$

where $\Delta Q_\alpha = \int_{t_0}^{t} dt' I_\alpha^{(Q)}(t')$ is the heat absorbed by reservoir α. The first and second laws of thermodynamics are essential tools when analyzing the performance

of a thermodynamic device, as they allow us to derive bounds on efficiency and power. In both laws, particle, energy, and heat currents play central roles and are hence necessary to calculate. Moreover, heat currents, chemical power, or work are often the desired output of a thermodynamic device or the resource being consumed to perform a useful task. This motivates the need for a quantum mechanical description of transported quantities, currents, and their fluctuations.

2.2 Quantum transport, currents and fluctuations

Rather than immediately delving into discussions of specific transport methods, it is useful to first state the transport problem in an abstract, method-independent way: quantum transport studies the time evolution of observables associated with subsystems through their currents and fluctuations. It is often convenient to view the dynamics in the Heisenberg picture, where the operators carry the time dependence rather than the density matrix. An operator $\hat{X}(t)$ in the Heisenberg picture is defined as

$$\hat{X}^{\mathrm{H}}(t) = \hat{U}^{\dagger}(t,t_0)\hat{X}(t)\hat{U}(t,t_0), \tag{2.8}$$

and evolves according to the Heisenberg equation of motion

$$\partial_t \hat{X}^{\mathrm{H}}(t) = \frac{i}{\hbar}\Big[\hat{H}^{\mathrm{H}}(t), \hat{X}^{\mathrm{H}}(t)\Big] + \hat{U}^{\dagger}(t,t_0)(\partial_t \hat{X}(t))\hat{U}(t,t_0). \tag{2.9}$$

We again consider a system coupled to reservoirs, allowing for the exchange of energy and particles described by the general time-dependent Hamiltonian $\hat{H}(t) = \hat{H}_{\mathrm{S}}(t) + \sum_\alpha (\hat{H}_\alpha(t) + \hat{V}_\alpha(t))$. We are often interested in the change of an observable associated with a reservoir over time, for example, the electrical charge accumulated in an electrode or the amount of energy absorbed. For a generic observable $\hat{X}_\alpha$ of reservoir α without any explicit time dependence in the Schrödinger picture, an associated current operator is defined by

$$\hat{I}_\alpha^{(X)}(t) := \partial_t \hat{X}_\alpha^{\mathrm{H}}(t) = \frac{i}{\hbar}\Big[\hat{H}^{\mathrm{H}}(t), \hat{X}_\alpha^{\mathrm{H}}(t)\Big]. \tag{2.10}$$

Integrating the expectation value of the current gives the average change in the observable during the evolution

$$\Delta X_\alpha(t) := \mathrm{tr}\Big\{\Delta \hat{X}_\alpha^{\mathrm{H}}(t)\hat{\rho}(t_0)\Big\} = \int_{t_0}^{t} dt'\, \mathrm{tr}\Big\{\hat{I}_\alpha^{(X)}(\tau)\hat{\rho}(t_0)\Big\}, \tag{2.11}$$

where we defined

$$\Delta \hat{X}_\alpha^{\mathrm{H}}(t) := \hat{X}_\alpha^{\mathrm{H}}(t) - \hat{X}_\alpha^{\mathrm{H}}(t_0). \tag{2.12}$$

As discussed in the introduction, we are also interested in characterizing the fluctuations in the output of a thermodynamic device, which are captured by the variance in the change of $\hat{X}_\alpha$

$$\begin{aligned}\mathrm{Var}[\Delta\hat{X}_\alpha(t)] = \int_{t_0}^{t} d\tau \int_{t_0}^{t} d\tau' \Big(&\mathrm{tr}\Big\{\hat{I}_\alpha^{(X)}(\tau)\hat{I}_\alpha^{(X)}(\tau')\hat{\rho}(t_0)\Big\} \\ &- \mathrm{tr}\Big\{\hat{I}_\alpha^{(X)}(\tau)\hat{\rho}(t_0)\Big\}\,\mathrm{tr}\Big\{\hat{I}_\alpha^{(X)}(\tau')\hat{\rho}(t_0)\Big\}\Big).\end{aligned} \tag{2.13}$$

At this stage, we view $\Delta\hat{X}_\alpha^{\mathrm{H}}(t)$ as a Heisenberg-picture operator and define its variance accordingly. In quantum mechanics, however, the statistics associated with transport depend on the chosen measurement protocol and operator ordering [58]. In general, Eq. (2.13) is not guaranteed to coincide with the variance obtained from e.g., the two-point measurement scheme [58, 59]. The time derivative of the variance is used to define the *noise* in a current

$$S_{\alpha\alpha}^{(X)}(t) = \partial_t \mathrm{Var}[\Delta\hat{X}_\alpha(t)] = \int_{t_0}^{t} d\tau \langle\langle \{\hat{I}_\alpha^{(X)}(t), \hat{I}_\alpha^{(X)}(\tau)\}\rangle\rangle. \tag{2.14}$$

Here $\{\hat{X},\hat{Y}\} = \hat{X}\hat{Y} + \hat{Y}\hat{X}$ is the anticommutator and $\langle\langle \hat{X}\hat{Y}\rangle\rangle = \langle \hat{X}\hat{Y}\rangle - \langle\hat{X}\rangle\langle\hat{Y}\rangle$. A common assumption in quantum transport is that when a reservoir is uncoupled from the system, the observable $\hat{X}_\alpha$ does not change. In other words, $[\hat{H}_{\mathrm{S}}(t), \hat{X}_\alpha] = [\hat{H}_\beta(t), \hat{X}_\alpha] = 0$, meaning that the current operator is determined by

$$\hat{I}_\alpha^{(X)}(t) = \sum_\beta \frac{i}{\hbar}[\hat{V}_\beta^{\mathrm{H}}(t), \hat{X}_\alpha^{\mathrm{H}}(t)]. \tag{2.15}$$

Furthermore, it is often assumed that only $\hat{V}_\alpha(t)$ has a non-vanishing commutator with $\hat{X}_\alpha$. We now move on to discussing specific methods for carrying out quantum transport calculations.

2.3 Scattering theory

Scattering theory or Landauer-Büttiker theory deals with coherent quantum transport between reservoirs through a central system acting as a scatterer. It is a well-established framework that has been tested experimentally in many systems [60–63]. It also allows for the derivation of universal relations that are applicable as long as the assumptions underpinning scattering theory are well motivated. The main assumption made in scattering theory is that interactions between particles are weak, such that they can be included on a mean-field level. This is necessary since the scattering is treated as a single-particle problem. Effects of decoherence and inelastic scattering can be included using dephasing and Büttiker probes,

which are fictitious reservoirs with occupation numbers fixed by imposing conditions on the average currents flowing into them [64]. In this picture, the reservoirs function as boundary conditions, injecting particles into the lead according to some average occupation $f_\alpha(E)$, where α is an index labelling the reservoir. In the lead, the particles propagate coherently toward the central region. In the central region, they are scattered, after which they propagate to one of the reservoirs where they equilibrate. For detailed explanations of scattering theory, see Refs. [60–63, 65]. To describe the particles, we introduce two sets of ladder operators: $\hat{a}_{\alpha i}(E), \hat{a}^\dagger_{\alpha i}(E)$ for the incident particles propagating away from reservoir α in channel i and $\hat{b}_{\alpha i}(E), \hat{b}^\dagger_{\alpha i}(E)$ for the scattered particles propagating towards the reservoirs in channel i of lead α. Here $\hat{a}^\dagger_{\alpha i}(E)$ creates a particle moving towards the scattering region and $\hat{b}^\dagger_{\alpha i}(E)$ creates a scattered particle with energy E in channel i, the lead connected to α. If the system is fermionic, the ladder operators fulfill anticommutation relations

$$\begin{aligned}
\{\hat{a}_{\alpha i}(E), \hat{a}^\dagger_{\beta j}(E')\} &= \delta_{ij}\delta_{\alpha\beta}\delta(E-E'),\\
\{\hat{a}^\dagger_{\alpha i}(E), \hat{a}^\dagger_{\beta j}(E')\} &= 0,\\
\{\hat{a}_{\alpha i}(E), \hat{a}_{\beta j}(E')\} &= 0.
\end{aligned} \tag{2.16}$$

The fermionic operators of the scattered particles $\hat{b}^\dagger_{\alpha i}(E)$ fulfill the same anticommutation relations. A consequence of the fermionic operator obeying the anticommutation relations is the Pauli exclusion principle, which states that two fermions can never occupy the same state.

If the system is instead bosonic, the ladder operators fulfill commutation relations

$$\begin{aligned}
[\hat{a}_{\alpha i}(E), \hat{a}^\dagger_{\beta j}(E')] &= \delta_{ij}\delta_{\alpha\beta}\delta(E-E'),\\
[\hat{a}^\dagger_{\alpha i}(E), \hat{a}^\dagger_{\beta j}(E')] &= 0,\\
[\hat{a}_{\alpha i}(E), \hat{a}_{\beta j}(E')] &= 0.
\end{aligned} \tag{2.17}$$

Furthermore, the particles injected from the reservoir are described by the reservoir's average occupation

$$\left\langle \hat{a}^\dagger_{\alpha i}(E)\hat{a}_{\beta j}(E') \right\rangle = \delta_{ij}\delta_{\alpha\beta} f_\alpha(E)\delta(E-E'). \tag{2.18}$$

The fermionic average occupations are bounded by $0 \leq f_\alpha(E) \leq 1$ while the bosonic ones are only constrained to be positive $0 \leq f_\alpha(E)$. If the reservoir is thermal, it is described by

$$f_\alpha(E) = \frac{1}{e^{(E-\mu_\alpha)/T_\alpha} \mp 1}, \tag{2.19}$$

which is the Fermi-Dirac distribution with the lower sign or the Bose-Einstein

distribution with the upper sign, depending on whether the reservoir is fermionic or bosonic. There are interesting situations where the average occupation might not be thermal, such as when the system is smaller than typical thermalization scales, the dynamics occur faster than thermalization times, or some driving is present [66–70]. We will, however, only consider the situation where the reservoir states are diagonal in their energy eigenbasis. Furthermore, we need to compute expectation values of the ladder operators for the scattered particles, such as $\langle \hat{b}^\dagger_{\alpha i}(E')\hat{b}_{\beta i}(E)\rangle$. This is, however, not as simple since it describes a mix of scattered particles from all the reservoirs. To circumvent this problem, we use the scattering matrix $s(E)$ to model the central scattering region

$$s(E) = \begin{bmatrix} t_{11}(E) & t_{12}(E) & \dots \\ t_{21}(E) & t_{22}(E) & \dots \\ \vdots & \vdots & \ddots \end{bmatrix} \tag{2.20}$$

where $t_{\alpha\beta}(E)$ are energy-dependent matrices of dimension $n_\alpha \times n_\beta$, describing the transmission amplitudes from the n_β channels of the lead connected to reservoir β into the n_α channels of the lead connected to reservoir α. The scattering matrix relates the incoming to the scattered particles by [62, 71, 72]

$$\hat{b}_{\alpha i}(E) = \sum_{\beta j} s_{\alpha i \beta j}(E)\hat{a}_{\beta j}(E), \tag{2.21}$$

$$\hat{b}^\dagger_{\alpha i}(E) = \sum_{\beta j} s^*_{\alpha i \beta j}(E)\hat{a}^\dagger_{\beta j}(E). \tag{2.22}$$

For this to be possible, the particles must interact weakly such that we can treat the scattering as a single particle problem. For more details on how the mean field effects of interactions can be incorporated, see Ref. [73]. The main assumption on the scattering matrix is that it must fulfill particle number conservation, giving rise to the unitarity condition,

$$\sum_\beta t_{\alpha\beta}(E)t^\dagger_{\alpha'\beta}(E) = \mathbb{I}_\alpha \delta_{\alpha\alpha'}, \tag{2.23}$$

where $\mathbb{I}_\alpha$ is the $n_\alpha \times n_\alpha$ identity matrix. To describe the propagating particles inside the leads, we introduce their field operators. We assume that the leads are much longer than their width, such that the propagation is essentially one-dimensional. In this case, the coefficients for the field operators can be written as products of

transversal and longitudinal wavefunctions. We expand the field operators as

$$\hat{\Psi}_\alpha(\mathbf{r},t) = \sum_i \int dE e^{-iEt/\hbar} \frac{\Phi_{\alpha i}(r_\perp)}{\sqrt{h v_i(E)}} \left[\hat{a}_{\alpha i}(E) e^{-ik_i(E)z} + \hat{b}_{\alpha i}(E) e^{ik_i(E)z}\right], \quad (2.24)$$

$$\hat{\Psi}^\dagger_\alpha(\mathbf{r},t) = \sum_i \int dE e^{iEt/\hbar} \frac{\Phi^*_{\alpha i}(r_\perp)}{\sqrt{h v_i(E)}} \left[\hat{a}^\dagger_{\alpha i}(E) e^{ik_i(E)z} + \hat{b}^\dagger_{\alpha i}(E) e^{-ik_i(E)z}\right]. \quad (2.25)$$

Here transversal wavefunction of lead α with energy E_i is denoted as $\Phi_{\alpha i}(r_\perp)$. Since the length of a lead is much longer than its width, the transversal wave functions are not involved in the propagation, and the longitudinal wave functions take the form of plane waves. Furthermore we let $k_i(E) = \sqrt{2m(E-E_i)}/\hbar$ denote the wave number, h Planck's constant, $v_i(E) = \hbar k_i(E)/m$ the particle speed, and E_i the energy eigenvalue of the transverse wavefunction. The factor $1/\sqrt{h v_i(E)}$ implements unit flux normalization [62, 71, 72]. With the key objects of scattering theory in place, we move on to deriving current operators.

2.3.1 Currents in scattering theory

To define a current operator, we consider the time derivative of the operator for particle density $\hat{n}_\alpha(\mathbf{r},t) = \hat{\Psi}^\dagger_\alpha(\mathbf{r},t)\hat{\Psi}_\alpha(\mathbf{r},t)$. In the lead where propagation is free, the single particle Hamiltonian is $\hat{H} = \hat{\mathbf{P}}^2/2m$ where $\hat{\mathbf{P}}$ and m are the momentum operator and mass of the particle [62]. This leads to

$$\begin{aligned}\frac{\partial}{\partial t}\hat{n}_\alpha(\mathbf{r},t) &= \frac{i}{\hbar}(\hat{H}\hat{\Psi}^\dagger_\alpha(\mathbf{r},t)\hat{\Psi}_\alpha(\mathbf{r},t) - \hat{\Psi}^\dagger_\alpha(\mathbf{r},t)\hat{\Psi}_\alpha(\mathbf{r},t)\hat{H}) \\ &= \nabla\frac{i\hbar}{2m}\left\{(\nabla\hat{\Psi}^\dagger_\alpha(t,\mathbf{r}))\hat{\Psi}_\alpha(t,\mathbf{r}) - \hat{\Psi}^\dagger_\alpha(t,\mathbf{r})(\nabla\hat{\Psi}_\alpha(t,\mathbf{r}))\right\} \\ &= -\nabla\hat{\boldsymbol{i}}^{(N)}_\alpha(\mathbf{r},t),\end{aligned} \quad (2.26)$$

where $\hat{\boldsymbol{i}}^{(N)}_\alpha(\mathbf{r},t)$ is the particle current density operator [65]. The current operator is obtained by integrating over the transversal coordinates $r_\perp$ and assuming that transversal wavefunctions are stationary, such that we only need to carry out derivatives in the z coordinate [62, 65, 71, 72]

$$\hat{I}^{(N)}_\alpha(z,t) = \frac{i\hbar}{2m}\int dr_\perp \left\{\frac{\partial\hat{\Psi}^\dagger_\alpha(\mathbf{r},t)}{\partial z}\hat{\Psi}_\alpha(\mathbf{r},t) - \hat{\Psi}^\dagger_\alpha(\mathbf{r},t)\frac{\partial\hat{\Psi}_\alpha(\mathbf{r},t)}{\partial z}\right\}. \quad (2.27)$$

Next, we use the standard approximation that quantities depending on the energy vary slowly compared to the energy scale $E-E'$ [62, 71, 72]. With this approximation, $k_i(E') \approx k_i(E) = v_i(E)m/\hbar$, $v_i(E') \approx v_i(E)$ and $\Phi_{\alpha i}(E) \approx \Phi_{\alpha i}(E')$. Under

this assumption, we can use the orthonormality of the wavefunctions, i.e.

$$\int dr_\perp \Phi^*_{\alpha i}(E, r_\perp)\, \Phi_{\alpha j}(E, r_\perp) = \delta_{ij}, \tag{2.28}$$

which leads to a simplified expression

$$\hat{I}^{(N)}_\alpha(z,t) = \frac{1}{h}\sum_i \int dE dE' e^{-i\frac{E-E'}{\hbar}t} \left\{ \hat{b}^\dagger_{\alpha i}(E')\hat{b}_{\alpha i}(E) - \hat{a}^\dagger_{\alpha i}(E')\hat{a}_{\alpha i}(E) \right\}. \tag{2.29}$$

This form of the current operator lends itself to a natural interpretation: the change in the number of particles in reservoir alpha is given by the difference in the number of scattered particles in the lead and particles being ejected from reservoir α. Next, in order to be able to take the expectation value of the operator, we rewrite it in terms of only the ladder operators for the injected particles using Eq. (2.21)

$$\hat{I}^{(N)}_\alpha(t) = \frac{1}{h}\sum_{\beta,\gamma} \int dE dE' e^{-i\frac{E-E'}{\hbar}t} \boldsymbol{\mathcal{A}}^{E',E}_{\alpha i,\beta j,\gamma k} \hat{a}^\dagger_{\beta j}(E')\hat{a}_{\gamma k}(E), \tag{2.30}$$

where we defined [71]

$$\boldsymbol{\mathcal{A}}^{E',E}_{\alpha i,\beta j,\gamma k} \equiv s^*_{\alpha i,\beta j}(E') s_{\alpha i,\gamma k}(E) - \delta_{\alpha i,\beta j}\delta_{\alpha i,\gamma k}. \tag{2.31}$$

Finally, we take the expectation value and find the famous Landauer formula for the average current

$$\begin{aligned} I^{(N)}_\alpha &= \left\langle \hat{I}^{(N)}_\alpha(t) \right\rangle = \frac{1}{h}\sum_{\beta,\gamma} \int dE dE' e^{-i\frac{E-E'}{\hbar}t} \boldsymbol{\mathcal{A}}^{E',E}_{\alpha i,\beta j,\gamma k} \delta_{\beta\gamma}\delta_{ij}\delta(E'-E) f_\beta(E) \\ &= \frac{1}{h}\sum_\beta \int dE D_{\alpha\beta}(E)(f_\beta(E) - f_\alpha(E)). \end{aligned} \tag{2.32}$$

Here, we introduced the transmission function of the scattering region, which relates the flux of particles between different leads

$$D_{\alpha\beta}(E) \equiv \mathrm{tr}\left\{ t_{\alpha\beta}(E) t^\dagger_{\alpha\beta}(E) \right\} \leq n_\alpha. \tag{2.33}$$

The transmission function has the symmetry

$$D_{\alpha\beta}(E) = D^{\mathrm{tr}}_{\beta\alpha}(E) \tag{2.34}$$

where $D^{\mathrm{tr}}_{\alpha\beta}(E)$ denotes the transmission probability of a time-reversed dual system [62, 71, 72]. For example, if we describe the transport of charged particles and the scattering region is pierced by a magnetic field $\mathbf{B}$, time-reversal symmetry

(TRS) is broken. Then, in the time-reversed dual system, the magnetic field is inverted, meaning that

$$D_{\alpha\beta}(E;\mathbf{B}) = D^{\mathrm{tr}}_{\beta\alpha}(E;\mathbf{B}) = D_{\beta\alpha}(E;-\mathbf{B}). \tag{2.35}$$

Thus, if time-reversal symmetry is fulfilled, the transmission probabilities are symmetric $D_{\alpha\beta}(E) = D_{\beta\alpha}(E)$. Additionally, for a specific system, it is possible to explicitly model the scattering matrix to make experimental predictions. However, one of the powers of scattering theory is the ability to use an arbitrary scattering matrix and derive general results that hold in a wide variety of systems.

The energy current operator is defined as

$$\hat{I}^{(E)}_{\alpha}(z,t) = \frac{i\hbar}{2m}\int dr_{\perp}\left\{\frac{\partial\hat{\Psi}^{\dagger}_{\alpha}(\mathbf{r},t)}{\partial z}\hat{H}\hat{\Psi}_{\alpha}(\mathbf{r},t) - \hat{\Psi}^{\dagger}_{\alpha}(\mathbf{r},t)\hat{H}\frac{\partial\hat{\Psi}_{\alpha}(\mathbf{r},t)}{\partial z}\right\}. \tag{2.36}$$

Applying the same approximations as we did earlier for the particle current yields

$$\hat{I}^{(E)}_{\alpha}(z,t) = \frac{1}{2h}\int dEdE' e^{-i(E-E')t/\hbar}(E+E')\sum_{\beta,\gamma}\left\{\boldsymbol{\mathcal{A}}^{E',E}_{\alpha i,\beta j,\gamma k}\hat{a}^{\dagger}_{\beta j}(E')\hat{a}_{\gamma_k}(E)\right\}. \tag{2.37}$$

Calculating the expectation value, we arrive at the following expression for the average energy current

$$I^{(E)}_{\alpha} = \left\langle \hat{I}^{(E)}_{\alpha}(t)\right\rangle = \frac{1}{h}\int dEE\sum_{\beta} D_{\alpha\beta}(E)(f_{\beta}(E) - f_{\alpha}(E)). \tag{2.38}$$

This again has a clear physical interpretation: the energy current into a reservoir is given by the amount of energy carried by the particles flowing into the reservoir, i.e., the energy flow is mediated by the particle flow.

Finally, we are interested in treating entropy production on a fluctuating level. We consider large reservoirs that are not affected by the transport and assume that the energy levels of the reservoirs do not interact with each other. This results in a fluctuating entropy current into reservoir α

$$\hat{I}^{(\Sigma)}_{\alpha}(t) = \frac{k_{\mathrm{B}}}{2h}\int dEdE' e^{-i(E-E')t/\hbar}\log\left[\frac{1\pm f_{\alpha}(E)}{f_{\alpha}(E)}\right]\sum_{\beta,\gamma}\left\{\boldsymbol{\mathcal{A}}^{E',E}_{\alpha i,\beta j,\gamma k}\hat{a}^{\dagger}_{\beta j}(E')\hat{a}_{\gamma_k}(E)\right\}, \tag{2.39}$$

where the upper sign is for bosonic systems and the lower sign is for fermionic system which we will use as a convention for the rest of the thesis. For more

details, see Refs. [59, 74–76]. The expectation value reads as

$$\left\langle \hat{I}_\alpha^{(\Sigma)}(t) \right\rangle = \frac{k_\mathrm{B}}{h} \int dE \log\left[\frac{1 \pm f_\alpha(E)}{f_\alpha(E)}\right] \sum_\beta D_{\alpha\beta}(E)(f_\beta(E) - f_\alpha(E)). \tag{2.40}$$

If the reservoir is thermal with a temperature T_α and a chemical potential μ_α, the above expression recovers the Clausius relation

$$I_\alpha^{(\Sigma)} = \frac{I_\alpha^{(E)} - \mu_\alpha I_\alpha^{(N)}}{T_\alpha}. \tag{2.41}$$

The total average entropy production rate σ is given by the sum of entropy flows

$$\sigma = \sum_\alpha I_\alpha^{(\Sigma)} \geq 0, \tag{2.42}$$

which is always positive [77]. If the transmission function is symmetric, we can express the total entropy production in a convenient form

$$\sigma = \frac{k_\mathrm{B}}{2h} \sum_{\alpha,\beta\neq\alpha} \left\{ \int_0^\infty dE D_{\alpha\beta}(E) \log\left[\frac{F_{\beta\alpha}^{\pm}(E)}{F_{\alpha\beta}^{\pm}(E)}\right] \left(F_{\beta\alpha}^{\pm}(E) - F_{\alpha\beta}^{\pm}(E)\right) \right\}. \tag{2.43}$$

where we defined $F_{\alpha\beta}^{\pm}(E) \equiv f_\alpha(E)(1 \pm f_\beta(E))$. This expression has recently been used in Refs [42, 43, 78] to prove general bounds on entropy production.

In this work, we will discuss a number of relations that apply to any of these currents. Thus, we define a generic current operator

$$\hat{I}_\alpha^{(\nu)} = \frac{1}{h} \sum_{\beta,\gamma} \int dE dE' e^{-i\frac{E-E'}{\hbar}t} x_\alpha^{(\nu)}(E,E') \boldsymbol{\mathcal{A}}_{\alpha i \beta j \gamma k}^{E',E} a_{\beta j}^\dagger(E') a_{\gamma k}(E), \tag{2.44}$$

where $x_\alpha^{(\nu)}(E,E')$ acts as a generalized charge which reduces to the particle current for $x_\alpha^{(N)}(E,E') = 1$, the energy current for $x_\alpha^{(E)}(E,E') = (E+E')/2$ and the entropy current for $x_\alpha^{(\Sigma)}(E,E') = \log\left[(1 \pm f_\alpha(E))/f_\alpha(E)\right]$. Whenever we use a single energy argument in the charge, this means $x_\alpha^{(\nu)}(E) = x_\alpha^{(\nu)}(E,E)$. The average of this generic current operator is given by

$$I_\alpha^{(\nu)} = \left\langle \hat{I}_\alpha^{(\nu)} \right\rangle = \frac{1}{h} \int dE x_\alpha^{(\nu)}(E) \sum_\beta D_{\alpha\beta}(E)(f_\beta(E) - f_\alpha(E)). \tag{2.45}$$

Having established the relevant current operators and their averages in scattering theory, we now turn our attention to describing their fluctuations.

2.3.2 Current noise in scattering theory

To study the fluctuation of the currents, we define the deviation of the current operators

$$\delta\hat{I}_\alpha^{(\nu)}(t) = \hat{I}_\alpha^{(\nu)}(t) - \left\langle \hat{I}_\alpha^{(\nu)}(t) \right\rangle . \tag{2.46}$$

We use the deviations to define the *symmetrized fluctuations* through the following correlator, which is time translation invariant in the absence of external time-dependent fields [61, 63, 79]:

$$S_{\alpha\beta}^{(\nu)}(t,t') = S_{\alpha\beta}^{(\nu)}(t-t') = \frac{1}{2}\left\langle \left\{ \delta\hat{I}_\alpha^{(\nu)}(t), \delta\hat{I}_\beta^{(\nu)}(t') \right\} \right\rangle . \tag{2.47}$$

We choose to study the fluctuations in the frequency domain, which is often called the *noise power*. To do this, we take the Fourier transform

$$\begin{aligned} \int_{-\infty}^{\infty} dt' e^{-i\omega' t'} \int_{-\infty}^{\infty} dt e^{-i\omega t} S_{\alpha\beta}^{(\nu)}(t-t') &= 2\pi\delta(\omega+\omega') S_{\alpha\beta}^{(\nu)}(\omega) \\ &= \left\langle \left\{ \delta\hat{I}_\alpha^{(\nu)}(\omega), \delta\hat{I}_\beta^{(\nu)}(\omega') \right\} \right\rangle . \end{aligned} \tag{2.48}$$

Next, we evaluate the expectation values of Eq. (2.48). This involves taking the expectation value of quartic products of ladder operators. For non-interacting particles, this can be done using Wick's theorem. For states diagonal in the number basis, Wick's theorem results in

$$\begin{aligned} \left\langle \hat{a}_{\alpha i}^\dagger(E_1)\hat{a}_{\beta j}(E_2)\hat{a}_{\gamma k}^\dagger(E_3)\hat{a}_{\delta l}(E_4) \right\rangle &= \left\langle \hat{a}_{\alpha i}^\dagger(E_1)\hat{a}_{\beta j}(E_2) \right\rangle \left\langle \hat{a}_{\gamma k}^\dagger(E_3)\hat{a}_{\delta l}(E_4) \right\rangle \\ &+ \left\langle \hat{a}_{\alpha i}^\dagger(E_1)\hat{a}_{\delta l}(E_4) \right\rangle \left\langle \hat{a}_{\beta j}(E_2)\hat{a}_{\gamma k}^\dagger(E_3) \right\rangle . \end{aligned} \tag{2.49}$$

Using this, we find

$$\begin{aligned} S_{\alpha\beta}^{(\nu)}(\omega) =& \frac{1}{h} \sum_{\gamma\delta} \sum_{ij} \sum_{mn} \int dE \boldsymbol{\mathcal{A}}_{\alpha i,\gamma m,\delta n}^{E,E+\hbar\omega} \boldsymbol{\mathcal{A}}_{\beta j,\delta n,\gamma m}^{E+\hbar\omega,E} x_\alpha^{(\nu)}(E) x_\beta^{(\nu)}(E+\hbar\omega) \\ &\times \left\{ f_\gamma(E)(1 \pm f_\delta(E+\hbar\omega)) + (1 \pm f_\gamma(E)) f_\delta(E+\hbar\omega) \right\} . \end{aligned} \tag{2.50}$$

We restrict ourselves to working with the *zero-frequency noise*, which takes the following form [61, 79]:

$$\begin{aligned} S_{\alpha\beta}^{(\nu)} = S_{\alpha\beta}^{(\nu)}(0) &= \frac{1}{2}\int_{-\infty}^{\infty} dt \left\langle \{\delta\hat{I}_{\alpha}^{(\nu)}(t), \delta\hat{I}_{\beta}^{(\nu)}(0)\} \right\rangle \\ &= \frac{1}{h}\sum_{\gamma\delta}\sum_{ij}\sum_{mn}\int dE \boldsymbol{\mathcal{A}}_{\alpha i,\gamma m,\delta n}^{E,E}\boldsymbol{\mathcal{A}}_{\beta j,\delta n,\gamma m}^{E,E} x_{\alpha}^{(\nu)}(E)x_{\beta}^{(\nu)}(E) \\ &\quad \times \{f_{\gamma}(E)(1 \pm f_{\delta}(E)) + (1 \pm f_{\gamma}(E))f_{\delta}(E)\}\,. \end{aligned} \tag{2.51}$$

Here again, the plus signs are for bosons, and the minus signs are for fermions. The noise in a current is given by the autocorrelator

$$S_{\alpha\alpha}^{(\nu)} = \frac{1}{2}\int_{-\infty}^{\infty} dt \left\langle \{\delta\hat{I}_{\alpha}^{(\nu)}(t), \delta\hat{I}_{\alpha}^{(\nu)}(0)\} \right\rangle. \tag{2.52}$$

Notice that since we assumed time-translation invariance, the expression of (2.51) coincides with the steady state limit of the noise introduced in Eq. (2.14). Moreover, we make a split of the noise into a "classical" part and a "quantum" part

$$S_{\alpha\alpha}^{(\nu)} = S_{\alpha\alpha}^{(\nu)\mathrm{cl}} + S_{\alpha\alpha}^{(\nu)\mathrm{qu}}. \tag{2.53}$$

This is merely a useful mathematical split of the noise, and in any experiment, one would measure the full noise. There also exist other common ways to divide the noise, for example, into shot noise and thermal noise [61]. The classical part contains terms quadratic in the scattering matrix elements and is given by

$$S_{\alpha\alpha}^{(\nu)\mathrm{cl}} = \frac{1}{h}\int dE (x_{\alpha}^{\nu}(E))^2 \left\{ \sum_{\beta\neq\alpha} D_{\alpha\beta}(E)\left(F_{\alpha\beta}^{\pm}(E) + F_{\beta\alpha}^{\pm}(E)\right)\right\}. \tag{2.54}$$

For fermionic systems, the factor $F_{\alpha\beta}^{-}(E)$ can be interpreted as the probability of a particle being present in α and a hole in β at energy E, implementing the Pauli exclusion principle. For the bosonic case, the factor $F_{\alpha\beta}^{+}(E)$ can instead be understood as the product of emission from reservoir α and absorption into β. The classical component of the noise can be interpreted as arising from single-particle transfers. For particle current, the classical part of the noise is simply a summation of particle transfer rates between reservoirs. By defining the single particle transfer rates [62]

$$\Gamma_{\alpha}^{\rightarrow} = \tfrac{1}{h}\textstyle\sum_{\beta\neq\alpha}\int dE D_{\alpha\beta}(E)F_{\alpha\beta}^{\pm}(E), \tag{2.55a}$$

$$\Gamma_{\alpha}^{\leftarrow} = \tfrac{1}{h}\textstyle\sum_{\beta\neq\alpha}\int dE D_{\alpha\beta}(E)F_{\beta\alpha}^{\pm}(E), \tag{2.55b}$$

the classical particle current noise is given by the sum of rates, while the average particle current is given by their differences

$$S_{\alpha\alpha}^{(N)\mathrm{cl}} = \Gamma_\alpha^{\rightarrow} + \Gamma_\alpha^{\leftarrow}, \quad I_\alpha^{(N)} = \Gamma_\alpha^{\leftarrow} - \Gamma_\alpha^{\rightarrow}. \tag{2.56}$$

The quantum part of the noise contains quartic terms in the scattering matrix elements and only contributes when the system is out of equilibrium

$$S_{\alpha\alpha}^{(\nu)\mathrm{qu}} = \pm\frac{1}{h}\int dE \sum_{\beta\neq\alpha}\sum_{\gamma\neq\alpha} \mathrm{tr}\left\{t_{\alpha\beta}t_{\alpha\beta}^\dagger t_{\alpha\gamma}t_{\alpha\gamma}^\dagger\right\}(x_\alpha^{(\nu)})^2(f_\beta - f_\alpha)(f_\gamma - f_\alpha). \tag{2.57}$$

Effects of correlated two-particle transfers are described by the quantum noise, resulting in larger noise for a bosonic system due to bunching and smaller noise in a fermionic system due to anti-bunching. These correlations are, however, not a result of an interaction between particles. They are instead a result of coherent superposition of scattering amplitudes together with the bosonic and fermionic exchange statistics.

2.4 Nonequilibrium Green's functions method

The Nonequilibrium Green's Function (NEGF) method is a more flexible approach to quantum transport compared to scattering theory. An important difference is its ability to treat interacting or nonlinear systems using perturbation theory. It also allows for the treatment of time-dependent Hamiltonians and transient behaviour. While scattering theory can treat periodically driven systems using Floquet methods [63], the NEGF method is not limited to this case. Moreover, the NEGF method allows one to more easily explore quantities that are defined on the level of a microscopic Hamiltonian, compared to scattering theory. This will be useful when we later on in Sec. 3.2 compare different definitions of dynamical activity. For linear systems, it is possible to translate between the NEGF method and scattering theory using Fisher-Lee relations [80–82]. We now briefly discuss the NEGF method for quantum transport in linear bosonic systems, only giving a snapshot of the method. We base our introduction primarily on Ref. [83], which contains many more details and further references on the subject. We consider a system described by a collection of vibrational displacements $\hat{u}_j$. For example, in a three-dimensional lattice of atoms, the index j could refer to the n-th atom's displacement in the forward direction. We will now introduce a number of nonequilibrium Green's functions. The greater Green's function $G^>$ is defined as a matrix by

$$G_{jk}^>(t,t') = -\frac{i}{\hbar}\,\mathrm{tr}\{\hat{u}_j(t)\hat{u}_k(t')\hat{\rho}(t_0)\}, \tag{2.58}$$

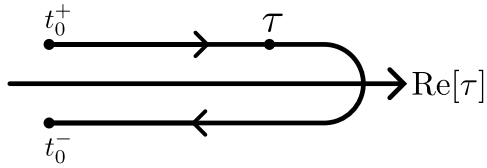

Figure 2.2: Schwinger-Keldysh contour $\mathcal{C}$. The contour runs from t_0^+ on the upper, forward branch up to a maximum time t_M, and then back to t_0^- on the lower, backward branch. If a time τ_b is succeeded by τ_a on the contour, we write $\tau_b \succ \tau_a$. For more details, see Ref. [83].

where $\hat{u}_j(t) = \hat{U}^\dagger(t,t_0)\hat{u}_j\hat{U}(t,t_0)$ is the operator for the displacement in the Heisenberg picture. The lesser Green's function is defined by

$$G^<_{jk}(t,t') = G^>_{kj}(t',t). \tag{2.59}$$

From these, the retarded Green's function is defined by

$$G^r_{jk}(t,t') = \Theta(t-t')\left(G^>_{jk}(t,t') - G^<_{jk}(t,t')\right) \tag{2.60}$$

along with the advanced Green's function

$$G^a_{jk}(t,t') = G^r_{kj}(t',t). \tag{2.61}$$

The time-evolution of the density matrix in the Schrödinger picture and of the operators in the Heisenberg picture can be thought of as two-sided, with $\hat{U}(t,t_0)$ providing the forward evolution from time t_0 to t and $\hat{U}^\dagger(t,t_0) = \hat{U}(t_0,t)$ the backward evolution, creating a loop. It is convenient to describe this time evolution using the Schwinger-Keldysh contour in the complex time plane. We denote the contour by $\mathcal{C}$ and the time on the contour as τ. The contour starts in t_0 on the forward branch in the upper complex time plane and runs up to a maximum time t_M. It then continues in the lower half of the complex plane on the backward branch from t_M to the initial time t_0, see Fig. 2.2. Ordering along this contour is implemented by the contour-ordering operator $T_\mathcal{C}$. Contour ordering coincides with ordinary time ordering on the upper branch and with anti-time ordering on the lower branch [83, 84]. Any point on the lower branch is considered later on the contour than any point on the upper branch, regardless of their physical times. The time evolution operator on the contour for τ_b succeeding τ_a is defined as

$$\hat{U}(\tau_b,\tau_a) = T_\mathcal{C}\exp\left\{-\frac{i}{\hbar}\int_{\tau_a}^{\tau_b} d\tau \hat{H}(\tau)\right\}, \quad \tau_b \succ \tau_a. \tag{2.62}$$

Like in the case of the time ordering operator, the contour ordering operator should be applied on the power series expansion in $\hat{H}(\tau)$ of $\hat{U}(\tau_2, \tau_1)$. We also have the group property $\hat{U}(\tau_c, \tau_a) = \hat{U}(\tau_c, \tau_b)\hat{U}(\tau_b, \tau_a)$, if $\tau_c \succ \tau_b \succ \tau_a$ and the inverse $\hat{U}^{-1}(\tau_b, \tau_a) = \hat{U}(\tau_a, \tau_b)$. Next, we use $\hat{U}(\tau_2, \tau_1)$ to define an operator in the Heisenberg picture on the contour

$$\hat{X}(\tau) = \hat{U}^{-1}(\tau, t_0^+)\hat{X}\hat{U}(\tau, t_0^+), \tag{2.63}$$

where t_0^+ belongs to the upper branch. If the Hamiltonian is the same on the upper and lower branches, the operator on the contour coincides with the usual operator in the Heisenberg picture. We are now ready to introduce the contour-ordered Green's function

$$\begin{aligned} G(\tau, \tau') &= -\frac{i}{\hbar}\operatorname{tr}\{T_{\mathcal{C}}\hat{u}(\tau)\hat{u}^T(\tau')\hat{\rho}(t_0)\} \\ &= -\frac{i}{\hbar}\Theta(\tau, \tau')\operatorname{tr}\{\hat{u}(\tau)\hat{u}^T(\tau')\hat{\rho}(t_0)\} - \frac{i}{\hbar}\Theta(\tau', \tau)\operatorname{tr}\{\hat{u}(\tau')\hat{u}^T(\tau)\hat{\rho}(t_0)\}. \end{aligned} \tag{2.64}$$

Here, the contour ordering is written using the Heaviside function on the contour, which is defined by $\Theta(\tau', \tau) = 1$ if $\tau' \succ \tau$ and $\Theta(\tau', \tau) = 0$ otherwise. Moreover, for ease of notation, we collected all the vibrational displacements into a column vector $\hat{u}(\tau)$. The contour ordered GF is useful since, by finding its Dyson equation (2.73), we can calculate all the other relevant GFs from it. Furthermore, while this is not the focus of this thesis, the Schwinger-Keldysh contour is useful when dealing with non-linear transport, as it allows for the use of perturbation theory and Feynman diagrams when other approaches, such as imaginary time, fail. This is because the Schwinger-Keldysh contour allows one to avoid any reference to the time-evolved nonequilibrium density operator in the interaction picture.

Having introduced the basic building blocks of the NEGF method, we apply it to the case of linear bosonic transport with the Hamiltonian

$$\hat{H} = \frac{1}{2}\hat{p}^T\hat{p} + \frac{1}{2}\hat{u}^T\mathbf{K}\hat{u} \tag{2.65}$$

where $\hat{u}_i = \sqrt{m_i}\hat{x}_i$ denote the rescaled positions of the oscillators, such that $\hat{u}$ and $\hat{p}$ are column vectors containing all the scaled positions and momenta of the network, and $\mathbf{K}$ is a symmetric and positive definite spring constant matrix. The canonical commutation relations for the positions and momenta at equal time on the contour are expressed by

$$\left[\hat{u}(\tau), \hat{p}^T(\tau)\right] = \hat{u}(\tau)\hat{p}^T(\tau) - \hat{p}(\tau)\hat{u}^T(\tau) = i\hbar\mathbf{I}. \tag{2.66}$$

Taking time derivatives of the contour-ordered GF, one finds

$$\frac{\partial^2 G(\tau,\tau')}{\partial\tau^2} = -\frac{i}{\hbar}\,\mathrm{tr}\big\{T_{\mathcal{C}}\ddot{\hat{u}}(\tau)\hat{u}^T(\tau')\hat{\rho}(t_0)\big\} - \frac{i}{\hbar}\delta(\tau,\tau')\,\mathrm{tr}\big\{[\dot{\hat{u}}(\tau),\hat{u}^T(\tau')]\hat{\rho}(t_0)\big\}. \tag{2.67}$$

Here, we used the delta function on the contour $\delta(\tau,\tau') = \frac{d}{d\tau}\Theta(\tau,\tau')$, which has the property that $y(\tau) = \int d\tau'\delta(\tau,\tau')y(\tau')$. Simplifying (2.67) using the Heisenberg equation and the canonical commutation relation of Eq. (2.66) results in [83]

$$\left(\frac{\partial^2}{\partial\tau^2} + \mathbf{K}\right) G(\tau,\tau') = -\delta(\tau,\tau')\mathbf{I}. \tag{2.68}$$

We observe that the contour-ordered GF has the same significance as the GF used in the context of linear differential equations, i.e., it represents the system's impulse response.

As of yet, we have not connected the NEGFs to a transport situation. To do this, we partition the harmonic network into a central region S interacting with reservoirs labeled by Greek letters α and write the Hamiltonian in terms of a system Hamiltonian, bath Hamiltonians, and coupling Hamiltonians

$$\begin{aligned} H =& \hat{H}_{\mathrm{S}} + \sum_{\alpha} \hat{H}_{\alpha} + \hat{V}_{\alpha} \\ =& \frac{1}{2}\hat{p}_{\mathrm{S}}^T\hat{p}_{\mathrm{S}} + \frac{1}{2}\hat{u}_{\mathrm{S}}^T\mathbf{K}^{\mathrm{S}}\hat{u}_{\mathrm{S}} + \sum_{\alpha}\hat{H}_{\alpha} + \hat{u}_{\alpha}^T\mathbf{V}^{\alpha\mathrm{S}}\hat{u}_{\mathrm{S}}. \end{aligned} \tag{2.69}$$

We have separated the spring constant matrix into two parts

$$\mathbf{K} = \begin{pmatrix} \mathbf{K}^{\mathrm{S}} & \mathbf{V}^{\mathrm{S}\alpha} & \mathbf{V}^{\mathrm{S}\beta} & \dots \\ \mathbf{V}^{\alpha\mathrm{S}} & \mathbf{K}^{\alpha} & 0 & \dots \\ \mathbf{V}^{\beta\mathrm{S}} & 0 & \mathbf{K}^{\beta} & 0 \\ \vdots & \vdots & 0 & \ddots \end{pmatrix} = \mathbf{k} + \mathbf{V} \tag{2.70}$$

where $\mathbf{k}$ is the spring constant matrix for the uncoupled subsystems, and $\mathbf{V}$ contains the couplings between the system and the baths

$$\mathbf{k} = \begin{pmatrix} \mathbf{K}^{\mathrm{S}} & 0 & \dots \\ 0 & \mathbf{K}^{\alpha} & 0 \\ \vdots & 0 & \ddots \end{pmatrix}, \quad \mathbf{V} = \begin{pmatrix} 0 & \mathbf{V}^{\mathrm{S}\alpha} & \mathbf{V}^{\mathrm{S}\beta} & \dots \\ \mathbf{V}^{\alpha\mathrm{S}} & 0 & 0 & \dots \\ \mathbf{V}^{\beta\mathrm{S}} & 0 & 0 & 0 \\ \vdots & \vdots & 0 & \ddots \end{pmatrix}. \tag{2.71}$$

Defining the uncoupled greens functions $g(\tau,\tau')$ as solutions to

$$\left(\frac{\partial^2}{\partial\tau^2}+\mathbf{k}\right)g(\tau,\tau')=-\delta(\tau,\tau')\mathbf{I}, \tag{2.72}$$

one finds the Dyson equation for the coupled ones

$$\begin{aligned} G(\tau,\tau') &= g(\tau,\tau')+\int_{\mathcal{C}} d\tau'' g(\tau,\tau'')\mathbf{V}G(\tau'',\tau') \\ &= g(\tau,\tau')+\int_{\mathcal{C}} d\tau'' G(\tau,\tau'')\mathbf{V}g(\tau'',\tau'). \end{aligned} \tag{2.73}$$

For shorthand, we will refer to the convolution as $G=g+g\mathbf{V}G=g+G\mathbf{V}g$. To proceed, one considers specific initial conditions for the uncoupled systems

$$g_{xy}(\tau,\tau')=-\frac{i}{\hbar}\,\mathrm{tr}\left\{\hat{\rho}_{\mathrm{S}}(t_0)\bigotimes_{\alpha}\hat{\rho}_{\alpha}(t_0)T_{\mathcal{C}}\hat{u}_x(\tau)\hat{u}_y^T(\tau')\right\}, \tag{2.74}$$

where we let x,y denote either S or one of the reservoir indices. For example, by choosing the initial state to be thermal

$$\hat{\rho}_x(t_0)=\frac{e^{-\hat{H}_x/k_{\mathrm{B}}T_x}}{\mathrm{tr}\left\{e^{-\hat{H}_x/k_{\mathrm{B}}T_x}\right\}} \tag{2.75}$$

with $\hat{H}_x=\frac{1}{2}\hat{p}_x^T\hat{p}_x+\frac{1}{2}\hat{u}_x^T\mathbf{K}^x\hat{u}_x$ one can solve Eq. (2.72) and construct the full nonequilibrium GF from the uncoupled ones via Eq. (2.73) [83].

With this solution, we can apply the NEGF framework to calculate the energy current into the reservoir α through

$$I_{\alpha}^{(E)}(t)=\mathrm{tr}\left\{\frac{d\hat{H}_{\alpha}(t)}{dt}\hat{\rho}(t_0)\right\}=-\frac{i}{\hbar}\frac{\partial}{\partial t'}\,\mathrm{tr}\left\{G_{\mathrm{S}\alpha}^{<}(t,t')\mathbf{V}^{\alpha\mathrm{S}}\right\}\Big|_{t'=t}. \tag{2.76}$$

Thus, in order to calculate the current, we need an expression for $G_{\mathrm{S}\alpha}^{<}(t,t')$. We easily obtain this from the Dyson equation (2.73) using Langreth's theorem [83]

$$G_{\mathrm{S}\alpha}^{<,>}(t,t')=\int_{t_0}^{t}dt''G_{\mathrm{SS}}^{r}(t,t'')V^{\mathrm{S}\alpha}g_{\alpha}^{<,>}(t'',t')+G_{\mathrm{SS}}^{<,>}(t,t'')V^{\mathrm{S}\alpha}g_{\alpha}^{a}(t'',t'). \tag{2.77}$$

By directly inserting Eq. (2.77) back into Eq. (2.76) one finds an expression for the current which is valid in the transient regime. We will, however, consider the steady state by setting $t_0\to-\infty$ and $t\to\infty$ so that we can use the convolution theorem

$$G_{\mathrm{S}\alpha}^{<,>}(\omega)=G_{\mathrm{SS}}^{r}(\omega)\mathbf{V}^{\mathrm{S}\alpha}g_{\alpha}^{<,>}(\omega)+G_{\mathrm{SS}}^{<,>}(\omega)\mathbf{V}^{\mathrm{S}\alpha}g_{\alpha}^{a}(\omega). \tag{2.78}$$

Next, we define the bath self-energies

$$\Sigma_\alpha(\tau,\tau') = \mathbf{V}^{\mathrm{S}\alpha} g_\alpha(\tau,\tau')\mathbf{V}^{\alpha\mathrm{S}}, \tag{2.79}$$

which together with Eq. (2.78) results in the Meir-Wingreen formula for the energy current

$$\lim_{t\to\infty} I_\alpha^{(E)}(t) = -\int_{-\infty}^{\infty} \frac{d\omega}{4\pi}\hbar\omega\,\mathrm{tr}\big\{G^<_{\mathrm{SS}}(\omega)\Sigma^>_\alpha(\omega) - G^>_{\mathrm{SS}}(\omega)\Sigma^<_\alpha(\omega)\big\}. \tag{2.80}$$

The Meir-Wingreen formula can also be derived for interacting systems and electronic systems [85, 86]. Furthermore, in the case of ballistic transport, which we are discussing here, this equation can be simplified. From the Dyson equation for the central system S and the relations between the NEGFs, we find

$$\begin{aligned} G^<_{\mathrm{SS}}(\omega) &= \sum_\alpha G^r_{\mathrm{SS}}(\omega)\Sigma^<_\alpha(\omega)G^a_{\mathrm{SS}}(\omega), \\ G^a_{\mathrm{SS}}(\omega) - G^r_{\mathrm{SS}}(\omega) &= i\sum_\alpha G^r_{\mathrm{SS}}(\omega)\Gamma_\alpha(\omega)G^a_{\mathrm{SS}}(\omega), \end{aligned} \tag{2.81}$$

where we introduced the spectral function for the lead α,

$$\Gamma_\alpha(\omega) = i(\Sigma^r_\alpha(\omega) - \Sigma^a_\alpha(\omega)). \tag{2.82}$$

Furthermore, assuming that the reservoirs are large enough that they are unaffected by the transport, and that they fulfill the Kubo-Martin-Schwinger relation, we have[1]

$$\Sigma^<_\alpha(\omega) = -if_\alpha(\omega)\Gamma_\alpha(\omega), \quad \Sigma^>_\alpha(\omega) = -i(1+f_\alpha(\omega))\Gamma_\alpha(\omega). \tag{2.83}$$

By defining

$$\mathbf{T}_{\alpha\beta}(\omega) = \Gamma_\alpha(\omega)G^r_{\mathrm{SS}}(\omega)\Gamma_\beta(\omega)G^a_{\mathrm{SS}}(\omega), \tag{2.84}$$

which is related to the transmission function by $D_{\alpha\beta}(\omega) = \mathrm{tr}\{\mathbf{T}_{\alpha\beta}(\omega)\}$ using the Caroli formula [87], we are able to simplify the current and recover the Landauer formula

$$I_\alpha^{(E)} = \int_0^\infty \frac{d\omega}{2\pi}\hbar\omega\sum_\beta \mathrm{tr}\{\mathbf{T}_{\alpha\beta}(\omega)\}(f_\beta(\omega) - f_\alpha(\omega)). \tag{2.85}$$

This derivation of the Landauer formula is more general than the one made in the previous section using scattering theory, since it does not rely on one-dimensional leads or additional assumptions of slow energy dependence. For more details on the relation between the NEGF method and scattering theory for non-interacting systems, see Ref. [82]. Also, for the NEGF method, we can consider the noise in

[1] Here we use $f_\alpha(\omega) = f_\alpha(\hbar\omega)$ for shorthand.

the current. We will, however, postpone discussing this until Sec. 2.6.2, where we give a short introduction to full-counting statistics.

2.5 Gorini–Kossakowski–Sudarshan–Lindblad master equation

In this section, we give a brief introduction to the Gorini–Kossakowski–Sudarshan –Lindblad (GKSL) master equation, which allows for the treatment of transport in nonlinear or interacting systems. Both scattering theory and the NEGF method can be applied to situations where the coupling between reservoirs and the system is strong. However, the former can only treat interactions at the mean field level, and while the NEGF allows for perturbative treatment of nonlinear terms in the Hamiltonian, or the coupling between system and enviroment see e.g. Refs. [73, 88]. However, this often does not yield general expressions for currents and noise that are amenable to proving universal bounds on precision. In most systems utilized in quantum technology, interactions or nonlinearities are present. One common approach to dealing with such a system is to assume that the coupling between it and the environment is weak, which allows us to derive a master equation. We consider a system interacting with a number of baths described by the following Hamiltonian

$$\hat{H} = \hat{H}_{\mathrm{S}} + \sum_{\alpha} (\hat{H}_{\alpha} + \hat{V}_{\alpha}). \tag{2.86}$$

This is the same setting as in Eq. (2.1) but with the additional assumption that there is no explicit time dependence in the Hamiltonian. The coupling Hamiltonian between system and bath α is, in general, given by

$$\hat{V}_{\alpha} = \sum_{k} \hat{A}_{\alpha k} \otimes \hat{B}_{\alpha k} = \sum_{k} \hat{A}^{\dagger}_{\alpha k} \otimes \hat{B}^{\dagger}_{\alpha k} \tag{2.87}$$

where $\hat{A}_{\alpha k}$ is an operator of the system and $\hat{B}_{\alpha k}$ is an operator of bath α. Notice that extra care is needed when the operators are fermionic in order to ensure proper anti-commutation relations [89–91]. The time evolution of the total system density matrix is given

$$\hat{\rho}(t) = \hat{U}(t, t_0)\hat{\rho}(t_0)\hat{U}^{\dagger}(t, t_0). \tag{2.88}$$

However, in practice, one rarely has access to the full density operator. One might only be able to measure a subsystem locally, or one might not even know the detailed Hamiltonian of the environment needed to find the full time-evolution operator. Thus, we resort to studying the reduced system density operator $\hat{\rho}_{\mathrm{S}}(t) = \mathrm{tr}_{\mathrm{E}}\{\hat{\rho}(t)\}$, where $\mathrm{tr}_{\mathrm{E}}\{\cdot\}$ is the partial trace over environment degrees of freedom. As a consequence, one needs to model the dynamics of $\hat{\rho}_{\mathrm{S}}(t)$, which, however, is no

longer governed by the von Neumann equation

$$\frac{d}{dt}\hat{\rho}(t) = -\frac{i}{\hbar}[\hat{H}, \hat{\rho}(t)], \qquad \frac{d}{dt}\hat{\rho}_{\mathrm{S}}(t) \neq -\frac{i}{\hbar}[\hat{H}_{\mathrm{S}}, \hat{\rho}_{\mathrm{S}}(t)]. \tag{2.89}$$

There exist methods to obtain equations of motion where approximations are applied in a systematic manner, such as the Nakajima-Zwanzig approach [52, 92–95]. We will, however, only outline a brief derivation of the famous GKSL equation based primarily on Ref. [96]. For further details on the GKSL equation in the context of quantum thermodynamics, see Ref. [52]. We will assume that the Hamiltonian has no explicit time dependence for simplicity, it is, however, possible to treat the time-dependent case, see e.g. Ref. [97]. Defining the coupling Hamiltonian $\hat{V} = \sum_\alpha \hat{V}_\alpha$, the von Neumann equation in the interaction picture reads as

$$\frac{d}{dt}\hat{\rho}^{\mathrm{I}}(t) = -\frac{i}{\hbar}\Big[\hat{V}^{\mathrm{I}}(t), \hat{\rho}^{\mathrm{I}}(t)\Big]. \tag{2.90}$$

Integrating and inserting the von Neumann equation back into itself, in combination with tracing out the environment, results in an equation of motion for the reduced density operator

$$\frac{d}{dt}\hat{\rho}^{\mathrm{I}}_{\mathrm{S}}(t) = -\frac{1}{\hbar^2}\int_0^t dt' \mathrm{tr}_{\mathrm{E}}\left\{\Big[\hat{V}^{\mathrm{I}}(t), \Big[\hat{V}^{\mathrm{I}}(t'), \hat{\rho}^{\mathrm{I}}(t')\Big]\Big]\right\}. \tag{2.91}$$

Here we assumed

$$\mathrm{tr}_{\mathrm{E}}\{[\hat{V}^{\mathrm{I}}(t), \hat{\rho}(0)]\} = 0, \tag{2.92}$$

which can always be made the case by redefining the system Hamiltonian to contain mean-field effects from the environment. Next, utilizing the weak coupling, we make the Born approximation $\hat{\rho}(t) \approx \hat{\rho}_{\mathrm{S}}(t) \bigotimes_\alpha \hat{\rho}_\alpha$ and the Markov approximation, which assumes that the bath correlation time τ_{B} is much shorter than the typical timescale over which the system evolves $\tau_{\mathrm{S}} \gg \tau_{\mathrm{B}}$. This allows us to replace $\hat{\rho}^{\mathrm{I}}(t') \approx \hat{\rho}^{\mathrm{I}}(t)$ in the integral of Eq. (2.91) and extend the upper integration limit to infinity [96]. For the bath correlations to decay, it is necessary to assume that the bath is infinitely large with a continuous spectrum. To continue, we assume that the spectrum of $H_{\mathrm{S}} = \sum_\epsilon \epsilon \left|\epsilon\right\rangle\!\left\langle\epsilon\right| = \sum_\epsilon \epsilon\hat{\Pi}(\epsilon)$ is discrete and denote the eigenvalues of the system Hamiltonian as ϵ with the projector onto the eigenspace of ϵ as $\hat{\Pi}(\epsilon)$. We use the projectors to define

$$\hat{A}_{\alpha k}(\omega) = \sum_{\epsilon' - \epsilon = \omega} \hat{\Pi}(\epsilon)\hat{A}_{\alpha k}\hat{\Pi}(\epsilon') \tag{2.93}$$

and express the time evolution of the system and environment operators in the interaction picture as

$$\hat{A}^{\mathrm{I}}_{\alpha k}(\omega;t) = e^{iH_{\mathrm{S}}t/\hbar}\hat{A}_{\alpha k}(\omega)e^{-iH_{\mathrm{S}}t/\hbar} = e^{-i\omega t}\hat{A}_{\alpha k}(\omega), \tag{2.94}$$

$$\hat{B}^{\mathrm{I}}_{\alpha k}(t) = e^{iH_{\alpha}t/\hbar}\hat{B}_{\alpha k}e^{-iH_{\alpha}t/\hbar}. \tag{2.95}$$

Here, we used the assumption that the Hamiltonian has no explicit time-dependence. In combination with the earlier approximations, we find the following expression for the evolution of the reduced density matrix

$$\frac{d}{dt}\hat{\rho}_{\mathrm{S}}(t) = \sum_{\omega,\omega'}\sum_{\alpha,k,\beta,j} e^{i(\omega'-\omega)t}\int_0^{\infty} dt' e^{i\omega t'}\,\mathrm{tr}_{\mathrm{E}}\left\{\hat{B}^{\mathrm{I}}_{\alpha k}(t)\hat{B}^{\mathrm{I}}_{\beta j}(t-t')\bigotimes_{\alpha}\hat{\rho}_{\alpha}\right\}\times \\ \times\left\{\hat{A}_{\beta j}(\omega)\hat{\rho}^{\mathrm{I}}_{\mathrm{S}}(t)\hat{A}^{\dagger}_{\alpha k}(\omega') - \hat{A}^{\dagger}_{\alpha k}(\omega')\hat{A}_{\beta j}(\omega)\hat{\rho}^{\mathrm{I}}_{\mathrm{S}}(t)\right\} + \mathrm{h.c.} \tag{2.96}$$

Furthermore we assume that the reservoirs are in stationary states $[\hat{H}_{\alpha},\hat{\rho}_{\alpha}] = 0$ which implies that the bath correlation functions obey

$$\mathrm{tr}_{\alpha}\left\{\hat{B}^{\mathrm{I}}_{\alpha k}(t)\hat{B}^{\mathrm{I}}_{\alpha k'}(t-t')\hat{\rho}_{\alpha}\right\} = \mathrm{tr}_{\alpha}\left\{\hat{B}^{\mathrm{I}}_{\alpha k}(t')\hat{B}^{\mathrm{I}}_{\alpha k'}(0)\hat{\rho}_{\alpha}\right\}. \tag{2.97}$$

The last approximation we use is the secular approximation, which assumes that $|\omega-\omega'| \gg 1/\tau_{\mathrm{S}}$, allowing us to disregard the rotating terms where $\omega' \neq \omega$. This leads to

$$\frac{d}{dt}\hat{\rho}_{\mathrm{S}}(t) = \sum_{\omega}\sum_{\alpha,k,\beta,j}\gamma_{\alpha k\beta j}(\omega)\left(\hat{A}_{\beta j}(\omega)\hat{\rho}_{\mathrm{S}}(t)\hat{A}^{\dagger}_{\alpha k}(\omega) - \frac{1}{2}\left\{\hat{A}^{\dagger}_{\alpha k}(\omega)\hat{A}_{\beta j}(\omega),\hat{\rho}_{\mathrm{S}}(t)\right\}\right), \tag{2.98}$$

where we neglected the Lamb-Shift Hamiltonian

$$\hat{H}_{\mathrm{LS}} = \sum_{\omega,\alpha,k,\beta,j}\mathrm{Im}\left[\int_0^{\infty} dt' e^{i\omega t'}\,\mathrm{tr}_{\alpha}\left\{\hat{B}^{\mathrm{I}}_{\alpha k}(t)\hat{B}^{\mathrm{I}}_{\beta j}(t-t')\bigotimes_{\alpha}\hat{\rho}_{\alpha}\right\}\right]\hat{A}^{\dagger}_{\alpha k}(\omega)\hat{A}_{\beta j}(\omega), \tag{2.99}$$

since it commutes with the system Hamiltonian. The Lamb-shift Hamiltonian leads to a renormalization of the system energy levels due to the coupling with the environment, for more details see e.g. Refs. [52, 96]. The prefactor in Eq. (2.98) is defined by the bath correlation function

$$\gamma_{\alpha k\beta j}(\omega) = \int_{-\infty}^{\infty} dt' e^{i\omega t'}\,\mathrm{tr}_{\mathrm{E}}\left\{\hat{B}^{\mathrm{I}}_{\alpha k}(t')\hat{B}^{\mathrm{I}}_{\beta j}(0)\bigotimes_{\alpha}\hat{\rho}_{\alpha}\right\}. \tag{2.100}$$

Since we assumed that the baths are independent and initially prepared in a product state, the operators of different baths are uncorrelated, i.e., $\gamma_{\alpha k\beta j}(\omega) =$

$\delta_{\alpha\beta}\gamma^{\alpha}_{kj}(\omega)$. The matrix $[\boldsymbol{\gamma}^{\alpha}(\omega)]_{kj} = \gamma^{\alpha}_{kj}(\omega)$ is positive as a result of Bochner's theorem [96], allowing us to diagonalize it using a unitary transformation $\boldsymbol{\gamma}^{\alpha}(\omega) = \boldsymbol{u}^{\alpha}(\omega)\boldsymbol{\Lambda}^{\boldsymbol{\alpha}}(\omega)(\boldsymbol{u}^{\alpha}(\omega))^{\dagger}$ where $\boldsymbol{u}^{\alpha}(\omega)(\boldsymbol{u}^{\alpha}(\omega))^{\dagger} = \boldsymbol{I}$ and $\boldsymbol{\Lambda}(\omega) = \mathrm{diag}\{\lambda^{\alpha}_1(\omega), ..., \lambda^{\alpha}_n(\omega)\}$ with $\lambda^{\alpha}_l(\omega)$ being the l-th eigenvalue of $\boldsymbol{\gamma}^{\alpha}(\omega)$ with the corresponding eigenvector $\boldsymbol{u}^{\alpha}_l(\omega)$. By defining the jump operators

$$\hat{L}_{\alpha l}(\omega) = \sum_k \sqrt{\lambda^{\alpha}_l(\omega)}[(\boldsymbol{u}^{\alpha}(\omega))^{\dagger}]_{lk}\hat{A}_{\alpha k}(\omega), \tag{2.101}$$

and transforming back to the Schrödinger picture, we finally arrive at the standard GKSL form

$$\frac{d}{dt}\hat{\rho}_{\mathrm{S}}(t) = \hat{\mathcal{L}}\hat{\rho} = -\frac{i}{\hbar}[\hat{H}_{\mathrm{S}}, \hat{\rho}_{\mathrm{S}}(t)] + \sum_{\alpha,l,\omega}\mathcal{D}[\hat{L}_{\alpha l}(\omega)]\hat{\rho}_{\mathrm{S}}(t) \tag{2.102}$$

where $\mathcal{D}[\hat{L}]\hat{\rho} = \hat{L}\hat{\rho}\hat{L}^{\dagger} - \{\hat{L}^{\dagger}\hat{L}, \hat{\rho}\}/2$. Here, the dynamics have been separated into a coherent part caused by the system Hamiltonian and an incoherent part due to the interaction with the environment. Moreover, this master equation is local in time and Completely Positive and Trace Preserving (CPTP), meaning that it preserves the trace, hermiticity, and positivity of $\hat{\rho}_{\mathrm{S}}(t)$ at all times. For the rest of the thesis, we will use the collective index j to refer to both ω and l. For thermal reservoirs, the bath correlators obey the KMS relation

$$\mathrm{tr}\Big\{\hat{B}^{\mathrm{I}}_{\alpha k}(t)\hat{B}^{\mathrm{I}}_{\alpha j}(0)\hat{\rho}_{\alpha}\Big\} = \mathrm{tr}\Big\{\hat{B}^{\mathrm{I}}_{\alpha j}(-t - \hbar i/k_{\mathrm{B}}T_{\alpha})\hat{B}^{\mathrm{I}}_{\alpha k}(0)\hat{\rho}_{\alpha}\Big\}, \tag{2.103}$$

which results in the condition of Local Detailed Balance (LDB)

$$\boldsymbol{\gamma}^{\alpha}_{kj}(-\omega) = e^{-\hbar\omega/k_{\mathrm{B}}T_{\alpha}}\boldsymbol{\gamma}^{\alpha}_{jk}(\omega). \tag{2.104}$$

Local detailed balance ensures that the dynamics will be thermodynamically consistent and implies that the jump operators come in pairs of two $j, \tilde{j}$, which obey

$$\hat{L}_{\alpha j} = e^{\sigma_{\alpha j}/2}\hat{L}^{\dagger}_{\alpha\tilde{j}}. \tag{2.105}$$

Here $\sigma_{\alpha j} = -\sigma_{\alpha\tilde{j}}$ is the entropy change in reservoir α due to $\hat{L}_{\alpha j}$. In particular, since

$$\hat{L}_{\alpha l}(-\omega) = e^{-\hbar\omega/2k_{\mathrm{B}}T_{\alpha}}\hat{L}^{\dagger}_{\alpha l}(\omega), \tag{2.106}$$

if $j = (\omega, l)$ then $\tilde{j} = (-\omega, l)$.

2.5.1 Jump unravelings and transport

We have not yet connected the GKSL equation to quantum transport, and how one does this depends on the details of how the system is coupled to its environment. One useful interpretation of the GKSL equation is that it represents the average over a continuously monitored stochastic evolution where the environment performs unread measurements on the system. As a consequence, it is in principle possible to monitor the interaction between the system and bath continuously. To describe this, one commonly unravels Eq. (2.102) into a stochastic master equation. The two most common types of unravelings are jump and diffusive unravelings; we will only cover the former, following Ref. [98] closely. A general CPTP map can be written as

$$\hat{\rho}_{\mathrm{S}} \mapsto \sum_j \hat{M}_j \hat{\rho}_{\mathrm{S}} \hat{M}_j^\dagger, \tag{2.107}$$

where $\{\hat{M}_j\}$ is a set of Kraus operators obeying $\sum_j \hat{M}_j^\dagger \hat{M}_j = \mathbf{I}$. We can interpret this as a generalized measurement where j labels the different outcomes. To describe the measurement, we define a random state conditioned on the outcome j

$$\hat{\rho}_{\mathrm{S}} \mapsto \frac{\hat{M}_j \hat{\rho}_{\mathrm{S}} \hat{M}_j^\dagger}{\mathrm{tr}\left\{\hat{M}_j \hat{\rho}_{\mathrm{S}} \hat{M}_j^\dagger\right\}}. \tag{2.108}$$

This post-selected state represents our knowledge of the system based on the observed outcome j. If we disregard the outcomes and instead average over them, we recover the original CPTP map of Eq. (2.107). The goal is to associate these measurement outcomes with the transport of a quantity between the environment and the system. Focusing on the GKSL equation, we define an effective non-Hermitian Hamiltonian

$$\hat{H}_{\mathrm{eff}} = \hat{H}_{\mathrm{S}} - \frac{i\hbar}{2} \sum_{\alpha j} \hat{L}_{\alpha j}^\dagger \hat{L}_{\alpha j}, \tag{2.109}$$

and the set of the Kraus operators

$$\hat{M}_0 = 1 - i\hat{H}_{\mathrm{eff}} dt, \quad \hat{M}_{\alpha j} = \sqrt{dt}\hat{L}_{\alpha j}. \tag{2.110}$$

The interaction with the environment causes so-called *quantum jumps*, and we imagine that by introducing detectors, we can continuously monitor these events. In an infinitesimal time step dt the evolution generated by the GKSL equation can be expanded as

$$e^{\hat{\mathcal{L}} dt} \hat{\rho}_{\mathrm{S}} = \hat{M}_0 \hat{\rho} \hat{M}_0^\dagger + \sum_{\alpha j \neq 0} \hat{M}_{\alpha j} \hat{\rho}_{\mathrm{S}} \hat{M}_{\alpha j}^\dagger, \tag{2.111}$$

where we can condition on the different measurement outcomes. By continuing the procedure for more time steps, the GKSL equation is unraveled. The first term in

Eq. (2.111) corresponds to a no jump evolution, while the second term gives the jump evolution [98]. The probability of seeing a jump j induced by reservoir α in a time step dt is given by

$$p_{\alpha j} = dt\,\mathrm{tr}\Big\{\hat{L}_{\alpha j}\hat{\rho}_{\mathrm{S}}\hat{L}_{\alpha j}^{\dagger}\Big\} \ll 1. \tag{2.112}$$

If this jump is observed in the time interval, the updated state conditioned on the outcome is given by

$$\hat{\rho}_{\mathrm{S}}^{c}(t+dt) = \frac{\hat{L}_{\alpha j}\hat{\rho}_{\mathrm{S}}^{c}(t)\hat{L}_{\alpha j}^{\dagger}}{\mathrm{tr}\Big\{\hat{L}_{\alpha j}\hat{\rho}_{\mathrm{S}}^{c}(t)\hat{L}_{\alpha j}^{\dagger}\Big\}}. \tag{2.113}$$

The unnormalized no-jump evolution is described by the non-Hermitian effective Hamiltonian.

$$\hat{\rho}_{\mathrm{S}}^{c}(t+dt) = \hat{\rho}_{\mathrm{S}}^{c}(t) - \frac{idt}{\hbar}(\hat{H}_{\mathrm{eff}}\hat{\rho}_{\mathrm{S}}^{c}(t) - \hat{\rho}_{\mathrm{S}}^{c}(t)\hat{H}_{\mathrm{eff}}^{\dagger}). \tag{2.114}$$

Thus, the system evolves during a sequence of time steps where either a jump is observed, causing a discontinuous update of the state, or no jump is observed, causing a smooth, continuous evolution. The no jump evolution contains both the unitary dynamics generated by the system Hamiltonian, but also effects of the environment, since the observation of no jumps carries information. This sequence of jumps and smooth evolution is called a quantum trajectory. A quantum jump trajectory is specified by an initial state $\hat{\rho}_{\mathrm{S}}(0)$ and a sequence of jumps j_q caused by reservoir α_q at times t_q

$$\varphi_t = \{\hat{\rho}_{\mathrm{S}}(0), (j_1, t_1, \alpha_1), \ldots, (j_N, t_N, \alpha_N)\}. \tag{2.115}$$

By using the subscript t, we emphasise that the trajectory also includes the time after the last jump. We define a classical random variable $d\breve{C}_{\alpha j}(\varphi_t)$ which takes the value 1 when a jump occurs due to the jump operator $\hat{L}_{\alpha j}$ and the value 0 otherwise in the time increment dt. With $p_{\alpha j}^{c}(t) = dt\,\mathrm{tr}\Big\{\hat{L}_{\alpha j}^{\dagger}\hat{L}_{\alpha j}\hat{\rho}_{\mathrm{S}}^{c}(t)\Big\}$, the evolution of the conditional density matrix can be written as a stochastic master equation [98]

$$\hat{\rho}_{\mathrm{S}}^{c}(t+dt) = \frac{1-\sum_{\alpha j\neq 0} d\breve{C}_{\alpha j}(\varphi_t)}{1-\sum_{\alpha j\neq 0} p_{\alpha j}^{c}(t)}\hat{M}_0\hat{\rho}_{\mathrm{S}}^{c}(t)\hat{M}_0^{\dagger} + \sum_{\alpha j\neq 0} d\breve{C}_{\alpha j}(\varphi_t)\frac{\hat{M}_{\alpha j}\hat{\rho}_{\mathrm{S}}^{c}(t)\hat{M}_{\alpha j}^{\dagger}}{p_{\alpha j}^{c}(t)}. \tag{2.116}$$

Since we assumed that the time steps are short we never observe more than one jump in a given step, meaning that $d\breve{C}_{\alpha j}(\varphi_t)d\breve{C}_{\beta k}(\varphi_t) = d\breve{C}_{\alpha j}(\varphi_t)\delta_{\alpha\beta}\delta_{jk}$ and $dtdC_{\alpha j}(\varphi_t) = 0$. With these properties Eq. (2.116) can be expanded to leading

order in dt [98]

$$\hat{\rho}_{\mathrm{S}}^{c}(t+dt)-\hat{\rho}_{\mathrm{S}}^{c}(t)=dt\hat{\mathcal{L}}\hat{\rho}_{\mathrm{S}}^{c}(t)+\sum_{\alpha j\neq 0}\left(d\breve{C}_{\alpha j}(\varphi_t)-dt\left\langle\hat{L}_{\alpha j}^{\dagger}\hat{L}_{\alpha j}\right\rangle_{c}\right)\times \\ \times\left(\frac{\hat{L}_{\alpha j}\hat{\rho}_{\mathrm{S}}^{c}(t)\hat{L}_{\alpha j}^{\dagger}}{\left\langle\hat{L}_{\alpha j}^{\dagger}\hat{L}_{\alpha j}\right\rangle_{c}}-\hat{\rho}_{\mathrm{S}}^{c}(t)\right), \tag{2.117}$$

where $\left\langle\hat{X}\right\rangle_{c}=\mathrm{tr}\left\{\hat{X}\hat{\rho}_{\mathrm{S}}^{c}(t)\right\}$. The time evolution of the unconditional density matrix is recovered by averaging over quantum trajectories. However, this is true for multiple different unravelings. Despite this, the transport of an observable which we are interested in describing, and its statistics, is dependent on whether the unraveling is, e.g., a jump or diffusive unraveling.

With this, we are now ready to tackle transport. Naturally, we can think of $d\breve{C}_{\alpha j}(\varphi_t)$ as the change in a counting observable $\breve{C}_{\alpha j}(\varphi_t)$ that counts the number of jumps in channel j of bath α that occurred in the time interval $[0,t]$. A generic counting observable is then defined by

$$\breve{X}(\varphi_t)=\sum_{\alpha j}x_{\alpha j}\breve{C}_{\alpha j}(\varphi_t), \tag{2.118}$$

where $x_{\alpha j}$ is a generalized charge associated with jump j induced by bath α. We point out that $\breve{X}(\varphi_t)$ is a classical stochastic variable which is generated by the underlying quantum dynamics. Since we are able to monitor the jumps, we are able to assign the charges we associate with each jump, allowing us to construct a variety of counting observables such as particle, energy, and entropy changes. This is, for instance, useful when defining quantities such as the dynamical activity, which will be commented on in more detail when we discuss full-counting statistics. The stochastic current associated with the counting observable is defined by

$$\breve{I}^{(X)}(\varphi_t)=\frac{d\breve{X}(\varphi_t)}{dt}. \tag{2.119}$$

Averaging over quantum trajectories, we find [98]

$$I^{(X)}(t)=\left\langle\breve{I}^{(X)}(\varphi_t)\right\rangle_{\varphi_t}=\frac{1}{dt}\sum_{\alpha j}x_{\alpha j}\left\langle d\breve{C}_{\alpha j}(\varphi_t)\right\rangle_{\varphi_t}=\sum_{\alpha j}x_{\alpha j}\,\mathrm{tr}\left\{\hat{L}_{\alpha j}^{\dagger}\hat{L}_{\alpha j}\hat{\rho}_{\mathrm{S}}(t)\right\}. \tag{2.120}$$

Quite intuitively, the average current at time t is given by the expected number of jumps weighted by their associated charge. Next, we show the expression for the

steady-state noise in the stochastic current [98]

$$S^{(X)} = \lim_{t\to\infty} \frac{d}{dt} \mathrm{Var}[\breve{X}(\varphi_t)]_{\varphi_t} = S^{(X)\mathrm{wh}} + S^{(X)\mathrm{co}}, \tag{2.121}$$

where the noise is divided into white noise

$$S^{(X)\mathrm{wh}} = \sum_{\alpha j} x_{\alpha j}^2 \, \mathrm{tr}\Big\{ \hat{L}_{\alpha j}^\dagger \hat{L}_{\alpha j} \hat{\rho}_{\mathrm{S}}(\infty) \Big\} \tag{2.122}$$

and colored noise stemming from correlations between jumps

$$S^{(X)\mathrm{co}} = 2 \int_0^\infty dt' \left(\mathrm{tr}\Big\{ \hat{\mathcal{I}}^{(X)} e^{\mathcal{L}t'} \hat{\mathcal{I}}^{(X)} \hat{\rho}_{\mathrm{S}}(\infty) \Big\} - \Big(I^{(X)} \Big)^2 \right). \tag{2.123}$$

Here $\hat{\mathcal{I}}^{(X)}$ is the current super operator

$$\hat{\mathcal{I}}^{(X)} \hat{\rho}_{\mathrm{S}}(t) = \sum_{\alpha j} x_{\alpha j} \hat{L}_{\alpha j} \hat{\rho}_{\mathrm{S}}(t) \hat{L}_{\alpha j}^\dagger, \tag{2.124}$$

related to the average current by $I^{(X)}(t) = \mathrm{tr}\Big\{ \hat{\mathcal{I}}^{(X)} \hat{\rho}_{\mathrm{S}}(t) \Big\}$. One might notice that this split of noise into white noise and colored noise is quite similar to the split of classical and quantum noise made for scattering theory, see Eq. (2.53). We will comment more on the similarities in Sec. 3.2.5.

2.6 Full-Counting-Statistics

We have now explored how scattering theory, the NEGF method, and quantum jumps can be used to describe the transport of quantities such as particles, energy, and entropy. We have derived currents that are related to the average amount of change in a quantity during transport. Furthermore, we discussed how these currents can display fluctuations on a fundamental level, leading to some variance in the amount of a quantity being transported. In fact, one can consider the full probability distribution of changes in a quantity during transport, resulting in a more detailed understanding of transport on a fluctuating level. Of course, studying these probability distributions and describing their general characteristics is a challenging task. One effective method for this is using Full-Counting-Statistics (FCS), which is also a powerful tool for calculating currents and their associated noise. We will begin by outlining the method in the context of quantum jumps and will then give a brief description of the method using the two-point-measurement scheme applicable to scattering theory and the NEGF method.

2.6.1 Full-Counting-Statistics and quantum jumps

We are interested in the probability distribution $P(x,t) = P(\breve{X}(t) = x)$, where x can take the values belonging to the set $\mathcal{X} = \{\mathcal{X}_i\}$. We can use this probability distribution to calculate the first and second moments

$$\begin{aligned} \left\langle \breve{X}(\varphi_t) \right\rangle_{\varphi_t} &= \sum_x xP(x,t) = \int_0^t dt' I^{(X)}(t'), \\ \mathrm{Var}[\breve{X}(\varphi_t)]_{\varphi_t} &= \sum_x \left(x - \left\langle \breve{X}(\varphi_t) \right\rangle_{\varphi_t} \right)^2 P(x,t). \end{aligned} \tag{2.125}$$

To describe $P(x,t)$, we follow Ref. [98] and introduce an x-resolved density matrix $\hat{\rho}_x(t)$, which is a unnormalized state associated with trajectories where we observe a net change x at time t. This unnormalized density matrix evolves according to

$$\hat{\rho}_x(t+dt) = \hat{M}_0 \hat{\rho}_x(t) \hat{M}_0^\dagger + \sum_{\alpha j \neq 0} \hat{M}_{\alpha j} \hat{\rho}_{x - x_{\alpha j}}(t) \hat{M}_{\alpha j}^\dagger. \tag{2.126}$$

From this, the sought-after probability distribution is given by $P(x,t) = \mathrm{tr}\{\hat{\rho}_x(t)\}$. The evolution of $P(x,t)$ is easier to describe by performing a Fourier transform

$$\hat{\rho}_\xi(t) = \sum_{x \in \mathcal{X}} e^{ix\xi} \hat{\rho}_x(t), \tag{2.127}$$

where ξ is a conjugate variable to x called a counting field. With the initial condition $\hat{\rho}_\xi(0) = \hat{\rho}(0)$, the evolution of $\hat{\rho}_\xi(t)$ is given by a tilted Liouvillian [98]

$$\begin{aligned} \frac{d}{dt}\hat{\rho}_\xi(t) &= \hat{\mathcal{L}}_\xi \hat{\rho}_\xi(t) \\ &= -\frac{i}{\hbar}[\hat{H}_\mathrm{S}, \hat{\rho}_\xi(t)] + \sum_{\alpha j} \left(e^{i\xi x_{\alpha j}} \hat{L}_{\alpha j} \hat{\rho}_\xi(t) \hat{L}_{\alpha j}^\dagger - \frac{1}{2}\{\hat{L}_{\alpha j}^\dagger \hat{L}_{\alpha j}, \hat{\rho}_\xi(t)\} \right). \end{aligned} \tag{2.128}$$

The solution of the tilted Liouvillian at time t is expressed as $\hat{\rho}_\xi(t) = e^{\hat{\mathcal{L}}_\xi t}\hat{\rho}(0)$. By performing an inverse Fourier transform, the original probability distribution is expressed as

$$\sum_{\mathcal{X}_i} \delta(x - \mathcal{X}_i) P(\mathcal{X}_i, t) = \int_{-\infty}^{\infty} \frac{d\xi}{2\pi} e^{-ix\xi} \,\mathrm{tr}\{\hat{\rho}_\xi(t)\}. \tag{2.129}$$

FCS allows us to calculate currents and their noise. This is done by the introduction of the characteristic function and the Cumulant Generating Function (CGF). The

characteristic function is defined as the Fourier transform of $P(x,t)$

$$C(\xi,t) = \mathrm{tr}\{\hat{\rho}_\xi(t)\} = \mathrm{tr}\Big\{e^{\hat{\mathcal{L}}_\xi t}\hat{\rho}(0)\Big\}, \tag{2.130}$$

which allows for the calculation of the n-th moment as

$$\Big\langle \breve{X}^n(\varphi_t)\Big\rangle_{\varphi_t} = \int dx \sum_{\mathcal{X}_i} \delta(x-\mathcal{X}_i)x^n P(\mathcal{X}_i,t) = (-i)^n \frac{\partial^n}{\partial \xi^n} C(\xi,t)\Big|_{\xi=0}. \tag{2.131}$$

We are, however, usually more interested in calculating the cumulants. For instance, the noise in a current is the time derivative of the second cumulant. To facilitate this, we define the cumulant generating function

$$\chi(\xi,t) = \ln C(\xi,t), \tag{2.132}$$

from which we calculate the n-th cumulant by differentiation

$$\Big\langle\Big\langle (\breve{X}(\varphi_t))^n\Big\rangle\Big\rangle_{\varphi_t} = (-i)^n \frac{\partial^n}{\partial \xi^n}\chi(\xi,t)\Big|_{\xi=0}. \tag{2.133}$$

While it is generally not easy to find a closed expression for the CGF, it is feasible in the context of quantum jumps in the long-time limit. By letting $\lambda_0(\xi)$ denote the eigenvalue of the tilted Liouvillian with the largest real part, the CGF in the long-time limit can be expressed as [98]

$$\chi(\xi,t) \approx \lambda_0(\xi)t, \tag{2.134}$$

where $\lambda_0(\xi)$ is the eigenvalue of the tilted Liouvillian with the largest real part [98]. To study the cross-correlation between different quantities, we can introduce a counting field for each quantity and study their joint probability distribution. Next, we discuss how FCS can be implemented in the context of the two-point-measurement scheme and applied to scattering theory and the NEGF method.

2.6.2 Full-Counting-Statistics and the two-point measurement scheme.

There exist multiple, inequivalent ways to implement FCS for quantum transport, which, in general, will give different values for higher-order moments. This is, e.g., the case when the Hamiltonian displays explicit time dependence. One approach is to include a coupling to a quantum system acting as a measurement device such that during the time evolution, e.g., the characteristic function is encoded in the state of the measurement device [58, 99–101]. Another approach is to use the Two-Point-Measurement (TPM) scheme, where one considers making a measurement

of an observable at an initial and final time, studying the statistics of the change. We will briefly outline the second approach based on Ref. [102]. We will first make a general consideration of the FCS and then apply it to the quantum transport setting.

We consider measuring an observable $\hat{X}(t) = \sum_{x_t} x_t \, |x_t\rangle\langle x_t| = \sum_{x_t} x_t \hat{\Pi}_{x_t}$ at time 0 and later on at time t. Denoting the initial state of the system as $\hat{\rho}(0)$, the probability of seeing the two measurement outcomes is given by

$$P(x_t, x_0) = \mathrm{tr}\Big\{\hat{\Pi}_{x_t}\hat{U}(t,0)\hat{\Pi}_{x_0}\hat{\rho}(0)\hat{\Pi}_{x_0}\hat{U}^\dagger(t,0)\hat{\Pi}_{x_t}\Big\}. \tag{2.135}$$

We define a classical random variable for the difference in the measurement outcomes $\Delta x = x_t - x_0$ with the probability distribution

$$P(\Delta x) = \sum_{x_t, x_0} \delta(\Delta x - (x_t - x_0)) P(x_t, x_0). \tag{2.136}$$

As in the previous section, the characteristic function is defined as the Fourier transform of $P(\Delta x)$

$$C(\xi) = \int_{-\infty}^{\infty} d\Delta x e^{i\xi\Delta x} P(\Delta x) = \sum_{x_t, x_0} e^{i\xi(x_t - x_0)} P(x_t, x_0), \tag{2.137}$$

along with the cumulant generating function

$$\chi(\xi) = \ln C(\xi). \tag{2.138}$$

Again n-th moment and cumulant are given by

$$\langle \Delta x^n \rangle = (-i)^n \frac{\partial^n}{\partial \xi^n} M(\xi)\Big|_{\xi=0}, \quad \langle\langle \Delta x^n \rangle\rangle = (-i)^n \frac{\partial^n}{\partial \xi^n} \chi(\xi)\Big|_{\xi=0}. \tag{2.139}$$

Since the initial measurement destroys any coherences in the $\hat{X}$-basis we introduce the diagonal density matrix $\bar{\hat{\rho}}(0) = \sum_{x_0} \hat{\Pi}_{x_0}\hat{\rho}(0)\hat{\Pi}_{x_0}$. We are able to rewrite

$$\sum_{x_0} e^{-i\xi x_0}\hat{\Pi}_{x_0}\hat{\rho}(0)\hat{\Pi}_{x_0} = e^{-i\xi\hat{X}(0)/2}\bar{\hat{\rho}}(0)e^{-i\xi\hat{X}(0)/2} \tag{2.140}$$

and express the characteristic function as

$$C(\xi) = \mathrm{tr}\{\hat{\rho}_\xi(t)\}, \quad \hat{\rho}_\xi(t) = \hat{U}_{\xi/2}(t,0)\bar{\hat{\rho}}(0)\hat{U}^\dagger_{-\xi/2}(t,0). \tag{2.141}$$

Here, we defined a tilted time evolution operator

$$\hat{U}_\xi(t,0) = e^{i\xi\hat{X}(t)}\hat{U}(t,0)e^{-i\xi\hat{X}(0)} = T_+\exp\left\{-\frac{i}{\hbar}\int_0^t dt'\hat{H}_\xi(t')\right\}, \tag{2.142}$$

and Hamiltonian

$$\hat{H}_\xi(t) = e^{i\xi\hat{X}(t)}\hat{H}(t)e^{-i\xi\hat{X}(t)} - \hbar\xi\frac{\partial}{\partial t}\hat{X}(t). \tag{2.143}$$

Next, we will apply this to a transport situation where we assume the standard Hamiltonian in Eq. (2.1) without any explicit time dependence. We will focus on the change of an observable $\hat{X}_\alpha$ of reservoir α, such as its energy or number of particles. Furthermore, we will assume that $[\hat{H}_\alpha, \hat{X}_\alpha] = 0$ to ensure that the change in $\hat{X}_\alpha$ can be attributed to its transport. This means that $\hat{X}_\alpha$ is diagonal in the eigenbasis $\hat{H}_\alpha = \sum_{\epsilon_\alpha}\epsilon_\alpha|\epsilon_\alpha\rangle\langle\epsilon_\alpha|$, i.e. we can write $\hat{X}_\alpha = \sum_{\epsilon_\alpha} x_{\epsilon_\alpha}|\epsilon_\alpha\rangle\langle\epsilon_\alpha|$. Moreover, we consider initial states which are diagonal in the measurement basis, i.e. $\hat{\rho}(0) = \bar{\hat{\rho}}(0)$. This is also one way to make a more formal definition of the type of quantity we consider in transport in scattering theory, with the generic current Eq. (2.45). The situation would, however, be more subtle if one were to consider entropy production since the von Neumann entropy is not given by a quantum observable. The characteristic function is given by [102]

$$C_\alpha(\xi) = \mathrm{tr}\Big\{e^{i\xi\hat{X}_\alpha^{\mathrm{H}}(t)}e^{-i\xi\hat{X}_\alpha}\hat{\rho}(0)\Big\}. \tag{2.144}$$

Since we are dealing with steady-state transport, it is more convenient to consider the scaled cumulant generating function

$$\bar{\chi}_\alpha(\xi) = \lim_{t\to\infty}\frac{1}{t}\ln C_\alpha(\xi). \tag{2.145}$$

In the context of scattering theory, one finds the Levitov formula [65, 99, 103] which can be expressed as [43]

$$\begin{aligned}\bar{\chi}_\alpha(\xi) = \mp\frac{1}{h}\int_0^\infty dE\ln\Big[\det\Big[1\mp\sum_{\alpha\neq\beta}s_{\alpha\beta}(E)s^\dagger_{\alpha\beta}(E)\times\\ \times\Big(F^\pm_{\alpha\beta}(E)(e^{-i\xi x_\alpha(E)}-1)+F^\pm_{\beta\alpha}(E)(e^{+i\xi x_\alpha(E)}-1)\Big)\Big]\Big].\end{aligned} \tag{2.146}$$

Here, the weight $x_\alpha(E)$ is determined by the eigenvalue x_{E_α}. For instance, if $\hat{X}_\alpha = \hat{H}_\alpha$ then $x_\alpha(E) = E$ and if $\hat{X}_\alpha = \hat{N}_\alpha$ then $x_\alpha(E) = 1$. The terms $F^\pm_{\alpha\beta}(E)(e^{-i\xi x_\alpha(E)}-1)$ and $F^\pm_{\beta\alpha}(E)(e^{i\xi x_\alpha(E)}-1)$ can be understood as counting the emission, and absorption of particles from and to reservoir α weighted by

$x_\alpha(E)$. With the formula

$$\frac{\partial}{\partial\xi}\ln[\det[A(\xi)]] = \mathrm{tr}\Big\{A^{-1}(\xi)\frac{\partial}{\partial\xi}A(\xi)\Big\}, \tag{2.147}$$

one can verify that the derivatives of Eq. (2.146) result in the correct expressions of the currents and noise for scattering theory. An interesting difference to the CGF for quantum jumps is that we do not have the freedom of choosing the combination of weights which appear in Eq. (2.146), these are instead set by commutation relations. Fundamentally, this difference stems from the fact that the output current is a classical stochastic object being continuously monitored in the context of quantum jumps, while in the TPM, one only measures at two different times.

Using the NEGF method for harmonic junctions, which we discussed in Sec. (2.4), one finds a similar expression for the scaled CGF [104]

$$\begin{aligned}\bar{\chi}_\alpha(\xi) = -\int\frac{d\omega}{4\pi}\ln\det\Big\{1-\sum_{\beta\neq\alpha}\mathbf{T}_{\alpha\beta}(\omega)\\ \times\Big[(e^{-i\xi x_\alpha(\omega)}-1)F^+_{\alpha\beta}(\omega)+(e^{i\xi x_\alpha(\omega)}-1)F^+_{\beta\alpha}(\omega)\Big]\Big\},\end{aligned} \tag{2.148}$$

where $\mathbf{T}_{\alpha\beta}(\omega)$ is defined in Eq. (2.84). In the case of energy transport where $\hat{X}_\alpha = \hat{H}_\alpha$ the weight is given by $x_\alpha(\omega) = \hbar\omega$. The noise in the energy current for bosonic linear transport is then calculated as

$$\begin{aligned}S^{(E)}_\alpha =&(-i)^2\frac{\partial^2\bar{\chi}_\alpha(\xi)}{\partial^2(\xi)}\bigg|_{\xi=0}\\ =&\int_0^\infty\frac{d\omega}{2\pi}\sum_{\beta\neq\alpha}D_{\alpha\beta}(\omega)(\hbar\omega)^2(F_{\alpha\beta}(\omega)+F_{\beta\alpha}(\omega))+\\ &+\int_0^\infty\frac{d\omega}{2\pi}\,\mathrm{tr}\left\{\left(\hbar\omega\sum_\beta\mathbf{T}_{\alpha\beta}(\omega)(f_\alpha(\omega)-f_\beta(\omega))\right)^2\right\}.\end{aligned} \tag{2.149}$$

In the case where one is interested in calculating the crosscorrelations between two quantities which commute at all times, $[\hat{X}^{\mathrm{H}}_\alpha(t),\hat{Y}^{\mathrm{H}}_\alpha(t)]$, one could use two counting fields [104, 105] and

$$C_\alpha(\xi_X,\xi_Y) = \mathrm{tr}\Big\{e^{i(\xi_X\hat{X}^{\mathrm{H}}_\alpha(t)+\xi_Y\hat{Y}^{\mathrm{H}}_\alpha(t))}e^{-i(\xi_X\hat{X}_\alpha+\xi_Y\hat{Y}_\alpha)}\hat{\rho}(0)\Big\}. \tag{2.150}$$

Our introduction of FCS has been rather brief; for applications and more details, see e.g. Refs. [65, 73, 95, 98, 99, 103, 104, 106, 107].

CHAPTER 3

Dynamical activity and thermokinetic uncertainty relations

Fluctuations in equilibrium systems are well studied with results such as the fluctuation-dissipation theorem and its many applications. However, when we want to use a device to perform a thermodynamic task such as extracting work or performing refrigeration, we need to consider an out-of-equilibrium situation. Fluctuations can still have an important effect on performance, but the well-known equilibrium relations are no longer universally applicable. The range of possible behaviours is much larger out of equilibrium. Nevertheless, the study of fluctuations in out-of-equilibrium systems has led to the discovery of the thermodynamic [25–28], kinetic [29–33] and combined thermokinetic uncertainty relations [34, 35], which constrain fluctuations even far from equilibrium. These relations are bounds on the precision of observables that are valid in a wide range of systems. In the thermodynamic uncertainty relation, precision is bounded by entropy production, quantifying irreversibility, whereas in the kinetic uncertainty relation, it is bounded by the *dynamical activity*, quantifying the intensity of the underlying process.

These uncertainty relations were originally discovered in classical systems, with the generalization to quantum systems being an ongoing research topic [40–49]. An unavoidable question arises when trying to find KURs for quantum systems: *what does it mean for a quantum system to be active?* Beyond weak coupling scenarios, there exist three main approaches to defining quantities playing the role of dynamical activity for quantum systems. In Refs. [47, 49, 76, 108, 109], the probability of measuring a change of an observable during a process has been used. Another approach is the use of information geometry and the Quantum Fisher

Information (QFI) [45, 46, 50, 110, 111]. A third definition aimed at quantum transport is based on the symmetrized autocorrelator of the coupling Hamiltonian between system and a reservoir [44]. A key distinction of the first approach is its reliance on measurement outcomes and classical stochastic trajectories in contrast to the latter two, which are formulated directly at the level of quantum dynamics.

In this thesis, we are interested in exploring definitions of quantum activity which we can apply to quantum systems on a fundamental level, meaning that we wish not to rely upon the classical random variables and their probability distributions, which are generated by measuring a quantum system. At present, it is not clear if these two latter definitions of activity in quantum systems are equivalent. If they are not, we would like to understand what the differences are, for example, what type of dynamics are counted towards how "active" a system is. Ideally, we would want a notion of quantum activity with a clear physical meaning, theoretical and practical implications, and that recovers the classical behaviour in the appropriate limit. Moreover, we would like to find a definition which we can use for fully unitary dynamics, where we are not able to describe the evolution of the system through stochastic trajectories. Connecting these different approaches is the main focus of this chapter.

The rest of this chapter will be structured in the following way: in Sec 3.1 we introduce the classical thermodynamic and kinetic uncertainty relations with a focus on classical continuous-time Markov processes. We then discuss dynamical activity in quantum systems weakly coupled to an environment, where the analogy to the classical setting is most direct in Sec 3.2.1. After this, we briefly review the first two generalizations of dynamical activity beyond weak coupling in Sec. 3.2.2.1 and Sec. 3.2.2.2. We will then tackle the challenge of connecting the correlation-based activity to the information geometric approach in Sec 3.2.3. We will do this by introducing a *partial dynamical activity* in Sec. 3.2.3.2. We will also discuss the definition of quantum dynamical activity in systems with time-dependent Hamiltonians, introducing a definition based on parametrizing the speed of a protocol in Sec. 3.2.4.3. Along the way, we will also highlight opportunities for deriving quantum generalizations of the kinetic uncertainty relations.

3.1 Thermodynamic and Kinetic uncertainty relations in classical Markovian systems

In this section, we will introduce the thermodynamic and kinetic uncertainty relations in the context of classical stochastic thermodynamics, specifically focusing on continuous-time Markov processes (CTMP).

Fig. 3.1 shows four pictures from a movie of milk being added to a glass of coffee. The panels are labelled (a-d) in chronological order of the original film, but even

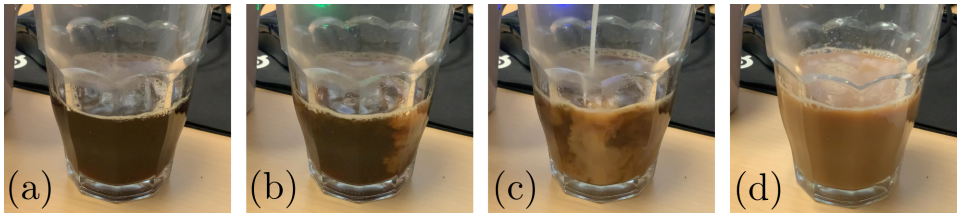

Figure 3.1: Frames from a video showing milk being added to a glass of coffee. The panels are labelled (a-d) in the chronological order of the film.

Figure 3.2: Frames from a video showing the oscillations of a watch movement. The panels are labelled (a-f) in the chronological order of the film.

if the labels were removed or the frames were placed in a non-chronological order, we would have little difficulty in determining the original sequence. This is due to the visible increase in entropy during the process. The glass of coffee starts in equilibrium in frame (a). Frames (b) and (c) display a nonequilibrium situation where milk has been added to the glass, but they have yet to fully mix. In frame (d), the coffee and milk have mixed and reached a new equilibrium. The irreversibility, or the breaking of time-reversal symmetry (TRS) and the production of (mixing) entropy, indicate that the system is out of equilibrium.

In Fig. 3.2, we show six frames from another movie that captures the oscillation of an escapement mechanism in a mechanical clock, in chronological order. This time, it is, however, substantially harder to tell a clear arrow of time in the sequence of events. Frame (a) looks almost identical to frame (f), and if we had placed the pictures in the wrong chronological order, it would be difficult to tell with this coarse-grained time. Even if we were to watch the full movie, it remains nontrivial to determine if it is played forward or backward. Only by closely observing the so-called pallet fork and the escape wheel can one deduce this. Is there still any entropy being produced by this clock? A running clock is, of course, a nonequilibrium system, and it is certainly breaking time-reversal symmetry. Indeed, a clock is producing entropy as it ticks. We have to keep winding the spring of a mechanical watch and changing the battery of a quartz clock. In fact, all of this energy is being dissipated just to produce a consistently timed sequence of ticks. In reality, no clock is perfectly stable and is subject to some fluctuations. We denote the expected number of ticks at time t by $\langle \text{ticks}(t) \rangle$ and its variance by $\text{Var}[\text{ticks}(t)]$. A "good" clock should make ticks with a high frequency, such that a user can time

events with good resolution, and the frequency should not fluctuate too much, otherwise the user cannot rely on the ticks. The performance can conveniently be characterized by the precision

$$\frac{\langle \text{ticks}(t) \rangle^2}{\text{Var}[\text{ticks}(t)]}. \tag{3.1}$$

It is a natural question to ask: how much more precise could this clock become if we kept improving its design? Furthermore, it turns out that there are a lot of things which "tick" in nature, for example, your heart, molecular machines, and motor proteins such as myosin. Molecular machines are crucial in the working of our bodies and cellular processes. Due to their small scale, they are affected by thermal fluctuations from their surrounding environment. Nevertheless, they still manage to accomplish directional processes, such as the movement of kinesin inside our cells or the rotary motor of a bacterial flagellum. Molecular machines essentially function by suppressing fluctuations through their chemical properties and energy expenditure, such as the usage of ATP [24, 112]. Simultaneously, they generate entropy by dissipating said energy. For example, if it were not for the ability of the myosin inside your muscles to generate directional movement, overcoming thermal fluctuations, you would not have been able to pick up this thesis or your cup of coffee in the morning. These are also important considerations when designing artificial molecular machines [113]. An important question arises: how, when and where do molecular machines expend energy and generate entropy in nature? Studying fluctuations can help in finding an answer.

These questions fall under the domain of stochastic thermodynamics, which deals with thermodynamics on the level of single fluctuating trajectories of small-scale systems. We can imagine modelling the behaviour of a molecular machine or some other fluctuating system by considering a coarse-grained, discrete set of states labelled by $k, l, \ldots$. We model the behaviour as a Markov jump process, where the rate of going from l to k due to transition m is denoted as W^m_{kl}. The probability to occupy state k at time t is denoted as $p_k(t)$ and evolves according to the master equation [114]

$$\dot{p}_k(t) = \sum_{m,l} (W^m_{kl} p_l(t) - W^m_{lk} p_k(t)). \tag{3.2}$$

To ensure the positivity and normalization of the probabilities, the rates must fulfill $W^m_{kl} \geq 0 \; \forall \; k \neq l$ and $\sum_k W^m_{kl} = 0$. A stochastic trajectory φ_t of the system states consists of N jumps occurring at times $t_1, \ldots, t_N$ due to transitions $m_1, \ldots, m_N$ and is given by

$$\varphi_t = \{k_0, (k_1, t_1, m_1), \ldots, (k_N, t_N, m_N)\}, \tag{3.3}$$

just as in Eq. (2.115). Here we include the subscript t to indicate that the trajectory also includes the time after the last jump. We also introduce the time-reversed path

$\tilde{\varphi}_t$, where the jumps occur in the opposite order. A stochastic counting observable is defined as a function of the trajectory,

$$\breve{X}(\varphi_t) = \sum_{m,kl} x_{kl}^m \breve{C}_{kl}^m(\varphi_t) = \sum_{q=1}^{N} x_{k_q k_{q-1}}^{m_q}, \tag{3.4}$$

where $\breve{C}_{kl}^m(\varphi_t)$ is a random variable, counting the number of transitions from l to k due to m during φ_t, and x_{kl}^m is a weight associated with the transition. An important example is the stochastic entropy production of the environment $\breve{\Sigma}_{\mathrm{E}}(\varphi_t)$, which, under the condition of Local Detailed Balance (LDB), has the weights

$$\sigma_{kl}^m = \ln\left[\frac{W_{kl}^m}{W_{lk}^m}\right] \tag{3.5}$$

and is expressed as

$$\breve{\Sigma}_{\mathrm{E}}(\varphi_t) = \sum_{m,kl} \sigma_{kl}^m \breve{C}_{kl}^m(\varphi_t). \tag{3.6}$$

The entropy change of the system is given by the change in Gibbs entropy, $\breve{\Sigma}_{\mathrm{S}}(\varphi_t) = -\ln p_{k_{\mathrm{N}}}(t_{\mathrm{N}}) + \ln p_{k_0}(t_0)$, which, together with Eq. (3.6), accounts for the total entropy change [24]

$$\breve{\Sigma}(\varphi_t) = \breve{\Sigma}_{\mathrm{E}}(\varphi_t) + \breve{\Sigma}_{\mathrm{S}}(\varphi_t). \tag{3.7}$$

Local detailed balance allows us to express the entropy production of the reservoirs in terms of the system trajectory, but is not trivially fulfilled and requires assumptions such as spatially separated equilibrium reservoirs with fast relaxation and weak coupling [115–118]. We label the probability of the system undergoing trajectory φ_t by $P(\varphi_t)$, letting us write the average of the counting observable as

$$\left\langle \breve{X}(\varphi_t) \right\rangle_{\varphi_t} = \int d\varphi_t P(\varphi_t) \breve{X}(\varphi_t). \tag{3.8}$$

Defining the escape rate

$$\lambda(k) = \sum_{m,l\neq k} W_{lk}^m \tag{3.9}$$

the probability of φ_t can be expressed as [24]

$$P(\varphi_t) = p_{k_0}(0) \left(\prod_{q=1}^{N} W_{k_q k_{q-1}}^{m_q} \right) \exp\left\{ -\int_0^t d\tau \lambda(k_\tau) \right\}. \tag{3.10}$$

The probability of the reversed path is given by

$$P(\tilde{\varphi}_t) = p_{k_N}(t_{\mathrm{N}}) \left(\prod_{q=1}^{N} W_{k_{q-1}k_q}^{m_q} \right) \exp\left\{ -\int_0^t d\tau \lambda(k_\tau) \right\}. \tag{3.11}$$

We can introduce an action $\mathcal{S}(\varphi_t) = -\ln P(\varphi_t) = -\frac{1}{2}\breve{\Sigma}(\varphi_t) + \breve{D}(\varphi_t)$, which weighs the probability according to

$$P(\varphi_t) = e^{-\mathcal{S}(\varphi_t)}. \tag{3.12}$$

Here $\frac{1}{2}\breve{\Sigma}(\varphi_t) = \frac{1}{2}\ln\frac{P(\varphi_t)}{P(\tilde{\varphi}_t)}$ is the part of the action which is antisymmetric in time, $\breve{\Sigma}(\varphi_t) = -\breve{\Sigma}(\tilde{\varphi}_t)$. Since we assumed LDB, the time antisymmetric part of $\mathcal{S}(\varphi_t)$ corresponds to the entropy change, which fulfills a detailed fluctuation theorem

$$\frac{P(\varphi_t)}{P(\tilde{\varphi}_t)} = e^{\breve{\Sigma}(\varphi_t)}, \tag{3.13}$$

implying the integral fluctuation theorem and the second law [16–24]

$$\left\langle e^{-\breve{\Sigma}(\varphi_t)} \right\rangle_{\varphi_t} = 1 \implies \left\langle \breve{\Sigma}(\varphi_t) \right\rangle_{\varphi_t} \geq 0. \tag{3.14}$$

The time-symmetric part

$$\breve{D}(\varphi_t) = -\frac{1}{2}\ln P(\varphi_t) P(\tilde{\varphi}_t), \tag{3.15}$$

is known as frenesy [118].

3.1.1 Thermodynamic uncertainty relations

Many interesting nonequilibrium systems could be modelled as a discrete-state continuous-time Markov process. Despite this richness, it turns out that there exist several bounds which constrain the possible behaviours of these systems and how precise a process can be. One such relation is the Thermodynamic Uncertainty Relation (TUR), which states that the precision of a counting observable is bounded by entropy change

$$\frac{\left(\left\langle \breve{X}(\varphi_t) \right\rangle_{\varphi_t} \right)^2}{\mathrm{Var}[\breve{X}(\varphi_t)]_{\varphi_t}} \leq \frac{1}{2} \left\langle \breve{\Sigma}(\varphi_t) \right\rangle_{\varphi_t}. \tag{3.16}$$

The TUR was first discovered in Ref. [25] with more general proofs for arbitrary connectivity and time-dependent protocols being presented in Refs. [25–28, 119]. The key assumptions for the validity of the TUR are the condition of LDB and that the observable has antisymmetric weights $x_{kl}^m = -x_{lk}^m$. The TUR has interesting applications both as a performance quantifier and as an inference tool. It states

that for a process to be precise, i.e. to occur with a strong directionality, it has to go along with a substantial average entropy production

$$\left\langle \breve{\Sigma}(\varphi_t) \right\rangle_{\varphi_t} = \int_0^t dt' \sum_{m,kl} \frac{1}{2} \ln \left[\frac{W_{kl}^m p_l(t')}{W_{lk}^m p_k(t')} \right] (W_{kl}^m p_l(t') - W_{lk}^m p_k(t')) \,. \tag{3.17}$$

Intuitively, for a process to occur with high precision, it must be probable, meaning the system together with the environment must end up in a higher entropy state. Moreover, by studying the precision of a counting observable, e.g. the motion of a motor protein, one is able to construct a nontrivial lower bound on the entropy production via (3.16). This strategy is referred to as thermodynamic inference [120]. In general, measuring the precision of a process is much easier than measuring the entropy production directly. Thus, the TUR allows us to identify where entropy is being produced, e.g., in cellular processes, and make a quantitative statement about its magnitude. Of course, it is highly nontrivial that one would be able to infer entropy production by such relatively simple means. This would apply to the ticks our clock from earlier, as long as it can be described as a Markov process fulfilling LDB at some fundamental level. TURs have also been investigated for Langevin dynamics and proven for the underdamped case. Interestingly, it turns out that a clock can break the TUR due to the effect of inertia in underdamped Langevin dynamics, violating LDB [121]. Moreover, LDB and the TUR can be violated due to the presence of e.g. magnetic fields [36, 122].

3.1.2 Kinetic uncertainty relations

While entropy and its change are central quantities in thermodynamics, they are not sufficient to fully describe a nonequilibrium system. This is illustrated by the blowtorch theorem, which originated in Ref. [123] and was expanded upon in Refs. [118, 124–126]. Although Ref. [124] offers a more precise mathematical formulation of the blowtorch theorem, its broader implication is that approaches based only on entropy production are incapable of identifying steady states in nonequilibrium systems. Without going into details it is possible to induce a steady-state distribution different from an equilibrium one just by changing the reactivity $r_{ij}^m = r_{ji}^m = \sqrt{W_{ji}^m W_{ij}^m}$ and leaving σ_{jk}^m unchanged [118, 124–126]. Since we can parametrize the transition rates as

$$W_{kl}^m = r_{kl}^m e^{\sigma_{kl}^m/2}, \tag{3.18}$$

this can be achieved by rescaling r_{ij}^m by a positive number. Indeed, the stochastic entropy production is left unchanged by this transformation since it only depends

on the ratios of the transition rates

$$\breve{\Sigma}(\varphi_t) = -\ln p_{k_N}(t_N) + \ln p_{k_0}(0) + \sum_{q=1}^{N} \ln \frac{W^{m_q}_{k_q k_{q-1}}}{W^{m_q}_{k_{q-1} k_q}}, \tag{3.19}$$

while the stochastic frenesy is affected since

$$\breve{D}(\varphi_t) = \int_0^t d\tau \lambda(k_\tau) - \sum_{q=1}^{N} \ln r^{m_q}_{k_q k_{q-1}}. \tag{3.20}$$

The entropy change plays a clear role in the action $\mathcal{S}(\varphi)$: it rewards paths with positive entropy change, and punishes those with negative. Frenesy, on the other hand, penalizes trajectories that spend long times in states with high escape rates via $\int_0^{t_M} dt \lambda_{k_t}$ and rewards paths which transition through links with large r^m_{ij}. Since kinetic aspects can play an important role in nonequilibrium, e.g. in linear response [118], they are interesting to investigate. Furthermore, the TUR is usually only a tight bound on precision close to equilibrium. Naturally, it seems like these kinetic aspects could play a key role in constraining the behavior of a system far from equilibrium. However, when formulating bounds on precision it is useful to consider a simpler frenetic observable. The stochastic dynamical activity is such a quantity. Defined as a counting observable where $x^m_{kl} = 1 \; \forall \; k, l, m$ it is symmetric with respect to time-reversal

$$\breve{\mathcal{A}}(\varphi_t) = \breve{\mathcal{A}}(\tilde{\varphi}_t) = \sum_{m,kl} \breve{C}^m_{kl}(\varphi_t) = \sum_{r=1}^{N} 1. \tag{3.21}$$

The dynamical activity $\breve{\mathcal{A}}(\varphi_t)$ counts the total number of jumps in a trajectory φ_t. Moreover, it bounds the precision of a process in a similar way to the entropy production in the Kinetic Uncertainty Relation (KUR)

$$\frac{\left(t\partial_t \left\langle \breve{X}(\varphi_t) \right\rangle_{\varphi_t}\right)^2}{\mathrm{Var}[\breve{X}(\varphi_t)]_{\varphi_t}} \leq \left\langle \breve{\mathcal{A}}(\varphi_t) \right\rangle_{\varphi_t}. \tag{3.22}$$

The KUR was first derived in Refs. [29, 30] with related bounds on the precision of clocks investigated in Refs. [40, 127]. Interestingly, the KUR does not rely on LDB, nor does it assume that the counting observable has antisymmetric weights. Moreover, the KUR often provides a tighter bound on precision compared to the TUR far from equilibrium, as kinetic aspects play a significant role in these regimes. However, close to equilibrium, the TUR generally becomes a tighter bound since thermal fluctuations, while not contributing to the change in $\breve{X}(\varphi)$, still influence

the dynamical activity. As shown in Ref. [127, 128], the KUR needs to be modified to be a tight bound in general. The KUR is a rather different statement compared to the TUR. It asserts that for a process to display high precision, there has to be a certain minimum average activity

$$\left\langle \breve{\mathcal{A}}(\varphi_t) \right\rangle_{\varphi_t} = \int_0^t dt' \sum_{m,kl,k\neq l} W_{kl}^m p_l(t). \tag{3.23}$$

We point out that the average dynamical activity can be understood as a sum of time-integrated probability fluxes out of the states.

3.1.3 Thermokinetic uncertainty relations

While the TUR and KUR capture different aspects of nonequilibrium dynamics, it has been found that they both are limiting cases of a deeper underlying bound known as the unified Thermodynamic Kinetic Uncertainty Relation (TKUR). Assuming LDB and antisymmetric weights as is done for the TUR, the TKUR states that

$$\begin{aligned} \frac{\left(t\partial_t \left\langle \breve{X}(\varphi_t) \right\rangle_{\varphi_t}\right)^2}{\mathrm{Var}[\breve{X}(\varphi_t)]_{\varphi_t}} &\leq \frac{\left\langle \breve{\Sigma}(\varphi_t) \right\rangle_{\varphi_t}}{2k_\mathrm{B}} \Xi\left[\frac{\left\langle \breve{\Sigma}(\varphi_t) \right\rangle_{\varphi_t}}{2k_\mathrm{B}\left\langle \breve{\mathcal{A}}(\varphi_t) \right\rangle_{\varphi_t}}\right] \leq \\ &\leq \min\left\{ \left\langle \breve{\Sigma}(\varphi_t) \right\rangle_{\varphi_t}/2k_\mathrm{B}, \left\langle \breve{\mathcal{A}}(\varphi_t) \right\rangle_{\varphi_t} \right\}. \end{aligned} \tag{3.24}$$

Here we introduced the functions $\Xi[x] \equiv x/\Omega^2[x]$ and $\Omega[x]$ as the inverse function of $x\tanh x$. The TKUR was derived in Ref. [34], and it describes how both irreversibility and activity limit precision. Moreover, it not only unifies these two different aspects, but it is also at least as tight as the TUR and KUR on their own, reducing to the TUR close to equilibrium and the KUR far from equilibrium. In the intermediate regime, it interpolates between the two bounds. This means that it is both a stricter limit on the performance of a device and a more powerful way to infer entropy production, given that one is able to measure the dynamical activity. Measuring the dynamical activity is, however, a non-trivial task generally.

3.1.4 TURs, KURs and TKURs in quantum systems

We have now discussed the role that fluctuations play in the thermodynamics of small-scale systems such as molecular machines and presented some of the general results bounding precision. Our discussion has been limited to classical systems. However, a focus of today's research is the construction of nanoscale and quantum technological devices. Due to their small size, these systems are also easily

influenced by fluctuations from their surrounding environment. Moreover, quantum devices, such as qubits, which utilize coherences, are more sensitive than their classical counterparts, as unwanted interactions with the environment can cause them to decohere. This is indeed one of the central difficulties in constructing quantum computers today. It is therefore desirable to understand how fluctuations affect quantum devices and how they can be controlled. While the study of small-scale thermodynamic devices might seem like a mostly theoretical endeavour, such devices have recently been realized, acting as engines [1] and as autonomous refrigerators used to perform on-chip cooling of qubits, allowing for faster resetting to the ground state in each round of computation [2, 3]. While the average cooling power of such a refrigerator is important, it may not be sufficient to accomplish its intended purpose. For example, imagine a refrigerator that provides a substantial but strongly fluctuating cooling power. Even if it, on average, removes heat from a working substance, it might at moments also inject heat, which, for a sensitive task, could make the device fail its intended goal. Therefore, precision is an important quantifier of performance.

Naturally, we would like to extend the TUR, KUR and TKURs to these sensitive quantum devices where fluctuations play an important role. This, however, turns out to be a challenge since quantum effects such as coherences lead to the violations of the classical bounds [4, 36–49]. On the one hand, this indicates that there are potential quantum advantages to achieving precision in a thermodynamic task. On the other hand, this spoils the applicability of the bounds for thermodynamic inference and as general trade-off relations for performance, which we would like to be able to rely upon. This motivates the recent investigation of the validity of the uncertainty relations and the generalization of them to quantum systems. This has been done using the GKSL equation in Refs. [40, 45, 46, 48], scattering theory in Refs. [36, 41, 42, 44] and methods based on repeated measurements in Refs. [47, 49].

As discussed in the chapter's introduction, this endeavour presents the question: *What does it mean for a quantum system to be "active"?* Depending on the system and regime, this question has clear answers, but in a general setting, it is not obvious at all, and there exist multiple different definitions of what a quantum dynamical activity is in the literature, based on, e.g. quantum jumps, Quantum Fisher Information (QFI) and correlators. Investigating the relation between different definitions and what their implications and potential problems are will be the focus of the rest of this chapter.

3.2 Dynamical activity in quantum systems

3.2.1 Dynamical activity as a jump rate — weak coupling

Before we make more general considerations of what a quantum mechanical notion of a dynamical activity might mean, we start by discussing the weak coupling regime, since it is analogous to the definition for a classical CTMP. As a starting point, we consider the GKSL equation (2.102) for which the average dynamical activity at time t is defined as

$$\mathcal{A}(t) = \int_0^t dt' \mathcal{K}(t'), \tag{3.25}$$

using the average dynamical activity rate

$$\mathcal{K}(t) = \sum_{\alpha,j} \mathrm{tr}\Big\{ \hat{L}^\dagger_{\alpha,j}(t) \hat{L}_{\alpha,j}(t) \hat{\rho}_\mathrm{S}(t) \Big\}. \tag{3.26}$$

We point out that this definition of activity is a directly measurable quantity, as one can, in principle, continuously monitor all jumps. Moreover, for the jump unravelling of the GKSL equation, we introduce a stochastic dynamical activity as a function of a quantum jump trajectory φ_t as defined in Eq. (2.115),

$$\breve{\mathcal{A}}(\varphi_t) = \sum_{\alpha j} \breve{C}_{\alpha j}(\varphi_t) = \sum_{q=1}^{N} 1. \tag{3.27}$$

This is a counting observable with all weights $x_{\alpha j} = 1$. It should, however, be noted that the dynamical activity is defined for the GKSL master equation, not the specific unravelling, as the same average dynamical activity is used for both jump and diffusive unravellings. Interestingly, by writing the reduced density matrix in its instantaneous diagonal basis $\hat{\rho}_\mathrm{S}(t) = \sum_n p_n(t) \left|n_t\right\rangle \left\langle n_t\right|$, the GKSL equation can be recast into the form of a classical rate equation,

$$\frac{d}{dt} p_n(t) = \frac{d}{dt} \left\langle n_t\right| \hat{\rho}_\mathrm{S}(t) \left|n_t\right\rangle = \sum_{\alpha,j,m} (w^{nm}_{\alpha j}(t) p_m(t) - w^{mn}_{\alpha j}(t) p_n(t)), \tag{3.28}$$

where the transition rates between the elements of the eigenbasis are defined by $w^{nm}_{\alpha j}(t) = \left| \left\langle n_t\right| \hat{L}_{\alpha,j}(t) \left|m_t\right\rangle \right|^2 \geq 0$ [129]. In this representation of the GKSL dynamics, the activity rate of Eq. (3.26) is expressed as [129]

$$\mathcal{K}(t) = \sum_{\substack{\alpha j, nm, \\ n \neq m}} w^{nm}_{\alpha j}(t) p_m(t), \tag{3.29}$$

which means that we can interpret the dynamical activity of Eq. (3.25) as the integrated sum of probability fluxes out of the populations in the instantaneous eigenbasis of $\hat{\rho}_{\mathrm{S}}(t)$, similarly to the classical case.

As a side note, if the jump operators fulfill LDB as defined in Eq. (2.105), the average entropy change of the system and the environment can be expressed as

$$\Sigma(t) = \int_0^t dt' \sigma(t'), \tag{3.30}$$

where the instantaneous entropy production rate is given by

$$\sigma(t) = \frac{1}{2} \sum_{\alpha j} \sum_{mn} \left(w_{\alpha j}^{nm}(t) p_m(t) - w_{\alpha \tilde{j}}^{mn} p_n(t) \right) \ln \left[\frac{w_{\alpha j}^{nm}(t) p_m(t)}{w_{\alpha \tilde{j}}^{mn}(t) p_n(t)} \right]. \tag{3.31}$$

This form of the entropy change highlights the fact that it is produced only through interaction with the environment [129]. Thus, both the dynamical activity and entropy production take a similar form to the case of the classical Markov process. However, it should be noted that since the rates $w_{\alpha j}^{mn}$ depend on the state $\hat{\rho}_{\mathrm{S}}(t)$, the dynamics are not that of a classical CTMP.

Naturally, the dynamical activity can also be defined through full counting statistics [98]. By setting all of the weights $x_{\alpha j} = 1$ in the tilted Liouvillian of Eq. (2.128), one counts all jumps, and the average dynamical activity is calculated as the first cumulant.

Another possible perspective on defining an activity-like quantity for quantum systems is through quantum noise. Consider a simple model of a Two-Level System (TLS) affected by a quantum noise source $\hat{B}$ with the corresponding Hamiltonian

$$\hat{H} = \frac{\hbar \varepsilon}{2} \hat{\sigma}_z + \hat{V} = \frac{\hbar \varepsilon}{2} \hat{\sigma}_z + \hat{\sigma}_x g \hat{B}, \tag{3.32}$$

where g is a parameter controlling the coupling strength. Assuming that the coupling is weak, the corresponding Fermi's golden rule transition rates of excitation $\Gamma_\uparrow$ and de-excitation $\Gamma_\downarrow$ are given by

$$\Gamma_\uparrow = \frac{g^2}{\hbar^2} S_{BB}^{\mathrm{ns}}[-\varepsilon], \quad \Gamma_\downarrow = \frac{g^2}{\hbar^2} S_{BB}^{\mathrm{ns}}[\varepsilon], \tag{3.33}$$

where $S_{BB}^{\mathrm{ns}}(\omega) = \int_{-\infty}^{\infty} dt e^{i\omega t} \langle \hat{B}^{\mathrm{H}}(t) \hat{B}^{\mathrm{H}}(0) \rangle$ [130]. Here we used $S_{BB}^{\mathrm{ns}}(\omega)$ to differentiate it from the symmetrized correlator, which we usually consider for transport. The positive and negative frequency parts of the spectral density of the quantum noise source correspond to the absorption and emission of energy by the noise source, respectively. If we assume that the TLS system starts out excited half the time and in its ground state the other half of the time, a natural notion of dynami-

cal activity rate in this weak coupling scenario would be given by the symmetrized spectral density, evaluated at $\omega = \varepsilon$,

$$\begin{aligned}\mathcal{K} &= \frac{1}{2}(\Gamma_\uparrow + \Gamma_\downarrow) \\ &= \frac{g^2}{2\hbar^2}(S^{\mathrm{ns}}_{BB}(\varepsilon) + S^{\mathrm{ns}}_{BB}(-\varepsilon)) = \frac{1}{2\hbar^2}\int_{-\infty}^{\infty} dt e^{i\varepsilon t}\langle\{g\hat{B}^{\mathrm{H}}(t), g\hat{B}^{\mathrm{H}}(0)\}\rangle.\end{aligned} \tag{3.34}$$

To clarify the role of the noise, we consider the case in which its source is from coupling to the position of a simple harmonic oscillator with spring constant k and mass m. The Hamiltonian of the oscillator can be expressed as

$$\hat{H} = \frac{1}{2m}\hat{p}^2 + \frac{1}{2}\Omega^2\hat{u}^2, \tag{3.35}$$

where $\hat{u} = \hat{x}\sqrt{m}$ is the rescaled position of the oscillator and $\Omega^2 = k/m$. The correlator in the rescaled position is given by

$$\langle\hat{u}(t)\hat{u}(0)\rangle = \frac{\hbar^2}{2\Omega}[f(\hbar\Omega)e^{i\Omega t} + [1 + f(\hbar\Omega)]e^{-i\Omega t}], \tag{3.36}$$

where $\hat{u}(t)$ is the operator in the Heisenberg picture, $f(\hbar\omega) = 1/(e^{\hbar\omega/k_{\mathrm{B}}T} - 1)$ is the Bose-Einstein distribution with temperature T [130]. The spectral density is given by

$$\begin{aligned}S^{\mathrm{ns}}_{uu}(\omega) &= \int_{-\infty}^{\infty} dt e^{i\omega t}\langle\hat{u}(t)\hat{u}(0)\rangle \\ &= \frac{\pi\hbar^2}{\Omega}[f(\hbar\Omega)\delta(\omega + \Omega) + [1 + f(\hbar\Omega)]\delta(\omega - \Omega)].\end{aligned} \tag{3.37}$$

Since the correlator of Eq. (3.36) is complex, the spectral density $S^{\mathrm{ns}}_{uu}(\omega)$ is not symmetric in frequency [130]. Moreover, the frequency asymmetry of the spectral function can be understood in the following way: the negative frequency part is a measure of the oscillator's ability to emit energy, and the positive frequency part is a measure of its ability to absorb energy through spontaneous and stimulated emission into the oscillator [130]. As a reminder, we point out that quantum noise also plays a role in the context of GKSL dynamics, as the rates entering the jump operators are set by the correlators of the bath operators, see e.g. Eq. (2.100).

There seems to be multiple potential avenues for defining a quantum dynamical activity beyond weak coupling. We could imagine trying to generalize the idea of counting the number of interactions with the environment, for example, using FCS, integrating a probability flux, or using quantum noise. In the coming section, we will explore some of these options.

3.2.2 Dynamical activity beyond weak coupling

The notion of activity as a series of jumps relies on measurement outcomes, which are essentially classical stochastic variables generated by underlying quantum dynamics. For GKSL dynamics, where the interaction between the environment and system is incoherent and weak, one is, in principle, able to observe these jumps continuously. As we will briefly discuss in Sec. 3.2.2.1, quantities based on measurement outcomes that can serve as dynamical activity can be found in more general situations. Both of these notions build upon classically registering definitive events that occurred, i.e. measurement outcomes.

When trying to find a meaningful notion of activity beyond this regime, the nature of quantum mechanics complicates the picture. In general, for fully unitary evolution, we can not treat dynamics as some definitive classical trajectory, e.g., in phase space or between energy eigenstates, since observing the system collapses the wavefunction. The picture becomes further complicated when we think about what type of evolution should be included in a general definition of activity. Is, for example, the rotating phase of an energy eigenstate some sort of activity? Could we think about some type of meaningful activity associated with, e.g., Rabi oscillations? We cannot expect to rely on such a classical notion of activity as a jump rate if we study, e.g., coherent energy transfer between two qubits. However, this might be an interesting situation to understand how precision in energy transfer is limited.

3.2.2.1 Dynamical activity based on measurement outcomes

In this section, we will give a brief recap of how a probability distribution, e.g. generated by measuring a quantum system, can be used to quantify activity [47, 49, 76, 108, 109]. We consider the probability $P(\varphi)$ of observing a trajectory of length N, $\varphi = \{\varphi_1, \varphi_2, \dots, \varphi_N\}$, which could, e.g., be a sequence of measurement outcomes. In addition, we consider a monitored quantity which takes a value for each of the measurement outcomes $\breve{X}(\varphi) = \{\breve{x}(\varphi_1), \breve{x}(\varphi_2), \dots, \breve{x}(\varphi_N)\}$. We are interested in the change of the monitored quantity and define a random variable $\Delta\breve{X}_N(\varphi) = \breve{x}(\varphi_N) - \breve{x}(\varphi_1)$. Moreover, we define a subset of trajectories where we observe no change in $\breve{X}(\varphi)$, $\Upsilon_N = \{\varphi | \breve{x}(\varphi_1) = \breve{x}(\varphi_q) \forall q \in 1, \dots, N\}$. The probability of observing such a trajectory is given by

$$P_0(N) = \sum_{\varphi \in \Upsilon_N} P(\varphi) \leq 1. \tag{3.38}$$

Interestingly, $P_0(N)$ has been shown to enter general bounds on fluctuations in Refs. [47, 49, 76, 108, 109]. For example, by using the Cauchy-Schwarz inequality,

one finds a bound on precision [47, 49, 76, 108]

$$\frac{\left\langle \Delta \breve{X}_N(\varphi) \right\rangle_\varphi^2}{\mathrm{Var}[\Delta \breve{X}_N(\varphi)]_\varphi} \leq \frac{1 - P_0(N)}{P_0(N)} = \frac{1}{P_0(N)} - 1. \tag{3.39}$$

Since $P_0(N)$ represents the probability that the monitored quantity remains unchanged, it effectively quantifies the inactivity of a process with respect to $\breve{X}(\varphi)$. Consequently, the expression $(1/P_0(N)) - 1$ can be interpreted as quantifying the activity at the level of the classical stochastic process induced by the measurements. Therefore, it is explicitly dependent on the measurements.

This discussion has been rather abstract, and we point the reader towards Ref. [49] for more concrete examples of how these concepts can be applied to a quantum system interacting with an environment. Moreover, in Ref. [49] $1-P_0(N)$ was connected to the dynamical activity (3.25), when $\breve{X}_N(\varphi)$ is used to construct a counting observable in the context of the GKSL equation. By considering a short time window Δt, for a jump unravelling of the GKSL equation, it follows that [49]

$$1 - P_0(N) = \Delta t \sum_k \mathrm{tr}\left\{ \hat{L}_k^\dagger \hat{L}_k \hat{\rho}_\mathrm{S} \right\} + \mathcal{O}(\Delta t^2), \tag{3.40}$$

and $1/P_0(N) - 1 = \Delta t \sum_k \mathrm{tr}\left\{ \hat{L}_k^\dagger \hat{L}_k \hat{\rho}_\mathrm{S} \right\} + \mathcal{O}(\Delta t^2)$. Thus, in the short time limit, Eq. (3.39) reproduces the classical KUR for a jump unravelling. Consequently, a drawback of using $1 - P_0(N)$ to quantify activity is that in the long-time limit, $P_0(N)$ is expected to decay exponentially, meaning that a bound like Eq. (3.39) becomes trivial.

As a side note, we point out the opportunity to adapt the concept of frenesy (3.15), which we discussed in Sec. 3.1.2, to a classical stochastic process generated by measuring a quantum system. As for the classical case, we can write the probability of observing a trajectory in terms of an action $\mathcal{S}(\varphi)$

$$P(\varphi) = e^{\ln P(\varphi)} = e^{-\mathcal{S}(\varphi)}, \quad \mathcal{S}(\varphi) = -\breve{\mathcal{S}}^-(\varphi) + \breve{D}(\varphi). \tag{3.41}$$

In analogy with the classical case, we have divided the action into a term that is anti-symmetric with respect to the time-reversal of the trajectory $\breve{\mathcal{S}}^-(\varphi) = -\breve{\mathcal{S}}^-(\tilde{\varphi}) = \frac{1}{2} \ln P(\varphi)/P(\tilde{\varphi})$ and a symmetric part $\breve{D}(\varphi) = \breve{D}(\tilde{\varphi}) = -\frac{1}{2} \ln P(\varphi)P(\tilde{\varphi})$ similar to Eq. (3.15). For a stochastic process describing a classical system, the stochastic entropy production is often given by $\breve{\Sigma}(\varphi) = \ln P(\varphi)/\widetilde{P}(\tilde{\varphi})$, where $\widetilde{P}(\varphi)$ is the probability of observing φ in a backward process. In Sec. 3.1, we discussed classical CTMPs under the assumption of local detailed balance and no driving $\widetilde{P}(\tilde{\varphi}) = P(\tilde{\varphi})$, meaning that the time-antisymmetric part of the action indeed corresponded to the physical entropy production (3.7). In general, $\breve{\mathcal{S}}^-(\varphi) \neq -\breve{\Sigma}(\varphi)/2$

due to e.g. driving, magnetic fields or even quantum effects [49]. While it might be the case that a decomposition $\ln P(\varphi) = \frac{1}{2}\ln P(\varphi)/\widetilde{P}(\tilde{\varphi}) + \frac{1}{2}\ln P(\varphi)\widetilde{P}(\tilde{\varphi})$ is more useful when connecting to the physical entropy production of a system this decomposition will not have the same (anti-)symmetry properties with respect to reversal of the trajectory.

We identify the time-symmetric part of the action $\breve{D}(\varphi)$ as frenesy. Although this frenesy is defined at the level of a classical probability distribution, the distribution itself can be generated by measuring a quantum system. This means, for instance, that $\breve{D}(\varphi)$ can be used as a frenesy in the context of quantum jumps by letting $P(\varphi)$ be the probability of observing a specific quantum trajectory (2.115). In classical stochastic thermodynamics, frenesy plays a role in, e.g. out-of-equilibrium linear response [118]. Whether frenesy for quantum systems can be applied in a similar manner remains an open question for future research.

Next, we move on to discussing definitions of dynamical activity made directly at the quantum level.

3.2.2.2 Dynamical activity for quantum transport from correlators

An additional definition of dynamical activity was recently introduced in Ref. [44] in the context of quantum transport. For the time-independent case of the transport Hamiltonian (2.1), the authors defined a generalized dynamical activity rate with respect to reservoir α as the symmetrized autocorrelator of the interaction Hamiltonian

$$\mathcal{K}_\alpha(t) = \frac{1}{2\hbar^2}\int_{-t}^{t} dt' \langle\langle \{\hat{V}_\alpha^{\mathrm{H}}(t), \hat{V}_\alpha^{\mathrm{H}}(t+t')\}\rangle\rangle, \tag{3.42}$$

where $\langle\langle \hat{X}\hat{Y}\rangle\rangle = \langle \hat{X}\hat{Y}\rangle - \langle\hat{X}\rangle\langle\hat{Y}\rangle$ and $\langle\hat{X}\rangle = \mathrm{tr}\Big\{\hat{X}\hat{\rho}(0)\Big\}$. Notice that this would correspond to the time derivative of the dynamical activity $\partial_t \mathcal{A}(t) = \mathcal{K}(t)$. In this thesis, we will refer to Eq. (3.42) as the correlator-based definition of the dynamical activity (rate). In Ref. [44], the authors investigated this definition in the context of fermionic non-interacting transport through quantum dots using the NEGF method and scattering theory. A general formula for non-interacting electronic transport through quantum dots was found in the steady state. In Appendix A we derive the corresponding formula for bosonic harmonic networks. This results in an expression

$$\begin{aligned}
\mathcal{K}_\alpha &= \lim_{t\to\infty} \mathcal{K}_\alpha(t) \\
&= \int_0^\infty \frac{d\omega}{2\pi}\,\mathrm{tr}\left\{4\mathbf{T}_{\alpha\alpha}(\omega) - \left(\sum_\beta \mathbf{T}_{\alpha\beta}(\omega)\right)^2\right\} F^+_{\alpha\alpha}(\omega) \\
&+ \int_0^\infty \frac{d\omega}{2\pi}\sum_{\beta\neq\alpha}\mathrm{tr}\{\mathbf{T}_{\alpha\beta}(\omega)\}(F^+_{\alpha\beta}(\omega) + F^+_{\beta\alpha}(\omega)),
\end{aligned} \tag{3.43}$$

where the main difference to the fermionic result presented in Ref. [44], is the expected replacement of the factors $F^{-}_{\alpha\beta}(\omega) \mapsto F^{+}_{\alpha\beta}(\omega)$ along with the bosonic average occupations. Furthermore, in Ref. [44] it was shown that for a Hamiltonian quadratic in ladder operators, Eq. (3.42) recovers the standard rate of jumps (3.26) for GKSL dynamics. Additionally, in Appendix B, we show that Eq. (3.42) generally recovers the standard definition of activity employed for the GKSL equation, after applying the Born, Markov and secular approximations. This derivation also applies to the case where there are interactions, i.e. when the Hamiltonian is not strictly quadratic. While it is clearly a good sign that Eq. (3.42) recovers the standard definition for GKSL dynamics, other definitions achieve similar results by e.g. recovering the classical activity, as demonstrated in Refs. [46, 50]. Furthermore, if we want to make a definition of quantum dynamical activity, we should have a clear physical picture in mind of what we mean by this. While Eq. (3.42) can be interpreted in terms of quantum jumps and quantum noise in the weak coupling limits, we cannot easily extrapolate this same meaning to strong coupling, where transport is coherent. We will establish an information geometric interpretation of Eq. (3.42) in Sec. 3.2.3.3.

3.2.3 Information geometric approach to dynamical activity

Another approach to defining activity, which we have only briefly mentioned until now, is the use of classical and quantum Fisher information and geometry. The QFI has previously been used to define a quantum dynamical activity in Refs. [46, 50] in the context of GKSL dynamics. These definitions recover the classical dynamical activity in Eq. (3.25) when the GKSL equation reduces to a classical rate equation, but contain additional quantum contributions in the general case. In particular, for a quantum state $\hat{\rho}(t)$ at time t, a quantum dynamical activity was defined as $t^2\mathcal{F}_{tt}(t)$, where $\mathcal{F}_{tt}(t)$ is the QFI with respect to time in Ref. [46]. In Ref. [50], an equivalent definition was used by considering $\hat{\rho}(t\theta)$, and the QFI for θ, $\mathcal{F}_{\theta\theta}(t) = t^2\mathcal{F}_{tt}(t)$. The classical and quantum Fisher information will be introduced in more detail in Sec. 3.2.3.1.

Moreover, in Ref. [40], where KURs for GKSL dynamics were derived, it was shown that the standard dynamical activity Eq. (3.25) could be calculated through a specific QFI in the steady-state limit. In the coming section, we will define a partial "dynamical activity" for a quantum system from a microscopic Hamiltonian using the QFI. We will show that, in special cases, this definition recovers the correlator-based definition of Eq. (3.42), and in general, the dynamical activity for GKSL dynamics in the steady state. An advantage of using the QFI is that it has a geometric interpretation since it is equivalent to the Bures metric. Moreover, we will also connect this definition to the QFI-based definitions of Refs. [46, 50] with a focus on interpreting what such a definition of activity would mean for a closed quantum system, identifying some potential conceptual issues. These issues are

especially prevalent when the Hamiltonian has explicit time dependence, something which was not the focus of Refs. [46, 50]. While doing this, we will also investigate what types of limits on precision these definitions of quantum dynamical activity give.

3.2.3.1 Classical and quantum Fisher information

Before we use the QFI to define a quantum mechanical notion of dynamical activity, we will give a quick walkthrough of the classical and quantum Fisher information. Let us consider a classical probability distribution $\{p(x|\mathbf{R})\}$, $\int dx p(x|\mathbf{R}) = 1$ for a random variable $\check{X}$. Here $p(x|\mathbf{R})$ is the conditional probability for the outcome x and $\mathbf{R} = [R_1, \dots, R_a, \dots]^T$ is a tuple of real numbers, parameterizing $p(x|\mathbf{R})$. The Classical Fisher Information (CFI) matrix is defined as

$$\mathcal{F}^{\mathrm{cl}}_{ab} = \int dx \frac{\partial^2 \ln p(x|\mathbf{R})}{\partial_{R_a}\partial_{R_b}} p(x|\mathbf{R}) = \int dx \frac{(\partial_{R_a} p(x|\mathbf{R}))(\partial_{R_b} p(x|\mathbf{R}))}{p(x|\mathbf{R})}. \tag{3.44}$$

If the random observable has discrete outcomes, the integration is replaced by a summation. Moreover, the CFI matrix introduces a Riemannian metric on a smooth statistical manifold, defining a distance between two probability distributions. The amount of information carried by $\check{X}$ about the parameter R_a is quantified by the CFI

$$\mathcal{F}^{\mathrm{cl}}_{aa} = \int dx \frac{(\partial_{R_a} p(x|\mathbf{R}))^2}{p(x|\mathbf{R})}. \tag{3.45}$$

To illustrate the CFI, let us consider the path probability $P(\varphi_t, \theta)$ of a classical CTMP in Eq. (3.10) when we rescale the transition rates uniformly by

$$W^m_{kl}(\theta) = (1+\theta) W^m_{kl}, \tag{3.46}$$

where $\theta \geq 0$. The original dynamics are recovered when we take $\theta \to 0$. By calculating the CFI in this limit, we find [30]

$$\lim_{\theta\to 0} \mathcal{F}^{\mathrm{cl}}_{\theta\theta}(t) = \int_0^t dt' \sum_{m,kl,k\neq l} W^m_{kl} p_l(t) = \left\langle \check{\mathcal{A}}(\varphi_t) \right\rangle_{\varphi_t}. \tag{3.47}$$

Here, the subscript θ means that the derivative is taken with respect to θ in the CFI (3.45). This particular parametrization of the CFI yields the average dynamical activity, and it provides a geometric interpretation: the classical dynamical activity is a measure of the speed of the evolution. Moreover, for time-independent rates, rescaling them corresponds exactly to letting the system evolve for a longer time $(1+\theta)t$, which in turn implies the KUR of Eq. (3.22) via the classical Cramér-

Rao bound when $\theta \to 0$

$$\frac{\left(\partial_\theta \left\langle \breve{X}(\varphi_t)\right\rangle_{\varphi_t}\right)^2}{\mathrm{Var}[\breve{X}(\varphi_t)]_{\varphi_t}} \leq \mathcal{F}^{\mathrm{cl}}_{\theta\theta}(t) \implies \frac{\left(t\partial_t \left\langle \breve{X}(\varphi_t)\right\rangle_{\varphi_t}\right)^2}{\mathrm{Var}[\breve{X}(\varphi_t)]_{\varphi_t}} \leq \left\langle \breve{\mathcal{A}}(\varphi_t)\right\rangle_{\varphi_t}. \tag{3.48}$$

This is indeed the fundamental principle behind the original KUR of Ref. [30], which, however, was derived using the Dechant-Sasa inequality [30].

We now come to the quantum case. When considering a probability distribution generated by performing measurements on a quantum system, a complication arises: measuring in different bases generates different classical probability distributions and hence different CFI. Measuring in one basis might yield a random variable which carries a lot of information about an unknown parameter, while another could yield very little information. To circumvent this issue the quantum Fisher information is introduced by maximizing the CFI over positive operator-valued measures [131]. Instead of the probability distribution $p(x|R)$, we now consider a density operator $\hat{\rho}(\mathbf{R})$ that is parametrized by a tuple of real numbers $\mathbf{R}$. The Bures distance $D_{\mathrm{B}}(\hat{\rho}_1, \hat{\rho}_2)$ between two density matrices $\hat{\rho}_1$ and $\hat{\rho}_2$ is defined using the fidelity as

$$D^2_{\mathrm{B}}(\hat{\rho}_1, \hat{\rho}_2) = 2 - 2\sqrt{\mathrm{Fid}(\hat{\rho}_1, \hat{\rho}_2)}, \quad \mathrm{Fid}(\hat{\rho}_1, \hat{\rho}_2) = \left(\mathrm{tr}\left\{\sqrt{\sqrt{\hat{\rho}_1}\hat{\rho}_2\sqrt{\hat{\rho}_1}}\right\}\right)^2. \tag{3.49}$$

If the rank of $\hat{\rho}(\mathbf{R})$ is unchanged when varying $\mathbf{R}$, the infinitesimal Bures distance is related to the Quantum Fisher Information (QFI) matrix $\mathcal{F}_{ab}$

$$D^2_{\mathrm{B}}(\hat{\rho}(\mathbf{R}), \hat{\rho}(\mathbf{R} + d\mathbf{R})) = \frac{1}{4}\sum_{ab} \mathcal{F}_{ab} dR_a dR_b. \tag{3.50}$$

The QFI matrix is defined as [132, 133]

$$\mathcal{F}_{ab} = \frac{1}{2}\,\mathrm{tr}\Big\{\rho(\mathbf{R})(\hat{\mathfrak{L}}_a\hat{\mathfrak{L}}_b + \hat{\mathfrak{L}}_b\hat{\mathfrak{L}}_a)\Big\}, \tag{3.51}$$

using the Symmetric Logarithmic Derivative (SLD) for the parameter R_a, which is implicitly defined through

$$\partial_{R_a}\hat{\rho}(\mathbf{R}) = \frac{1}{2}(\hat{\rho}(\mathbf{R})\hat{\mathfrak{L}}_a + \hat{\mathfrak{L}}_a\hat{\rho}(\mathbf{R})). \tag{3.52}$$

Thus, the QFI matrix is equivalent to the Bures metric $g_{ab} = \mathcal{F}_{ab}/4$. The quantum Fisher information is defined from the QFI matrix as

$$\mathcal{F}_{aa} = \mathrm{tr}\Big\{\rho(\mathbf{R})\hat{\mathfrak{L}}_a\hat{\mathfrak{L}}_a\Big\}. \tag{3.53}$$

The QFI originated from the field of quantum metrology, where it limits the precision of parameter estimation via the Quantum Cramér-Rao Bound (QCRB). Fundamentally, this stems from the fact that precision in parameter estimation is a matter of distinguishability, which is related to the distance between states [134]. The QFI is a measure of how strongly a parameter is encoded in a state, i.e., how different a state is if we make a small change to the parameter. Of course, the sensitivity to a parameter of any classical probability distribution derived from a quantum state will be limited by this underlying distinguishability. Moreover, the QFI also plays an important role in quantum phase transitions, thermometry and quantum thermodynamics, see e.g. Refs. [134–142].

To demonstrate the QFI and its role in quantum thermodynamics, let us pick a simple example by considering a Gibbs state

$$\hat{\rho}(T,\mu) = \frac{e^{-(\hat{H}-\mu\hat{N})/k_\mathrm{B}T}}{\mathrm{tr}\left\{e^{-(\hat{H}-\mu\hat{N})/k_\mathrm{B}T}\right\}}, \tag{3.54}$$

where the Hamiltonian and number operator commute $[\hat{H},\hat{N}]=0$. Here we use the temperature T and the chemical potential μ as parameters for the QFI. The derivatives with respect to the T and μ are calculated by

$$\begin{aligned}\partial_T\hat{\rho}(T,\mu) &= \frac{1}{k_\mathrm{B}T^2}\left(\left\langle\hat{H}-\mu\hat{N}\right\rangle - (\hat{H}-\mu\hat{N})\right)\hat{\rho}(T,\mu),\\ \partial_\mu\hat{\rho}(T,\mu) &= \frac{1}{k_\mathrm{B}T}\left(-\left\langle\hat{N}\right\rangle + \hat{N}\right)\hat{\rho}(T,\mu).\end{aligned} \tag{3.55}$$

Since $[\hat{\rho}(T,\mu),\hat{H}]=[\hat{\rho}(T,\mu),\hat{N}]=0$, we find simple expressions for the SLDs

$$\begin{aligned}\hat{\mathfrak{L}}_T &= \frac{1}{k_\mathrm{B}T^2}\left(\left\langle\hat{H}-\mu\hat{N}\right\rangle - (\hat{H}-\mu\hat{N})\right),\\ \hat{\mathfrak{L}}_\mu &= \frac{1}{k_\mathrm{B}T}\left(-\left\langle\hat{N}\right\rangle + \hat{N}\right).\end{aligned} \tag{3.56}$$

Inserting this into the definition of the QFI, we find the expressions [134, 136, 138, 139, 141, 142]

$$\begin{aligned}\mathcal{F}_{TT} &= \frac{1}{k_\mathrm{B}^2T^4}\langle\langle(\hat{H}-\mu\hat{N})^2\rangle\rangle = \frac{1}{k_\mathrm{B}T^2}\frac{\partial}{\partial T}\left\langle\hat{H}-\mu\hat{N}\right\rangle,\\ \mathcal{F}_{\mu\mu} &= \frac{1}{k_\mathrm{B}^2T^2}\langle\langle\hat{N}^2\rangle\rangle = \frac{1}{k_\mathrm{B}T}\frac{\partial}{\partial\mu}\left\langle\hat{N}\right\rangle.\end{aligned} \tag{3.57}$$

Hence, we see that the QFI for temperature and chemical potential is related to the susceptibilities, e.g. for $\mu=0$, the QFI for temperature is proportional to the specific heat $\mathcal{F}_{TT}=(\partial_T\langle\hat{H}\rangle)/k_\mathrm{B}T^2$. This example of the QFI is unrelated to the

definition of dynamical activity.

However, in general, for a mixed state, the SLDs do not take such a simple expression, and we cannot easily represent the QFI in terms of standard quantities. Using the spectral decomposition of a density matrix $\hat{\rho}(\mathbf{R}) = \sum_{i=0}^{d-1} p_i(\mathbf{R}) \left|\psi_i(\mathbf{R})\right\rangle \left\langle\psi_i(\mathbf{R})\right|$ the QFI matrix (3.51) can be expressed as [134]

$$\mathcal{F}_{ab} = \sum_{\substack{i,j=0,\\ p_i+p_j\neq 0}}^{d-1} \frac{2\,\mathrm{Re}[\langle\psi_i(\mathbf{R})|\left(\partial_{R_a}\hat{\rho}(\mathbf{R})\right)|\psi_j(\mathbf{R})\rangle\langle\psi_j(\mathbf{R})|\left(\partial_{R_b}\hat{\rho}(\mathbf{R})\right)|\psi_i(\mathbf{R})\rangle]}{p_i(\mathbf{R}) + p_j(\mathbf{R})}. \tag{3.58}$$

If the state is pure $\hat{\rho}(\mathbf{R}) = \left|\psi(\mathbf{R})\right\rangle \left\langle\psi(\mathbf{R})\right|$, the situation is simplified as the Bures metric reduces to the Fubini-Study metric and the QFI matrix becomes

$$\mathcal{F}_{ab} = 4\,\mathrm{Re}[\langle\partial_{R_a}\psi(\mathbf{R})|\partial_{R_b}\psi(\mathbf{R})\rangle - \langle\partial_{R_a}\psi(\mathbf{R})|\psi(\mathbf{R})\rangle\langle\psi(\mathbf{R})|\partial_{R_b}\psi(\mathbf{R})\rangle]. \tag{3.59}$$

Before we move on to discussing activity, we list some general properties of the QFI matrix $\mathcal{F}$ which we will use later on [134].

- $\mathcal{F}_{ab} = \mathcal{F}_{ba}$.
- $\mathcal{F}$ is positive semi-definite.
- $\mathcal{F}(\rho) = \mathcal{F}(\hat{U}\rho\hat{U}^\dagger)$ for a unitary $\hat{U}$ which is independent of $\mathbf{R}$.
- $\mathcal{F}$ is convex: $\mathcal{F}(p\hat{\rho}_1 + (1-p)\hat{\rho}_1) \leq p\mathcal{F}(\hat{\rho}_1) + (1-p)\mathcal{F}(\hat{\rho}_2)$ for $p \in [0,1]$.
- $\mathcal{F}$ is monotonic under a CPTP map ϕ, $\mathcal{F}(\hat{\rho}) \geq \mathcal{F}(\phi(\hat{\rho}))$.

For additional properties, see [134].

3.2.3.2 Partial dynamical activity

As we have stated earlier, we wish to use the quantum Fisher information to elaborate upon and connect the previously made definitions of quantum dynamical activity. We aim to make a notion of quantum activity with a clear physical meaning, theoretical and practical implications, and that recovers the classical behaviour in the appropriate limit. Moreover, we would like to find a definition which we can use for fully unitary dynamics, where it is not possible to describe the evolution of the system through stochastic trajectories. We make such a notion of activity by adapting the previous QFI-based definitions of activity used in Refs. [45, 46, 50] to count the dynamics generated by a specific part of a microscopic Hamiltonian. Specifically, we consider the parametrized, time-dependent Hamiltonian

$$\hat{H}_\theta(t) = \hat{H}_0(t) + \theta\hat{V}(t), \tag{3.60}$$

which we have separated into two parts $\hat{H}_0(t)$ and $\theta\hat{V}(t)$, where θ is a real number controlling the strength of $\hat{V}(t)$. Note that the definition of quantum activity

becomes more nuanced when the Hamiltonian has explicit time dependence, as discussed in Sec. 3.2.4.2 and Sec. 3.2.4.3. Moreover, we emphasize that we do not require $\hat{V}(t)$ to be weak. Instead we simply separate it out as a specific part of the dynamics, which we are interested in defining an activity with respect to, in a controlled and transparent manner. For example, if one is interested in a system interacting with an environment, one might take $\hat{H}_0 = \hat{H}_\mathrm{S} + \hat{H}_\mathrm{E}$ with $\hat{V}$ as the coupling Hamiltonian. In the limit of $\theta \to 1$, we recover the original Hamiltonian. The parameter θ is encoded in the state at time t by the unitary dynamics

$$\hat{\rho}_\theta(t) := \hat{U}_\theta(t,0)\hat{\rho}(0)\hat{U}_\theta^\dagger(t,0), \quad \hat{U}_\theta(t,0) := T_+ \exp\left\{-\frac{i}{\hbar}\int_0^t d\tau \hat{H}_\theta(\tau)\right\}. \tag{3.61}$$

where $\hat{\rho}(0)$ is the initial state of the system. We define a *Partial Dynamical Activity* (PDA) with respect to $\hat{V}(t)$ from the QFI as

$$\mathscr{A}(t) := \lim_{\theta\to 1}\frac{1}{4}\mathcal{F}_{\theta\theta}(t) = \lim_{\theta\to 1}\frac{1}{4}\,\mathrm{tr}\left\{\hat{\rho}_\theta(t)\hat{\mathfrak{L}}_\theta\hat{\mathfrak{L}}_\theta\right\}. \tag{3.62}$$

In the coming sections, we will show why this object can play the role of $\mathcal{A}(t)$ as defined in Eq. (3.25). Before this, we make some more general considerations and define a corresponding PDA rate as

$$\mathscr{K}(t) := \frac{\partial}{\partial t}\mathscr{A}(t). \tag{3.63}$$

When the initial state is pure $\hat{\rho}(0) = |\psi(0)\rangle\langle\psi(0)|$, the parametrized state and its variation are

$$|\psi_\theta(t)\rangle := \hat{U}_\theta(t,0)\,|\psi(0)\rangle\,, \quad |\partial_\theta\psi_\theta(t)\rangle := \partial_\theta\hat{U}_\theta(t,0)\,|\psi(0)\rangle\,. \tag{3.64}$$

The unitary evolution of a pure state is the most fundamental level of description in quantum mechanics, and it is therefore instructive to push the definition of quantum activity to this level. However, for a complicated system, e.g., a quantum transport setting, this is an intractable approach since we, in general, do not know the eigenstates of the full Hamiltonian, and we are not able to control the quantum state of, e.g., a reservoir in experiment and prepare the same pure initial state for each measurement. Thus, for practical calculations, we rely on a mixed state to describe experiments. Even if we only have access to the mixed state given by $\rho_\theta^{\mathrm{practical}}(t) = \phi(|\psi_\theta(t)\rangle\langle\psi_\theta(t)|)$, for a CPTP map ϕ, the monotonicity of the QFI tells us that

$$\mathcal{F}_{\theta\theta}(|\psi_\theta(t)\rangle) \geq \mathcal{F}_{\theta\theta}(\rho_\theta^{\mathrm{practical}}(t)), \tag{3.65}$$

meaning that the inability to obtain complete information about the pure state reduces sensitivity to θ and, consequently, the PDA. In the context of classical

Markov processes, a similar characteristic of dynamical activity is its dependence on the level of coarse-graining. Specifically, when using a coarse-grained model that lumps together certain microscopic states, transitions between them are overlooked, leading to the dynamical activity being underestimated compared to a more detailed model with less coarse-graining.

Next, we turn our attention to finding an expression of the PDA for a pure state. By taking a derivative of the Schrödinger equation with respect to θ, we find the following differential equation

$$i\hbar\partial_t\partial_\theta\hat{U}_\theta(t,0) = (\partial_\theta\hat{H}_\theta(t))\hat{U}_\theta(t,0) + \hat{H}_\theta(t)(\partial_\theta\hat{U}_\theta(t,0)). \tag{3.66}$$

We can solve this by using a variation of constants and making an ansatz

$$\partial_\theta\hat{U}_\theta(t,0) = \hat{U}_\theta(t,0)\hat{Y}(t), \tag{3.67}$$

for some operator $\hat{Y}(t)$. We insert the ansatz into the differential equation

$$\begin{aligned} i\hbar\partial_t\partial_\theta\hat{U}_\theta(t,0) =& \hat{H}_\theta(t)\hat{U}_\theta(t,0)\hat{Y}(t) + i\hbar\hat{U}_\theta(t,0)\partial_t\hat{Y}(t) \\ =& (\partial_\theta\hat{H}_\theta(t))\hat{U}_\theta(t,0) + \hat{H}_\theta(t)(\partial_\theta\hat{U}_\theta(t,0)), \end{aligned} \tag{3.68}$$

and solve for $\hat{Y}(t)$, finding

$$\hat{Y}(t) = \frac{-i}{\hbar}\int_0^t d\tau\hat{U}_\theta^\dagger(\tau,0)(\partial_\theta\hat{H}_\theta(\tau))\hat{U}_\theta(\tau,0). \tag{3.69}$$

With the expression for $\hat{Y}(t)$ we compute the derivative of the unitary as

$$\begin{aligned} \partial_\theta\hat{U}_\theta(t,0) &= \frac{-i}{\hbar}\hat{U}_\theta(t,0)\int_0^t d\tau\hat{U}_\theta^\dagger(\tau,0)(\partial_\theta\hat{H}_\theta(\tau))\hat{U}_\theta(\tau,0) \\ &= \frac{-i}{\hbar}\hat{U}_\theta(t,0)\int_0^t d\tau\hat{V}_\theta^{\mathrm{H}}(\tau), \end{aligned} \tag{3.70}$$

where $\hat{V}_\theta^{\mathrm{H}}(\tau) = \hat{U}_\theta^\dagger(\tau,0)\hat{V}(\tau)\hat{U}_\theta(\tau,0)$ is the operator in the Heisenberg picture, evolving under the θ-modified dynamics. Inserting this back into the QFI for a pure state results in

$$\begin{aligned} \frac{1}{4}\mathcal{F}_{\theta\theta}(t) &= \frac{1}{\hbar^2}\int_0^t d\tau\int_0^t d\tau'\langle\hat{V}_\theta^{\mathrm{H}}(\tau)\hat{V}_\theta^{\mathrm{H}}(\tau')\rangle - \langle\hat{V}_\theta^{\mathrm{H}}(\tau)\rangle\langle\hat{V}_\theta^{\mathrm{H}}(\tau')\rangle, \\ &= \frac{1}{\hbar^2}\int_0^t d\tau\int_0^t d\tau'\langle\langle\hat{V}_\theta^{\mathrm{H}}(\tau)\hat{V}_\theta^{\mathrm{H}}(\tau')\rangle\rangle, \end{aligned} \tag{3.71}$$

where $\langle\cdot\rangle = \langle\psi(0)|\cdot|\psi(0)\rangle$. By evaluating the QFI at $\theta = 1$, we find the partial

dynamical activity

$$\mathscr{A}(t) = \frac{1}{4}\mathcal{F}_{\theta\theta}(t)\Big|_{\theta=1} = \frac{1}{\hbar^2}\int_0^t d\tau \int_0^t d\tau' \langle\langle \hat{V}^{\mathrm{H}}(\tau)\hat{V}^{\mathrm{H}}(\tau')\rangle\rangle. \tag{3.72}$$

If we want to calculate the PDA rate, we simply take the time derivative

$$\begin{aligned}\mathscr{K}(t) = \frac{\partial}{\partial t}\mathscr{A}(t) &= \frac{1}{\hbar^2}\int_0^t d\tau \langle\{\hat{V}^{\mathrm{H}}(t), \hat{V}^{\mathrm{H}}(\tau)\}\rangle - 2\langle\hat{V}^{\mathrm{H}}(\tau)\rangle\langle\hat{V}^{\mathrm{H}}(t)\rangle \\ &= \frac{1}{\hbar^2}\int_0^t d\tau \langle\langle\{\hat{V}^{\mathrm{H}}(t), \hat{V}^{\mathrm{H}}(\tau)\}\rangle\rangle.\end{aligned} \tag{3.73}$$

These expressions are valid for a pure state.

If the initial state is mixed $\hat{\rho}(0) = \sum_{i=1}^{d} p_i \left|\psi_i\right\rangle \left\langle\psi_i\right|$, the QFI can instead be written as

$$\begin{aligned}\mathcal{F}_{\theta\theta}(t) &= 2\sum_{ij}\frac{(p_i - p_j)^2}{p_i + p_j}\left|\left\langle\psi_i\right|\hat{\mathcal{V}}_\theta(t)\left|\psi_j\right\rangle\right|^2, \\ \hat{\mathcal{V}}_\theta(t) &= i\hat{U}_\theta^\dagger(t,0)(\partial_\theta\hat{U}_\theta(t,0)) = \frac{1}{\hbar}\int_0^t d\tau V_\theta^{\mathrm{H}}(\tau).\end{aligned} \tag{3.74}$$

since the evolution (or encoding) is unitary [143]. While this expression is valid for a mixed initial state, it is, in general, hard to handle. However, using the convexity of the QFI together with Jensen's inequality [144, 145], an upper bound is provided by

$$\frac{1}{4}\mathcal{F}_{\theta\theta}(t) \leq \frac{1}{\hbar^2}\int_0^t d\tau \int_0^t d\tau' \langle\langle \hat{V}_\theta^{\mathrm{H}}(\tau)\hat{V}_\theta^{\mathrm{H}}(\tau')\rangle\rangle. \tag{3.75}$$

Here $\langle\hat{V}_\theta^{\mathrm{H}}(t)\rangle = \mathrm{tr}\Big\{\hat{V}_\theta^{\mathrm{H}}(t)\hat{\rho}(0)\Big\}$ is evaluated with the initial density matrix. From this, we can construct a general upper bound on the PDA by taking $\theta \to 1$,

$$\mathscr{A}(t) \leq \frac{1}{\hbar^2}\int_0^t d\tau \int_0^t d\tau' \langle\langle \hat{V}^{\mathrm{H}}(\tau)\hat{V}^{\mathrm{H}}(\tau')\rangle\rangle =: \mathscr{A}^{\mathrm{lim}}(t). \tag{3.76}$$

We can interpret $\mathscr{A}^{\mathrm{lim}}(t)$ as a limiting PDA. Interestingly, the time derivative of this limiting activity is similar to the definition of the correlator-based activity rate (3.42) as introduced in Ref. [44],

$$\frac{\partial}{\partial t}\mathscr{A}^{\mathrm{lim}}(t) = \frac{1}{\hbar^2}\int_0^t d\tau \langle\langle\{\hat{V}^{\mathrm{H}}(t), \hat{V}^{\mathrm{H}}(\tau)\}\rangle\rangle. \tag{3.77}$$

We can interpret the relation between $\mathscr{A}(t)$ and $\mathscr{A}^{\mathrm{lim}}(t)$ in the following way: for a pure state $\mathscr{A}(t) = \mathscr{A}^{\mathrm{lim}}(t)$ and the variance of $\hat{\mathcal{V}}(t)$, see Eq. (3.74) has a precise geometric meaning, it measures how strongly $\hat{V}(t)$ has been encoded in the state. However, when the state is mixed, the variance is enhanced compared to the PDA.

This enhancement leads to an overestimation of the PDA $\mathscr{A}(t) \leq \mathscr{A}^{\lim}(t)$ when using the variance. This overestimation is not related to the dynamics; it is instead a consequence of classical uncertainty.

There are some situations where the PDA for a mixed state can be represented in terms of quantities which are, in principle, measurable. This is the case for a system in thermal equilibrium at a temperature T, where we can write

$$\begin{aligned}\mathscr{A}(t) =& \int_0^t d\tau \int_0^t d\tau' \int_{-\infty}^{\infty} d\omega \frac{1}{4\pi\hbar^2} \Big(\tanh^2 \left[\frac{\hbar\omega}{2k_{\mathrm{B}}T}\right] e^{i\omega(\tau-\tau')} R_{VV}(\omega) \Big) \\ =& \frac{1}{\pi\hbar^2} \int_{-\infty}^{\infty} d\omega \tanh^2 \left[\frac{\hbar\omega}{2k_{\mathrm{B}}T}\right] \frac{\sin^2[\omega t/2]}{\omega^2} R_{VV}(\omega),\end{aligned} \tag{3.78}$$

using

$$R_{VV}(\omega) = \int_{-\infty}^{\infty} dt \langle\{\hat{V}^{\mathrm{H}}(t), \hat{V}^{\mathrm{H}}(0)\}\rangle e^{-i\omega t}. \tag{3.79}$$

For a derivation of Eq. (3.78) see Appendix C. Finding similar formulas for the PDA in terms of measurable quantities out of equilibrium remains a challenge for future work.

3.2.3.3 Partial dynamical activity in quantum transport

We now apply our definition of partial dynamical activity to the case of quantum transport, with the goal of deriving the correlator-based definition (3.42) [44]. To do this, we consider the typical case of a transport setting with Hamiltonian

$$\hat{H}_\theta = \hat{H}_{\mathrm{S}} + \sum_{\beta\neq\alpha} (\hat{H}_\beta + \hat{V}_\beta) + \hat{H}_\alpha + \theta\hat{V}_\alpha, \tag{3.80}$$

where the parametrization is applied only on the coupling to bath α. As a starting point, we use a pure initial state, which could be a complicated entangled state between the system and the baths. In this case, the partial dynamical activity with respect to the coupling between system and reservoir α is given by

$$\mathscr{A}_\alpha(t) = \frac{1}{\hbar^2} \int_0^t d\tau \int_0^t d\tau' \langle\langle \hat{V}_\alpha^{\mathrm{H}}(\tau) \hat{V}_\alpha^{\mathrm{H}}(\tau')\rangle\rangle. \tag{3.81}$$

The corresponding partial activity rate is given by

$$\mathscr{K}_\alpha(t) = \frac{1}{\hbar^2} \int_0^t d\tau \langle\langle \{\hat{V}_\alpha^{\mathrm{H}}(t), \hat{V}_\alpha^{\mathrm{H}}(\tau)\}\rangle\rangle, \tag{3.82}$$

and is closely related to the correlator-based definition of the activity rate of Eq. (3.42) [44], for a pure state. The only difference lies in the integration limits: $\int_0^t$ in $\mathscr{K}_\alpha(t)$ and $\frac{1}{2}\int_{-t}^t$ in Eq. (3.42). However, this is resolved when assuming

time-translation invariance. Thus, by starting from a geometric point of view, we have now found a clear interpretation of the activity rate in Eq. (3.42) for a pure initial state: It is the rate of change in the metric, which measures the distinguishability in the state with respect to the coupling strength, i.e., at which rate is the information about $\hat{V}_\alpha$ encoded in the state due to the evolution. While the pure state description is fundamental, a practical transport calculation requires a mixed initial state. If the initial density matrix is given by $\hat{\rho}(0) = \sum_{i=1}^{d} p_i \left|\psi_i\right\rangle \left\langle\psi_i\right|$, the PDA can instead be expressed as

$$\mathscr{A}_\alpha(t) = \frac{1}{2} \sum_{ij=1}^{d} \frac{(p_i - p_j)^2}{p_i + p_j} |\left\langle\psi_i\right| \hat{\mathcal{V}}_\alpha(t) \left|\psi_j\right\rangle|^2, \tag{3.83}$$

where

$$\hat{\mathcal{V}}_\alpha(t) := \frac{1}{\hbar} \int_0^t d\tau \hat{V}_\alpha^{\mathrm{H}}(\tau), \tag{3.84}$$

since the parametrized state is given by a unitary encoding [143]. If the initial state is known, one could, in principle, directly calculate this quantity. For instance, if the initial state is given by a tensor product of thermal states. Moreover, as discussed earlier, the PDA is upper-bounded by

$$\mathscr{A}_\alpha(t) \leq \mathscr{A}_\alpha^{\lim}(t) = \frac{1}{\hbar^2} \int_0^t d\tau \int_0^t d\tau' \langle\langle \hat{V}_\alpha^{\mathrm{H}}(\tau) \hat{V}_\alpha^{\mathrm{H}}(\tau') \rangle\rangle, \tag{3.85}$$

where the expectation values are taken with respect to $\hat{\rho}(0)$. Again, the only difference between the time derivative of the limiting PDA

$$\frac{\partial}{\partial t} \mathscr{A}_\alpha^{\lim}(t) = \frac{1}{\hbar^2} \int_0^t d\tau \langle\langle \{\hat{V}_\alpha^{\mathrm{H}}(t), \hat{V}_\alpha^{\mathrm{H}}(\tau)\} \rangle\rangle, \tag{3.86}$$

and the correlator-based activity is the integration limits. There exists a vast body of literature on methods to calculate the QFI in various settings, as it is a crucial quantity in the field of quantum metrology. It is, however, generally challenging to express it in terms of standard transport quantities and relate it to a directly measurable object. Therefore, an estimate in terms of $\mathscr{A}_\alpha^{\lim}(t)$ might be easier to find and more practical. As a next step, we verify that the PDA recovers the definition of dynamical activity used for GKSL dynamics.

3.2.3.4 Weak-coupling limit of the partial dynamical activity

In this section, we connect the partial dynamical activity Eq. (3.62) to the standard definition of dynamical activity (3.25) of the GKSL equation by considering the weak-coupling limit. In Appendix B we verified that the correlator-based activity [Eq. (3.42)] recovers the GKSL definition [Eq. (3.25)] in the weak coupling limit.

This means that the PDA Eq. (3.62) in the weak coupling limit must at least be upperbounded by the standard dynamical activity of Eq. (3.25). However, it is still instructive to investigate the PDA Eq. (3.62) directly in the weak coupling limit. To do this, we consider a system coupled to an environment via $\hat{V}$ that could consist of multiple baths, with the Hamiltonian

$$\hat{H}_\theta = \hat{H}_\mathrm{S} + \hat{H}_\mathrm{E} + \theta\hat{V}, \tag{3.87}$$

where $\hat{V}$ is the interaction Hamiltonian between system and environment. Following a standard derivation of the GKSL equation, one arrives at

$$\partial_t\hat{\rho}_\theta(t) = -\frac{i}{\hbar}[\hat{H}_\mathrm{S}, \hat{\rho}_\theta(t)] + \theta^2\sum_k \mathcal{D}[\hat{L}_k]\hat{\rho}_\theta(t), \tag{3.88}$$

where $\hat{\rho}_\theta(t)$ is the reduced density matrix of the system and $\hat{L}_k$ is a jump operator. Here θ is encoded by the GKSL dynamics. By defining the parametrized jump operators $\hat{L}_{k,\theta} = \theta\hat{L}_k$, the QFI can be calculated in the long-time limit [40, 146]

$$\mathcal{F}_{\theta\theta}(t) = 4t\sum_k \mathrm{tr}\Big\{(\partial_\theta\hat{L}_{k,\theta})^\dagger(\partial_\theta\hat{L}_{k,\theta})\hat{\rho}_\theta^\mathrm{ss}\Big\}. \tag{3.89}$$

Here we denoted the steady-state solution to Eq. (3.88) as $\hat{\rho}_\theta^\mathrm{ss}$. Thus, by taking $\theta \to 1$, the PDA becomes

$$\mathscr{A}(t) = \frac{1}{4}\mathcal{F}_{\theta\theta}(t)\big|_{\theta=1} = t\sum_k \mathrm{tr}\Big\{\hat{L}_k^\dagger\hat{L}_k\hat{\rho}^\mathrm{ss}\Big\}, \tag{3.90}$$

and, in the long-time limit, the PDA rate is identical to the standard definition

$$\lim_{t\to\infty}\mathscr{K}(t) = \lim_{t\to\infty}\frac{d}{dt}\mathscr{A}(t) = \sum_k \mathrm{tr}\Big\{\hat{L}_k^\dagger\hat{L}_k\hat{\rho}^\mathrm{ss}\Big\}. \tag{3.91}$$

Next, we make a few remarks and compare with the dynamical activities used in Refs. [40, 50]. In Ref. [40], the GKSL equation is deformed as

$$\partial_t\hat{\rho}_\theta(t) = -\frac{i}{\hbar}[\hat{H}_\mathrm{S}, \hat{\rho}_\theta(t)] + (\theta+1)\sum_k \mathcal{D}[\hat{L}_k]\hat{\rho}_\theta(t), \tag{3.92}$$

with the jump operators being parametrized by $\hat{L}_{k,\theta} = \sqrt{1+\theta}\hat{L}_k$ instead. This is equivalent to the parametrization we used in Eq. (3.88) and the corresponding QFI is equal to the dynamical activity in the steady-state $\mathcal{F}_{\theta\theta}(t)\big|_{\theta=0} = t\sum_k \mathrm{tr}\Big\{\hat{L}_k^\dagger\hat{L}_k\hat{\rho}^\mathrm{ss}\Big\}$. Next, we compare with the definition used in Ref. [50, 111], where a deformation

of the GKSL dynamics

$$\partial_t \hat{\rho}_\theta(t) = -\frac{i}{\hbar}[\theta \hat{H}_\mathrm{S}, \hat{\rho}_\theta(t)] + \theta \sum_k \mathcal{D}[\hat{L}_k]\hat{\rho}_\theta(t), \tag{3.93}$$

was used, and quantum dynamical activity was identified with the corresponding QFI. This definition, however, is not equivalent to the usual number of jumps and contains additional effects of coherence due to the unitary part of the dynamics. This parametrization of the GKSL dynamics has a physical significance since rescaling θ is equivalent to letting the system evolve for a longer time (as long as the Liouvillian has no explicit time dependence). Moreover, in Refs. [40, 50] an analogous definition of quantum activity was also used for closed quantum systems and shown to be connected to quantum speed limits. The different parametrizations Eq. (3.92) of Ref. [40] and Eq. (3.93) of Refs. [46, 50, 110] lead to different bounds on the precision of a counting observable via the quantum Cramér-Rao bound.

3.2.3.5 Partial dynamical activity and precision bounds

One of the key drives behind introducing a quantum mechanical notion of dynamical activity is the opportunity to find generalizations of the classical kinetic uncertainty relation (3.22) for quantum systems. In this section, we will apply the PDA for the transport problem to try to derive a quantum KUR. By doing this, we are motivated to expand our definition of activity to encompass the dynamics generated by the full Hamiltonian. Since the PDA (3.62) is defined through the QFI, we are able to utilize the quantum Cramér-Rao bound

$$\frac{(\partial_\theta \mathrm{tr}\{\hat{X}^\mathrm{H}_\theta \hat{\rho}(0)\})^2}{\mathrm{Var}[\hat{X}^\mathrm{H}_\theta(t)]} \leq \mathcal{F}_{\theta\theta}(t). \tag{3.94}$$

Focusing on the transport scenario of Eq (3.80), performing the derivative using Eq. (3.70) and setting $\theta = 1$, we find

$$\partial_\theta \mathrm{tr}\{\hat{X}^\mathrm{H}_\theta(t)\hat{\rho}(0)\}\Big|_{\theta=1} = \int_0^t d\tau \mathrm{tr}\left\{\frac{i}{\hbar}[\hat{V}^\mathrm{H}_\alpha(\tau), \hat{X}^\mathrm{H}(t)]\rho(0)\right\}, \tag{3.95}$$

which at first glance appears promising for obtaining a bound on the precision of an integrated current. If we pick $\hat{X}^\mathrm{H}(t) = \Delta\hat{X}^\mathrm{H}_\alpha(t) = \hat{X}^\mathrm{H}_\alpha(t) - \hat{X}^\mathrm{H}_\alpha(0)$ to be the change in an observable of reservoir α, such as its Hamiltonian or number operator in the standard transport scenario, the associated current operator is

$$\frac{\partial}{\partial t}\hat{X}^\mathrm{H}_\alpha(t) = \hat{I}^{(X)}_\alpha(t) = \frac{i}{\hbar}[\hat{V}^\mathrm{H}_\alpha(t), \hat{X}^\mathrm{H}_\alpha(t)]. \tag{3.96}$$

Note, however, that the operators inside of Eq. (3.95) have different time arguments, meaning that we cannot interpret it as a current operator directly. If we take a time derivative, we find

$$\begin{aligned}\partial_t\partial_\theta \mathrm{tr}\{\hat{X}^{\mathrm{H}}_\theta(t)\hat{\rho}(0)\}\Big|_{\theta=1} = \mathrm{tr}\left\{\frac{i}{\hbar}[\hat{V}^{\mathrm{H}}_\alpha(t),\hat{X}^{\mathrm{H}}_\alpha(t)]\hat{\rho}(0)\right\} + \\ + \int_0^t d\tau \mathrm{tr}\left\{\frac{i}{\hbar}[\hat{V}^{\mathrm{H}}_\alpha(\tau),\frac{i}{\hbar}[\hat{V}^{\mathrm{H}}_\alpha(t),\hat{X}^{\mathrm{H}}_\alpha(t)]]\hat{\rho}(0)\right\}.\end{aligned} \tag{3.97}$$

Thus, we can rewrite

$$\partial_\theta \mathrm{tr}\{\hat{X}^{\mathrm{H}}_\theta(t)\hat{\rho}(0)\}\Big|_{\theta=1} = \int_0^t d\tau\, \mathrm{tr}\Big\{\hat{I}^{(X)}_\alpha(\tau)\hat{\rho}(0)\Big\} + M(t), \tag{3.98}$$

where we defined

$$M(t) = \int_0^t d\tau \int_0^\tau d\tau' \frac{i}{\hbar}\,\mathrm{tr}\Big\{[\hat{V}^{\mathrm{H}}_\alpha(\tau'),\hat{I}^{(X)}_\alpha(\tau)]\hat{\rho}(0)\Big\}. \tag{3.99}$$

The first term in Eq. (3.98) is exactly the time-integrated current, while the second term $M(t)$ instead contains memory effects. It is, however, second-order in $\hat{V}^{\mathrm{H}}_\alpha(t)$, implying that at a first-order approximation in the coupling

$$\partial_\theta \mathrm{tr}\{\hat{X}^{\mathrm{H}}_\theta(t)\hat{\rho}(0)\}\Big|_{\theta=1} = \int_0^t d\tau\, \mathrm{tr}\Big\{\hat{I}^{(X)}_\alpha(\tau)\hat{\rho}(0)\Big\} + \mathcal{O}\Big(\hat{V}^2_\alpha\Big). \tag{3.100}$$

One might then try to use

$$\frac{\Big(\partial_\theta\,\mathrm{tr}\Big\{\Delta\hat{X}^{\mathrm{H}}_{\alpha,\theta}(t)\hat{\rho}(0)\Big\}\Big|_{\theta=1}\Big)^2}{\mathrm{Var}[\Delta\hat{X}^{\mathrm{H}}_\alpha(t)]} \leq 4\mathscr{A}_\alpha(t) \leq 4\mathscr{A}^{\mathrm{lim}}_\alpha(t) \tag{3.101}$$

as a weak coupling KUR, but this does not work since $\mathscr{A}_\alpha(t)$ is second order in $\hat{V}_\alpha$. In general, we cannot neglect the memory term, and we are left with

$$\frac{\Big(\mathrm{tr}\Big\{\Delta\hat{X}^{\mathrm{H}}_\alpha(t)\hat{\rho}(0)\Big\} + M(t)\Big)^2}{\mathrm{Var}[\Delta\hat{X}^{\mathrm{H}}_\alpha(t)]} \leq 4\mathscr{A}_\alpha(t) \leq 4\mathscr{A}^{\mathrm{lim}}_\alpha(t). \tag{3.102}$$

In principle, if one has control over the coupling strength between system and reservoir α in an experiment, one could directly measure $M(t)$ using the response and transport of $\hat{X}_\alpha(t)$

$$M(t) = \partial_\theta \mathrm{tr}\{\hat{X}^{\mathrm{H}}_\theta(t)\hat{\rho}(0)\}\Big|_{\theta=1} - \int_0^t d\tau\, \mathrm{tr}\Big\{\hat{I}^{(X)}_\alpha(\tau)\hat{\rho}(0)\Big\}. \tag{3.103}$$

As is evident, $M(t)$ is exactly the difference between the response of $\Delta\hat{X}^{\mathrm{H}}_{\alpha}(t)$ to increasing the coupling strength and its transport. I.e., how different increasing θ is from letting the system evolve for a longer time. Of course, this does not help us construct a general quantum KUR limiting the precision in a current. Still, one would be able to conclude whether $M(t)$ is positive or negative and if $M(t)$ has the same sign as $\langle\Delta\hat{X}^{\mathrm{H}}_{\alpha}(t)\rangle$, we have a quantum KUR without any corrections

$$\frac{\langle\Delta\hat{X}^{\mathrm{H}}_{\alpha}(t)\rangle^2}{\mathrm{Var}[\Delta\hat{X}^{\mathrm{H}}_{\alpha}(t)]} \leq \frac{(\partial_\theta\langle\Delta\hat{X}^{\mathrm{H}}_{\alpha}(t)\rangle)^2}{\mathrm{Var}[\Delta\hat{X}^{\mathrm{H}}_{\alpha}(t)]} \leq 4\mathscr{A}_{\alpha}(t) \leq 4\mathscr{A}^{\mathrm{lim}}_{\alpha}(t). \tag{3.104}$$

When $M(t)$ has the opposite sign of $\langle\Delta\hat{X}^{\mathrm{H}}_{\alpha}(t)\rangle$, we can no longer trivially neglect the term, and it remains a challenge for future works to relate $M(t)$ to standard transport quantities.

It is natural to first seek a kinetic uncertainty relation by relating the activity to the strength of the system-environment coupling. However, the appearance a "quantum correction" is not surprising, since the PDA does not take the full dynamics into account.

3.2.4 Total dynamical activity

In the previous section, we were left with the additional memory term in Eq. (3.102) when trying to derive a quantum KUR. Two approaches can be taken to address this issue: one can either view $M(t)$ as a "quantum correction" to a classical bound and attempt to relate it to some measurable quantities, or alternatively, one can ask the question if there are some aspects of the dynamics which the partial dynamical activity is missing. In this section, by following the latter inquiry, we will connect the partial dynamical activity (3.62) and the correlator-based dynamical activity (3.42) [44] to the information geometric quantum dynamical used in Refs. [45, 46, 50]. We will first consider the case when the Hamiltonian has no explicit time dependence in Sec. 3.2.4.1. When trying to derive a quantum KUR, we encounter the time-energy uncertainty relation [147]. The extension to time-dependent Hamiltonians is more subtle, and we will explore two different generalizations. In Sec. 3.2.4.2, we will explore a definition of activity based on a scaling of time and in Sec. 3.2.4.3, we will instead make a definition based on parametrizing the speed of a protocol. While both definitions are equivalent for a time-independent Hamiltonian, they have different conceptual implications and permit inequivalent bounds on precision in general.

3.2.4.1 Time independent Hamiltonians

We will now extend the PDA (3.62) to account for the full dynamics and explore how this total dynamical activity limits precision. Naturally, if we want to extend

the PDA to account for the full dynamics, we can do this by parameterizing the full Hamiltonian. To begin with, let us consider a time-independent Hamiltonian

$$\hat{H}_\theta = \theta \hat{H}, \tag{3.105}$$

and a pure initial state $\hat{\rho}(0) = |\psi(0)\rangle\langle\psi(0)|$. We point out that since the Hamiltonian is time independent, $\hat{U}_\theta(t,0) = \hat{U}(\theta t, 0)$ and scaling θ is equivalent to scaling t [50]. Since

$$\partial_\theta \hat{U}_\theta(t,0) = \frac{-it}{\hbar}\hat{U}_\theta(t,0)\hat{H}, \tag{3.106}$$

the QFI reads as

$$\mathcal{F}_{\theta\theta}(t) = 4\frac{t^2}{\hbar^2}(\langle\hat{H}^2\rangle - \langle\hat{H}\rangle^2) = 4\frac{t^2}{\hbar^2}\langle\langle\hat{H}^2\rangle\rangle. \tag{3.107}$$

Using this, we define a *Total Dynamical Activity* (TDA) as

$$\mathscr{A}(t) = \lim_{\theta\to 1}\mathcal{F}_{\theta\theta}(t) = \frac{t^2}{\hbar^2}\langle\langle\hat{H}^2\rangle\rangle. \tag{3.108}$$

This definition of activity is equivalent to the definitions used in Refs. [46, 50, 110, 111] for a closed quantum system. The only difference between these definitions lies in the factor of four, as we employed the Bures metric in this thesis, whereas Refs. [46, 50] utilized the QFI. Note that $\partial_t\langle\langle\hat{H}^2\rangle\rangle = 0$, meaning that the TDA is set by the initial superpositions in the eigenbasis. Furthermore, we remark that an energy eigenstate of $\hat{H}$, as expected, is not considered active, since for such a state $\langle\langle\hat{H}^2\rangle\rangle = 0$. Extending the discussion to mixed states, $\hat{\rho}(0) = \sum_i p_i |\psi_i\rangle\langle\psi_i|$, we have

$$\mathscr{A}(t) = \frac{t^2}{2\hbar^2}\sum_{ij}\frac{(p_i - p_j)^2}{p_i + p_j}|\langle\psi_i|\hat{H}|\psi_j\rangle|^2 \leq \mathscr{A}^{\lim}(t) = \frac{t^2}{\hbar^2}\langle\langle\hat{H}^2\rangle\rangle. \tag{3.109}$$

Here, it is important to note that the variance no longer directly quantifies the speed of evolution, since it can stem from statistical uncertainty rather than superpositions. For instance, due to the convexity of the QFI, the TDA of a thermal state is zero, despite having a nonzero variance in energy. Another way to see this is from the fact that θ is not encoded in a thermal state

$$\hat{U}_\theta(t,0)\frac{e^{-\hat{H}/k_\mathrm{B}T}}{\mathrm{tr}\left\{e^{-\hat{H}/k_\mathrm{B}T}\right\}}\hat{U}_\theta^\dagger(t,0) = \frac{e^{-\hat{H}/k_\mathrm{B}T}}{\mathrm{tr}\left\{e^{-\hat{H}/k_\mathrm{B}T}\right\}}. \tag{3.110}$$

This is true for any state diagonal in the eigenbasis of $\hat{H}$. Fundamentally, this stems from the fact that the measure of distance we use, the Bures, or the Fubini-Study

metric, does not distinguish between two states that only differ by a complex phase. Thus, the rotating phase of an energy eigenstate is not counted as activity. Here, we also get a clear distinction of what type of state is considered active for the different definitions of quantum dynamical activity. If one opts to use the TDA (3.108), the thermal system is considered inactive since there is no evolution, while the definition based on the variance $\mathscr{A}^{\lim}(t)$ would consider the statistical uncertainty as contributing to activity. Moreover, $\mathscr{A}^{\lim}(t)$ would in general be easier to measure and can, in fact, for a thermal state, be related to the specific heat via Eqs. (3.57). Depending on one's goals, this is a clear argument for adopting either the QFI-based or the variance-based definitions of dynamical activity. Furthermore, as we will see, the variance of energy is connected to quantum speed limits [148].

As we did in Sec. 3.2.3.5, we now try to use the total dynamical activity to limit the precision of observables in the same fashion as the KUR. This time, since increasing θ is equivalent to letting the system evolve for a longer time, we find for a general observable $\hat{X}$

$$\partial_\theta \operatorname{tr}\Big\{\hat{U}_\theta^\dagger(t,0)\hat{X}\hat{U}_\theta(t,0)\hat{\rho}(0)\Big\} = t\partial_t \operatorname{tr}\Big\{\hat{X}_\theta^{\mathrm{H}}(t)\hat{\rho}(0)\Big\} = t\operatorname{tr}\Big\{\hat{I}_\theta^{(X)}(t)\hat{\rho}(0)\Big\}. \quad (3.111)$$

Inserting this into the QCRB and setting $\theta = 1$ yields a constraint

$$\frac{\Big(t\partial_t\langle\hat{X}^{\mathrm{H}}(t)\rangle\Big)^2}{\langle\langle(\hat{X}^{\mathrm{H}}(t))^2\rangle\rangle} \leq 4\mathscr{A}(t) \leq 4\frac{t^2}{\hbar^2}\langle\langle\hat{H}^2\rangle\rangle, \quad (3.112)$$

where the second inequality is saturated for a pure state. While this is a general constraint on an observables current and its variance, it is not a new result. Indeed, (3.112) is equivalent to

$$\frac{1}{2}|\partial_t\langle\hat{X}^{\mathrm{H}}(t)\rangle| \leq \sqrt{\langle\langle(\hat{X}^{\mathrm{H}}(t))^2\rangle\rangle}\sqrt{\mathscr{A}(t)/t^2} \leq \sqrt{\langle\langle(\hat{X}^{\mathrm{H}}(t))^2\rangle\rangle}\sqrt{\langle\langle\hat{H}^2\rangle\rangle/\hbar^2}. \quad (3.113)$$

The last inequality is the observable-level form of the *time-energy uncertainty relation* underlying the Mandelstam-Tamm quantum speed limit [147, 148]. The connection to quantum speed limits, as related to the minimal time for a system to evolve into a distinguishable state has been made before in Refs. [46, 50, 110]. With this parallel, the activity definition (3.108) can be interpreted in terms of time-energy uncertainty, which indeed restricts the current and variance of an observable, similar to how the average number of jumps does in the original KUR (3.22). However, it should be noted that (3.112) is challenging to apply to a transport setting for two major reasons: $\mathscr{A}(t)$ is very large due to the size of the baths, and we are typically interested in the long-time limit, which would render (3.112) a trivial bound. This is due to the quadratic scaling in time of $\mathscr{A}(t)$. From the perspective of parameter estimation, the t^2 is expected in a unitary encoding. By waiting a

longer time, the sensitivity to θ is increased. However, when trying to interpret $\mathscr{A}(t)$ as an activity-like quantity, the t^2 scaling seems counterintuitive. We will comment more on this shortly, but before that, we note that the PDA in the context of quantum transport does not generally display this problem. This we can understand by comparing the PDA to the correlator-based definition of dynamical activity. In Ref. [44], the correlation-based activity was calculated for noninteracting fermionic transport, and the bosonic version is covered in Appendix A of this thesis. In both cases, in the steady-state limit $\partial_t \mathscr{A}^{\lim}(t)$ is constant, meaning that $\mathscr{A}(t)$ can at most have linear scaling in time. This is possible because both reservoirs (bosonic or fermionic) are assumed to be of infinite size, which makes the correlation functions decay, unlike the case of closed unitary dynamics, see Appendix A.

3.2.4.2 Total dynamical activity from parameterizing time

When we consider a time-dependent Hamiltonian $\hat{H}(t)$, there are multiple potential generalizations of the TDA which would reduce to Eq. (3.108) for a time-independent Hamiltonian. We will discuss two different parametrizations giving rise to inequivalent notions of activity and bounds on precision.

We first investigate the parametrization $\hat{H}_\theta(t) = \theta \hat{H}(\theta t)$. This parametrization is special since

$$\int_0^t d\tau \hat{H}_\theta(t) = \int_0^t d\tau \theta \hat{H}(\theta t) = \int_0^{t\theta} d\tau \hat{H}(\tau), \tag{3.114}$$

meaning that the unitary has the property

$$\hat{U}_\theta(t,0) = \hat{U}(\theta t, 0). \tag{3.115}$$

As a consequence, scaling θ remains equivalent to scaling time. If we define the TDA from this parametrization, we get the same expression as for the time-independent case, Eq. (3.109),

$$\mathscr{A}(t) = \frac{t^2}{2\hbar^2} \sum_{ij} \frac{(p_i - p_j)^2}{p_i + p_j} |\langle \psi_i | \hat{H}^{\mathrm{H}}(t) | \psi_j \rangle|^2 \leq \mathscr{A}^{\lim}(t) = \frac{t^2}{\hbar^2} \langle\langle (\hat{H}^{\mathrm{H}}(t))^2 \rangle\rangle. \tag{3.116}$$

This definition of a quantum dynamical activity is equivalent to the ones used in Refs. [46, 50, 110]. It is interesting to note that QFI for θ is closely related to the QFI for time due to Eq. (3.115). Concretely,

$$\mathcal{F}_{\theta\theta}(t) = t^2 \mathcal{F}_{tt}(t) \tag{3.117}$$

where $t^2\mathcal{F}_{tt}(t)$ was used as a definition of a quantum dynamical activity in Refs. [46, 110]. This, in turn, means that the bound (3.112) extends to the time-dependent

case if we use Eq. (3.116)

$$\frac{\left(t\partial_t\langle\hat{X}^{\mathrm{H}}(t)\rangle\right)^2}{\langle\langle(\hat{X}^{\mathrm{H}}(t))^2\rangle\rangle} \leq 4\mathscr{A}(t) \leq 4\frac{t^2}{\hbar^2}\langle\langle(\hat{H}^{\mathrm{H}}(t))^2\rangle\rangle. \tag{3.118}$$

Interesting connections to the geometry of quantum evolution [149] have been made for the QFI based on time [46, 50, 110]. We point out that $\langle\langle\hat{H}^2(t)\rangle\rangle$ often is used to quantify the speed of quantum evolution [148]. There are, however, situations where the variance does not give an insightful speed. This is the case for the Breit-Wigner state, which has finite average energy but infinite energy variance unless some sort of energy cutoff is introduced [148, 150]. Such issues are, however, not present in quantum systems with finite-dimensional discrete spectra.

Returning to Eq. (3.116), we note that it presents some conceptual issues when attempting to interpret it as an activity. To illustrate this, we use a two-level system with a time-independent Hamiltonian

$$\hat{H}_\theta = -\theta\hbar\omega\hat{\sigma}_z = \theta\hbar\omega(|e\rangle\langle e| - |g\rangle\langle g|). \tag{3.119}$$

The initial state $|+\rangle = (|g\rangle + |e\rangle)/\sqrt{2}$ results in the TDA

$$\mathscr{A}(t) = t^2\omega^2. \tag{3.120}$$

The quadratic scaling in time makes each precession around the Bloch sphere contribute a different amount of "activity", even though physically, they are all equivalent. The conceptual difficulties increase when we consider the time-dependent Hamiltonian

$$\hat{H}(t) = -\hbar\omega(t)\hat{\sigma}_z, \tag{3.121}$$

with the same initial state $|+\rangle$. The TDA reads as

$$\mathscr{A}(t) = t^2\omega^2(t). \tag{3.122}$$

In this case, $\mathscr{A}(t)$ is history agnostic, depending only on the instantaneous speed of evolution. To show the consequences of this local time-dependence, we consider a piecewise constant Hamiltonian

$$\hat{H}(t) = [\mathbf{1}_{[0,t_1]}(t) + \mathbf{1}_{[t_2,t_3]}(t)]\hbar\omega_z\hat{\sigma}_z + \mathbf{1}_{[t_1,t_2]}(t)\hbar\omega_x\hat{\sigma}_x, \tag{3.123}$$

where $0 \leq t_1 \leq t_2 \leq t_3$ and $\hat{\sigma}_x = |e\rangle\langle g| + |g\rangle\langle e|$. Here, we used the indicator function

$$\mathbf{1}_{[t_a,t_b]}(t) = \begin{cases} 1 & t \in [t_a, t_b], \\ 0 & \text{otherwise.} \end{cases} \tag{3.124}$$

Moreover, we consider the initial state $|+\rangle$, and we pick the time windows such that $\hat{U}(t_1, 0)|+\rangle = |+\rangle$. The evolution can be understood as follows: In the first time window $0 \leq t \leq t_1$, the state is precessing around the equator of the Bloch sphere, which $\mathscr{A}(t)$ counts as being "active". In the second time window $t_1 \leq t \leq t_2$, the state is not active since $\hat{\sigma}_x|+\rangle = |+\rangle$ while in the third time window the precession is restarted. This results in the following TDA

$$\mathscr{A}(t) = \begin{cases} \omega_z^2 t^2, & 0 \leq t \leq t_1, \\ 0, & t_1 \leq t \leq t_2, \\ \omega_z^2 t^2 & t_2 \leq t \leq t_3. \end{cases} \tag{3.125}$$

We emphasize that $\mathscr{A}(t)$ corresponds to Eq. (3.25), not the to activity rate. Here $\mathscr{A}(t)$ is very hard to interpret as something analogous to the classical activity. Due to the fact that the TDA is local in time, it is possible to extinguish it at a later time despite there being "activity" at an earlier time. This is very different from the standard number of jumps in Eq. (3.25), which instead accumulates over time. Furthermore, even though we would consider the system as being "inactive" in the second time window, when the precession is restarted in the third window, the activity does not pick up where it left off. Instead, due to the t^2 scaling, it jumps to a larger value, even though nothing has happened physically, but the change in time in our "clock". These strange properties call into question whether the parametrization used leads to a meaningful definition of activity for closed unitary dynamics when the Hamiltonian has explicit time-dependence.

An important distinction from the classical case is that we consider the quantum Fisher information (QFI) for the state of the system. In the classical case, the Fisher information that yielded the dynamical activity was defined from the probability of observing an entire trajectory, as in Eq. (3.10). In Refs. [46, 50] in the context of GKSL dynamics, a trajectory consisting of quantum jumps was encoded in the pure state of an auxiliary system.

However, there is no reason that we would desire a bound on the instantaneous current, such as (3.118), to be dependent on the entire evolution. As we noted earlier, the choice of parametrization $\hat{U}(\theta t, 0)$ is closely related to considering the QFI for time [46]. However, even for a classical rate equation with time-dependent rates, the classical Fisher Information with respect to time does not yield the standard dynamical activity Eq. (3.23). Instead, it is the parametrization $\theta W_{kl}^m(t)$ which would result in a CFI equal to the dynamical activity. Moreover, the classical KUR needs to be modified in order to hold for time-dependent rates, see Refs. [28, 151].

3.2.4.3 Total dynamical activity from parameterizing speed of protocol

As we have seen, basing the activity definition on rescaling time results in some potential conceptual difficulties. We can instead take inspiration from classical stochastic thermodynamics and rescale the speed of a protocol [28, 151]. To do this, we consider a Hamiltonian

$$\hat{H}(t,v) = \hat{H}(\lambda(tv)), \tag{3.126}$$

depending on a protocol $\lambda(tv)$ performed at a speed v, which under unitary dynamics yields a state

$$\hat{\rho}(t,v) = \hat{U}(t,0;v)\hat{\rho}(0)\hat{U}^{\dagger}(t,0;v). \tag{3.127}$$

We then parametrize the state as

$$\hat{\rho}_{\theta}(t,v) = \hat{\rho}(\theta t, v/\theta), \tag{3.128}$$

meaning that θ controls the speed of evolution. Scaling the speed of the protocol yields the parametrized unitary

$$\begin{aligned}\hat{U}_{\theta}(t,0;v) = \hat{U}(\theta t,0;v/\theta) &= T_{+}\exp\left\{-\frac{i}{\hbar}\int_{0}^{t\theta} d\tau \hat{H}(\lambda(\tau v/\theta))\right\} \\ &= T_{+}\exp\left\{-\frac{i}{\hbar}\int_{0}^{t} d\tau \theta \hat{H}(\lambda(\tau v))\right\}.\end{aligned} \tag{3.129}$$

Thus, this parametrization is equivalent to rescaling the total Hamiltonian as we did earlier for the time-independent case, with the QFI for a mixed initial state taking the form

$$\mathcal{F}_{\theta\theta}(t,v) = \frac{2}{\hbar^2}\sum_{ij}\frac{(p_i-p_j)^2}{p_i+p_j}|\left\langle\psi_i\right|\int_0^t d\tau \hat{H}^{\mathrm{H}}_{\theta}(\tau,v)\left|\psi_j\right\rangle|^2. \tag{3.130}$$

From this, we define the corresponding TDA as

$$\mathscr{A}(t,v) = \lim_{\theta\to 1}\mathcal{F}_{\theta\theta}(t,v) = \frac{1}{2\hbar^2}\sum_{ij}\frac{(p_i-p_j)^2}{p_i+p_j}|\left\langle\psi_i\right|\int_0^t d\tau \hat{H}^{\mathrm{H}}(\tau,v)\left|\psi_j\right\rangle|^2, \tag{3.131}$$

which is upper bounded by

$$\mathscr{A}(t,v) \leq \mathscr{A}^{\lim}(t,v) = \frac{1}{\hbar^2}\int_0^t d\tau \int_0^t d\tau' \langle\langle \hat{H}^{\mathrm{H}}(\tau,v)\hat{H}^{\mathrm{H}}(\tau',v)\rangle\rangle. \tag{3.132}$$

This parametrization yields a different bound on precision compared to (3.118), since

$$\partial_\theta \operatorname{tr}\Big\{\hat{X}^{\mathrm{H}}(\theta t, v/\theta)\hat{\rho}(0)\Big\} = (t\partial_t - v\partial_v)\operatorname{tr}\Big\{\hat{X}^{\mathrm{H}}(\theta t, v/\theta)\hat{\rho}(0)\Big\}. \tag{3.133}$$

Thus, using the QCRB, we find the following quantum KUR

$$\frac{\Big((t\partial_t - v\partial_v)\langle\hat{X}^{\mathrm{H}}(t,v)\rangle\Big)^2}{\langle\langle(\hat{X}^{\mathrm{H}}(t))^2\rangle\rangle} \leq 4\mathscr{A}(t,v) \leq 4\mathscr{A}^{\mathrm{lim}}(t,v). \tag{3.134}$$

The differential operator $t\partial_t - v\partial_v$ also appears in the formulations of the TUR, KUR and TKUR for time-dependent transition rates [28, 151]. Moreover, this definition of activity depends on the entire history of evolution in general. For example, if we again consider the Hamiltonian (3.121) with initial state $|+\rangle$, the TDA is calculated as

$$\mathscr{A}(t,v) = \left(\int_0^t d\tau\omega(\lambda(\tau v))\right)^2. \tag{3.135}$$

While the issue of t^2 scaling is still present, by parameterizing the speed of a protocol as in Eq. (3.128), we avoid some of the conceptual difficulties we encountered when we only rescaled time. Moreover, this activity bounds the precision in an observable (3.134) in an analogous fashion to the classical dynamical activity of a CTMP by including the sensitivity to the speed of the protocol [28, 151].

We have now investigated quite thoroughly how to define a quantum dynamical activity from a geometric perspective using the quantum Fisher information. This has, for instance, allowed us to derive the correlator-based activity definition (3.2.2.2) of Ref. [44], giving it a geometric interpretation. Moreover, we have seen that by considering the quantum dynamical activity for closed unitary dynamics, we obtain the time-energy uncertainty relation. However, at the same time, we identified some conceptual difficulties in the interpretation of activity. We have also found that defining the activity through the quantum Fisher information associated with the speed of a protocol yields a precision bound (3.134) analogous to the classical case [28, 151]. Still, identifying a notion of quantum dynamical activity that is both conceptually well motivated and operationally useful for precision bounds remains an open problem.

3.2.5 Estimating single particle transfer rates from noise

In this section, we will discuss how to estimate rates of single-particle transfers from particle current noise. The previous sections have been dedicated to discussing definitions of dynamical activity in quantum systems from a fundamental perspective. We are, however, sometimes interested in a more pragmatic way of

quantifying how "active" a system. The definitions based on quantum Fisher information have a clear interpretation and limit precision in a current, but they are not easily connected to standard measurable quantities in a transport scenario. Moreover, the correlator-based definition Eq. (3.42) [44] is likely to be difficult to measure since it is defined as a correlator in a joint bath system operator.

Furthermore, not all parts of an activity necessarily help us construct useful bounds on noise in quantum systems. This is, for example, the case in bosonic non-interacting transport as discussed in paper A. In such cases, reflection events are not needed to find a valid bound. It is therefore useful to estimate some parts of what we call activity from quantities which are easier to measure in practice. This is particularly appealing if the goal is thermodynamic inference of entropy production and we wish to avoid introducing additional difficult-to-measure quantities in our bounds.

To build intuition for how noise is related to transfer rates, we will consider a toy model of two reservoirs, $\alpha = \mathrm{L}, \mathrm{R}$, connected via an interface. The reservoirs are emitting non-interacting classical particles at rates γ_α which travel towards the interface where they are transmitted with probability D and reflected with probability $1 - D$. We assume that the number of particles emitted by reservoir α, $\breve{N}^{\mathrm{e}}_\alpha(t)$ between time 0 and t is Poisson distributed

$$p^{\mathrm{e}}_\alpha(\breve{N}^{\mathrm{e}}_\alpha(t) = n) = \frac{e^{-\gamma_\alpha t}(\gamma_\alpha t)^n}{n!}. \tag{3.136}$$

Since the particles are not influenced by each other at the interface, the number of particles transmitted $\breve{N}^{\mathrm{t}}_\alpha(t)$ from α at time t, given n attempts, follows a binomial distribution

$$p^{\mathrm{t}}_\alpha(\breve{N}^{\mathrm{t}}_\alpha(t) = k | \breve{N}^{\mathrm{e}}_\alpha(t) = n) = \frac{n!}{k!(n-k)!} D^k (1-D)^{n-k}, \tag{3.137}$$

which means that also $\breve{N}^{\mathrm{t}}_\alpha(t)$ is Poisson distributed

$$\begin{aligned} p^{\mathrm{t}}_\alpha(\breve{N}^{\mathrm{t}}_\alpha(t) = k) &= \sum_{n=k}^{\infty} p^{\mathrm{t}}_\alpha(\breve{N}^{\mathrm{t}}_\alpha(t) = k | \breve{N}^{\mathrm{e}}_\alpha(t) = n) p^{\mathrm{e}}_\alpha(\breve{N}^{\mathrm{e}}_\alpha(t) = n) \\ &= e^{-\gamma_\alpha t} \frac{(D\gamma_\alpha t)^k}{k!} \sum_{n=k}^{\infty} \frac{((1-D)\gamma_\alpha t)^{n-k}}{(n-k)!} = \frac{e^{-D\gamma_\alpha t}(D\gamma_\alpha t)^k}{k!}. \end{aligned} \tag{3.138}$$

We are interested in the net number of transfers across the interface between time 0 and t $\Delta\breve{N}(t) = \breve{N}^{\mathrm{t}}_{\mathrm{L}}(t) - \breve{N}^{\mathrm{t}}_{\mathrm{R}}(t)$, which is Skellam distributed [152]

$$p(\Delta\breve{N}(t) = m) = \sum_{k=-\infty}^{\infty} p^{\mathrm{t}}_{\mathrm{L}}(\breve{N}^{\mathrm{t}}_{\mathrm{L}}(t) = m + k) p^{\mathrm{t}}_{\mathrm{R}}(\breve{N}^{\mathrm{t}}_{\mathrm{R}}(t) = k), \tag{3.139}$$

with the corresponding cumulant generating function [152]

$$\chi(\xi) = \ln \left\langle e^{i\xi \Delta \breve{N}(t)} \right\rangle = tD\gamma_{\mathrm{L}}(e^{i\xi} - 1) + tD\gamma_{\mathrm{R}}(e^{-i\xi} - 1). \tag{3.140}$$

From the cumulant generating function, the average particle current and its noise are calculated as

$$I_{\mathrm{R}}^{(N)} = \partial_t \left\langle \Delta \breve{N} \right\rangle = D(\gamma_{\mathrm{L}} - \gamma_{\mathrm{R}}), \quad S_{\mathrm{RR}}^{(N)} = \partial_t \mathrm{Var}[\Delta \breve{N}] = D(\gamma_{\mathrm{L}} + \gamma_{\mathrm{R}}). \tag{3.141}$$

In this toy model, the average current is given by the difference in the rates of particles moving from L to R and from R to L and its noise is given by the sum of the rates. Notice that $S_{\mathrm{RR}}^{(N)}$ does not contain the rates of particles being reflected, $(1-D)\gamma_\alpha$. That the noise in a current takes the form of a sum of transfer rates is typical for systems where transfers are uncorrelated. The precision in the particle current obeys a KUR-like constraint[1]

$$\frac{\left(I_{\mathrm{R}}^{(N)}\right)^2}{S_{\mathrm{RR}}} \leq S_{\mathrm{RR}} = D(\gamma_{\mathrm{L}} + \gamma_{\mathrm{R}}). \tag{3.142}$$

It is only the rates of transfers contained in $S_{\mathrm{RR}}^{(N)}$ which are needed to constrain precision. By including e.g. the reflection events as done for the standard KUR, one obtains a bound which is not tight[2].

Particle transfers are generally not uncorrelated, and the current noise cannot be described by a weighted sum of rates. If, e.g. classical particles carry electrical charge, they could repel or attract each other, giving rise to correlations. Moreover, in quantum systems, transfers can become correlated even without any interaction due to quantum effects such as interference. This is indeed the case for scattering theory, see Sec. 2.3.2, where we discussed how bosonic particles displayed bunching while the fermionic ones displayed anti-bunching. As displayed in Eq. (2.53), the current noise in scattering theory was split into a classical part and a quantum part. The classical part [Eq. (2.54)] is indeed a sum of rates and contains single-particle effects. In the limit of weak transmission or small bias, this is the dominating term of the noise, since it is rarely the case that two particles with the same energy are scattered close together in time. In this limit, the current statistics in scattering theory are effectively captured by the toy model[3]. Also, in the case of the jump unravelling of the GKSL model when quantum jumps become uncorrelated, only the white noise remains, which is related to a sum of jump rates, see Eq. (2.121) and Eq. (2.122) [98].

It is thus a reasonable approach to estimate some useful parts of the activity, in

[1] This bound follows from $|\gamma_{\mathrm{L}} - \gamma_{\mathrm{R}}| \leq |\gamma_{\mathrm{L}} + \gamma_{\mathrm{R}}|$.
[2] Due to correlations, these reflection events are generally needed in the classical KUR (3.22).
[3] Energy dependence in the transmission D or the rates γ_α can be included.

this case, rates of single-particle transfers from the noise in a current. How this can be done for bosonic scattering theory is outlined in Sec. 4.1.1, while the fermionic case is covered in Sec. 4.1.2. The observation that current noise can be used to estimate single-particle transfer rates, once correlations are taken into account, is used to formulate pragmatic bounds on precision in the appended papers A and B of this thesis.

CHAPTER 4

Summary of appended papers

4.1 Kinetic Uncertainty Relations for Quantum Transport

The question that paper A addresses is whether it is possible to derive bounds on precision in the spirit of the classical KUR for coherent quantum transport beyond the weak coupling limit. In a semi-classical limit of scattering theory, where transport is primarily governed by single-particle transfers, we derive a local KUR. Away from this regime, bosonic and fermionic exchange statistics modify the bound in opposite ways due to bunching and anti-bunching, leading to a decrease and increase in precision, respectively.

We are interested in coherent transport, which is well described by scattering theory under the condition that many-body interactions are weak. Focusing on the single-channel case, a generic average current is given by

$$I_\alpha^{(\nu)} = \frac{1}{h}\int_0^\infty dE x_\alpha^{(\nu)}(E)\sum_\beta D_{\alpha\beta}(E)\left[f_\beta(E) - f_\alpha(E)\right]. \tag{4.1}$$

The noise in the current can be expressed in terms of a "classical" and "quantum" part $S_{\alpha\alpha}^{(\nu)} = S_{\alpha\alpha}^{(\nu)\mathrm{cl}} + S_{\alpha\alpha}^{(\nu)\mathrm{qu}}$ as discussed in Sec. 2.3. The classical noise term is

given by

$$S_{\alpha\alpha}^{(\nu)\mathrm{cl}} = \frac{1}{h}\int_0^\infty dE[x_\alpha^{(\nu)}(E)]^2\Big\{\sum_{\beta\neq\alpha} D_{\alpha\beta}(E)(F_{\alpha\beta}^{\pm}(E) + F_{\beta\alpha}^{\pm}(E))\Big\} \tag{4.2}$$

and the quantum part is

$$S_{\alpha\alpha}^{(\nu)\mathrm{qu}} = \pm\frac{1}{h}\int_0^\infty dE[x_\alpha^{(\nu)}(E)]^2\Big\{\sum_{\beta\neq\alpha} D_{\alpha\beta}(E)(f_\alpha(E) - f_\beta(E))\Big\}^2, \tag{4.3}$$

where the upper sign is for bosonic system and the lower sign is for fermionic systems.

In the regime where the system is either close to equilibrium, $|f_\alpha(E) - f_\beta(E)| \ll 1$, or the transmission probability is small, $D_{\alpha\beta}(E) \ll 1$, the dominating processes taking place are single-particle transfers. Therefore, the quantum part of the noise is negligible, such that the full noise is approximated well by the classical part of the noise $S_{\alpha\alpha}^{(\nu)} \approx S_{\alpha\alpha}^{(\nu)\mathrm{cl}}$. As discussed in Sec. 3.2.5, when there are only single-particle transfers, the bosonic and fermionic exchange statistics do not matter for the dynamics to the same extent[1], and the transfers become uncorrelated. In a classical Markov process where the transitions are Poissonian, i.e., uncorrelated, the noise in a counting observable takes the form of a sum of weighted transfer rates [98]. The same is true here, where the classical noise in the particle current is given by

$$S_{\alpha\alpha}^{(N)\mathrm{cl}} = \Gamma_\alpha^{\rightarrow} + \Gamma_\alpha^{\leftarrow} \equiv \mathcal{K}_\alpha^{\mathrm{cross}}\,, \tag{4.4}$$

and the rates of particle exchanges with the reservoir α are

$$\begin{aligned}\Gamma_\alpha^{\rightarrow} &= \frac{1}{h}\sum_{\beta\neq\alpha}\int_0^\infty dE D_{\alpha\beta}(E)F_{\alpha\beta}^{\pm}(E),\\ \Gamma_\alpha^{\leftarrow} &= \frac{1}{h}\sum_{\beta\neq\alpha}\int_0^\infty dE D_{\alpha\beta}(E)F_{\beta\alpha}^{\pm}(E).\end{aligned} \tag{4.5}$$

Notice that these rates only count transfers between reservoirs, and no contributions from a particle being reflected back into the reservoir from which it came. We call this limit the *semi-classical* limit of scattering theory in the sense that particle transfers become uncorrelated. However, quantum effects can still enter the transmission function and the average occupations.

The first main result of paper A is a local KUR in the semi-classical limit of

[1] The exchange statistics still enter average occupations and transfer rates via $F_{\alpha\beta}^{\pm}(E)$.

scattering theory. By using the two inequalities

$$x^2 + \frac{1}{4} \geq |x|, \quad |x+y| \geq |x-z| \forall x, z \geq 0, \tag{4.6}$$

a bound on the classical noise of a generic current is derived

$$S_{\alpha\alpha}^{(\nu)\mathrm{cl}} + \frac{y^2}{4} S_{\alpha\alpha}^{(N)\mathrm{cl}} - y \left| I_\alpha^{(\nu)} \right| \geq 0, \tag{4.7}$$

where a parameter $y > 0$ guarantees consistent units. Similar to the procedure used in Refs. [36, 42], we notice that (4.7) defines a positive quadratic form. Minimizing (4.7) with the optimal value $y = 2|I_\alpha^{(\nu)}|/S_{\alpha\alpha}^{(N)\mathrm{cl}}$ yields a KUR

$$\mathcal{K}_\alpha^{\mathrm{cross}} = S_{\alpha\alpha}^{(N)\mathrm{cl}} \geq \frac{\left(I_\alpha^{(\nu)}\right)^2}{S_{\alpha\alpha}^{(\nu)\mathrm{cl}}} \equiv \mathcal{P}_\alpha^{(\nu)\mathrm{cl}}. \tag{4.8}$$

There are a few differences between the bound (4.8) and the standard classical KUR (3.22). As discussed earlier, the $\mathcal{K}_\alpha^{\mathrm{cross}}$ does not count events where a particle from reservoir α is reflected into α while the activity used in the standard KUR does count these events. More importantly, the standard KUR uses the activity of the whole system, while (4.8) uses a *local* activity which counts the particle transfers with respect to a single reservoir. It is *necessary* to use a local activity in this regime to get a tight bound, since $\mathcal{P}_\alpha^{(\nu)\mathrm{cl}} \leq \sum_\alpha \mathcal{K}_\alpha^{\mathrm{cross}}$ could never be tight.

While the bound (4.8) has a clear conceptual interpretation, it is only valid in the semi-classical regime and in general, we cannot approximate the full noise by the classical part. To go beyond this limit, we analyze the quantum noise separately, highlighting the differences in achieving precision in bosonic and fermionic systems.

4.1.1 Bosonic bounds

For the bosonic case, the Cauchy-Schwarz inequality implies

$$S_{\alpha\alpha}^{(\nu)\mathrm{qu}} \geq \frac{h}{B_\alpha^\nu} \left(I_\alpha^{(\nu)}\right)^2, \tag{4.9}$$

where we defined the *bandwidth* $B_\alpha^\nu = \int_0^\infty dE \zeta_\alpha^\nu(E)$ using the indicator function $\zeta_\alpha^\nu(E) = 1$ if $E \in \mathrm{supp}\{x_\alpha^{(\nu)} \sum_\beta D_{\alpha\beta}(f_\alpha - f_\beta)\}$ and $\zeta_\alpha^\nu(E) = 0$ otherwise. This bound extends to the full noise $B_\alpha^\nu/h \geq (I_\alpha^{(\nu)})^2/S_{\alpha\alpha}^{(\nu)}$. These inequalities capture a completely different aspect of achieving precision in bosonic systems: the effect of quantum-mechanical bunching. The bandwidth B_α^ν is the energy range over which there is, on average, transport of the generalized charge $x_\alpha^\nu(E)$. The intuitive interpretation of this bound is that as the bandwidth decreases, the relative weight

of states with equal energy increases, leading to bunching. Consequently, a small bandwidth leads to large quantum noise at a fixed current and hence to a limited precision. Thus, to improve precision in bosonic systems, it is beneficial to spread out transport over a large energy interval. Infinite bandwidth would make the (4.9) trivial.

Since in the bosonic case the full noise is greater than the classical noise $S^{(\nu)}_{\alpha\alpha} \geq S^{(\nu)\mathrm{cl}}_{\alpha\alpha}$, we can extend the KUR (4.8) as

$$\mathcal{K}^{\mathrm{cross}}_{\alpha} \geq \frac{\left(I^{(\nu)}_{\alpha}\right)^2}{S^{(\nu)}_{\alpha\alpha}} \equiv \mathcal{P}^{(\nu)}_{\alpha}. \tag{4.10}$$

However, by taking into account the effect of bunching on precision, we construct a stricter bound by combining (4.9) and (4.8)

$$\mathcal{M}^{\nu}_{\alpha}\left[\mathcal{K}^{\mathrm{cross}}_{\alpha}\right] \equiv \frac{\mathcal{K}^{\mathrm{cross}}_{\alpha}}{1+\frac{h}{B^{\nu}_{\alpha}}\mathcal{K}^{\mathrm{cross}}_{\alpha}} \geq \mathcal{P}^{(\nu)}_{\alpha}. \tag{4.11}$$

In the limit of $B^{\nu}_{\alpha} \to \infty$ this bound reduces to $\mathcal{K}^{\mathrm{cross}}_{\alpha} \geq \mathcal{P}^{(\nu)}_{\alpha}$. When the bandwidth has a finite value, (4.11) is a stricter bound on precision compared to what is possible to show for a classical system. As a consequence, in bosonic non-interacting transport, precision is worse compared to classical transport.

To constrain precision in a similar way to the classical KUR, we found that $\mathcal{K}^{\mathrm{cross}}_{\alpha}$ contains the useful parts of the activity. In general, one might not have access to $\mathcal{K}^{\mathrm{cross}}_{\alpha}$ because the noise contains excess correlations due to the bosonic exchange statistics. As discussed in Sec. 3.2.5, one approach is to estimate the single-particle transfer rates in terms of more common transport observables. To estimate $\mathcal{K}^{\mathrm{cross}}_{\alpha}$ we bound the excess noise due to bunching by introducing the function $\delta S^{(\nu)}_{\alpha\alpha} \equiv S^{(\nu)}_{\alpha\alpha} - h(I^{(\nu)}_{\alpha})^2/B^{\nu}_{\alpha} \geq \mathcal{K}^{\mathrm{cross}}_{\alpha}$ which we use in the bound

$$\mathcal{M}^{\nu}_{\alpha}\left[\delta S^{(N)}_{\alpha\alpha}\right] \geq \mathcal{M}^{\nu}_{\alpha}\left[\mathcal{K}^{\mathrm{cross}}_{\alpha}\right] \geq \mathcal{P}^{(\nu)}_{\alpha}. \tag{4.12}$$

In the limit of $B^{\nu}_{\alpha} \to \infty$, this sequence of bound reduces to $S^{(N)}_{\alpha\alpha} \geq \mathcal{K}^{\mathrm{cross}}_{\alpha} \geq \mathcal{P}^{(\nu)}_{\alpha}$, i.e. the precision in a generic current is limited by the particle current noise.

4.1.2 Fermionic bounds

In the fermionic case, the situation is opposite compared to the bosonic, since for fermions $S^{(\nu)}_{\alpha\alpha} \leq S^{(\nu)\mathrm{cl}}_{\alpha\alpha}$, due to the Pauli exclusion principle. As a consequence, the classical bound breaks

$$\mathcal{K}^{\mathrm{cross}}_{\alpha} \ngeq \frac{\left(I^{(\nu)}_{\alpha}\right)^2}{S^{(\nu)}_{\alpha\alpha}}. \tag{4.13}$$

Since the classical KUR constrains precision by using the total activity, counting transitions in the entire system, one might expect that a more inclusive notion of activity could salvage (4.1.2)[2]. For example, by using the correlator-based definition (3.42) [44], which contains effects of reflection events. This is, however, not the case [44], even if one considers the correlation-based activity for multiple reservoirs[3].

Instead, we take a similar approach as we did for the bosonic case and establish a bound on the quantum part of the noise. Using Jensen's inequality, and defining the minimum reflection probability $R_\alpha \equiv \inf_{E\in A} D_{\alpha\alpha}(E)$, we prove a general lower bound on the fermionic quantum noise

$$S_{\alpha\alpha}^{(\nu)\mathrm{qu}} \geq -(1-R_\alpha)S_{\alpha\alpha}^{(\nu)\mathrm{cl}} \implies \frac{S_{\alpha\alpha}^{(\nu)}}{R_\alpha} \geq S_{\alpha\alpha}^{(\nu)\mathrm{cl}}. \tag{4.14}$$

With this bound, we extend the classical KUR (4.8) to hold for the full noise in a generic current, which results in the following sequence of bounds

$$\frac{1}{R_\alpha}\frac{S_{\alpha\alpha}^{(N)}}{R_\alpha} \geq \frac{1}{R_\alpha}\mathcal{K}_\alpha^{\mathrm{cross}} \geq \mathcal{P}_\alpha^{(\nu)}. \tag{4.15}$$

Here we used $S_{\alpha\alpha}^{(N)}/R_\alpha \geq \mathcal{K}_\alpha^{\mathrm{cross}}$ as an estimate of the rate of single-particle transfers. Notice that this bound is less strict than the classical counterpart (4.8) since $1 \geq R_\alpha \geq 0$. If the scatterer is fully transparent for some energy $R_\alpha = 0$, (4.15) becomes a trivial statement as the upper bound diverges. This, however, reflects the fact that for fermionic ballistic transport in a fully transparent conductor, it is theoretically possible to completely suppress the noise in, e.g., the particle current, while the current is finite. The suppression of noise in fermionic transport has been experimentally observed [153, 154]. Even though the bound is trivial for a fully transparent conductor, it still is a tight bound for any finite fixed value of R_α. As a final note, we point out that none of the results found in paper A required the transmission function $D_{\alpha\beta}(E)$ to be symmetric, meaning that the results hold independent of the status of time-reversal symmetry in the system. Furthermore, there were no assumptions on the reservoirs' occupation numbers, meaning that the bounds also hold for nonthermal systems.

[2] If one extends the activity to include the dynamics generated by the full Hamiltonian, this is the case, as demonstrated in Sec. 3.2.4.1.

[3] This can be easily verified in a two-terminal system at the high-transparency, low-temperature limit.

4.2 Combining kinetic and thermodynamic uncertainty relations in quantum transport

Paper B extends the logic of Paper A from KURs to the unified Thermodynamic Kinetic Uncertainty Relation (TKUR) for coherent quantum transport. This is done by first deriving a TKUR in the semi-classical limit of scattering theory after which the bounds on quantum noise (4.9) and (4.14) are applied to extend the TKUR beyond the semi-classical regime. Paper B also contains the generalization of these bounds to the multichannel case and bounds aimed at inference of entropy production.

The TKUR (3.24), first discovered in Ref. [151] for classical Markov processes and then extended to GKSL dynamics in Ref. [48], unites the thermodynamic and kinetic uncertainty relations in the sense that close to equilibrium, it reduces to the TUR, and the KUR far from equilibrium. In the intermediate regime the TKUR interpolates between the two bounds [151]. Furthermore, it is always a tighter bound compared to the separate bounds.

4.2.1 Unified thermokinetic uncertainty relation

The first main result of Paper B is a TKUR in the semi-classical limit of scattering theory. By applying Jensen's inequality we find that the sum of precisions is bounded by a function of transfer rates and entropy production

$$\sum_{\alpha} \mathcal{P}_{\alpha}^{(\nu)\mathrm{cl}} \leq \frac{\lambda\sigma}{k_{\mathrm{B}}} \Xi\left[\frac{\lambda\sigma}{k_{\mathrm{B}}\mathcal{K}^{\mathrm{cross}}}\right] \leq \min\left\{\lambda\sigma/k_{\mathrm{B}}, \mathcal{K}^{\mathrm{cross}}\right\}, \tag{4.16}$$

where $\Xi[x] \equiv x/\Omega^2[x]$ and $\Omega[x]$ is the inverse function of $x\tanh x$. In addition, we defined the total activity counting transfers between reservoirs

$$\mathcal{K}^{\mathrm{cross}} = \sum_{\alpha} \mathcal{K}_{\alpha}^{\mathrm{cross}}, \tag{4.17}$$

and the asymmetry in the transmissions,

$$\lambda \equiv \max_{E,\alpha,\beta} \frac{D_{\alpha\beta}(E) + D_{\beta\alpha}(E)}{2D_{\alpha\beta}(E)}. \tag{4.18}$$

The factor λ quantifies the asymmetry in the transmission function, and thereby the degree of Time-Reversal Symmetry (TRS) breaking. If the system has TRS, the transmission function is symmetric and $\lambda = 1$. For the extreme case of broken TRS where transport becomes unidirectional, the asymmetry diverges $\lambda \to \infty$. In this limit the bound reduces to a KUR, $\sum_{\alpha} \mathcal{P}_{\alpha}^{(\nu)\mathrm{cl}} \leq \mathcal{K}^{\mathrm{cross}}$.

The classical TUR can be violated due to the breaking of time-reversal symmetry,

e.g., in the presence of magnetic fields [36, 122]. This is a consequence of local-detailed balance not being fulfilled. It has been shown in various contexts that for fermionic ballistic transport, a bound on entropy production in a system with TRS can be generalized to a system without, by the inclusion of a numerical factor [36, 41–43]. If a similar numerical constant can be found for the TUR in bosonic systems[4] or for the TKUR (4.16) remains an open question.

A distinction between (4.16) and the standard TKUR lies in its ability to bound the sum of precisions across all terminals, whereas the original version (3.24) [151] limits the precision of a single current. This is in analogy with the KUR (4.8) of Paper A using an activity with respect to a single reservoir. Furthermore, TKURs that utilize the transfer rates of single reservoir $\mathcal{K}_\alpha^{\text{cross}}$, where also derived in Paper B. The generalization of TKUR of (4.16) beyond the semi-classical limit is analogous to the extension of the KUR performed in Paper A, using the multi-channel version of the bounds on the quantum noise.

4.2.2 Bound for inference of entropy production

An interesting use case of the TUR is to perform thermodynamic inference of the entropy production by measuring a current and its noise [120]. While this allows one to estimate a lower bound for the entropy production, it is, in general, only close to the true value when the system is near equilibrium. The TKUR, on the other hand, can be tight over a much wider range of circumstances, allowing it to provide an improved estimate of σ [151]. We derive a closely related but not equivalent bound to the TKUR for thermodynamic inference

$$\sum_\alpha \frac{1}{2} \ln \left[\frac{\sqrt{\boldsymbol{\mathcal{K}}_\alpha} + \sqrt{\boldsymbol{\mathcal{P}}_\alpha}}{\sqrt{\boldsymbol{\mathcal{K}}_\alpha} - \sqrt{\boldsymbol{\mathcal{P}}_\alpha}} \right] \sqrt{\boldsymbol{\mathcal{K}}_\alpha \boldsymbol{\mathcal{P}}_\alpha} \leq \frac{\lambda \sigma}{k_{\text{B}}}, \tag{4.19}$$

where $\boldsymbol{\mathcal{K}}_\alpha$ represents an estimate of $\mathcal{K}_\alpha^{\text{cross}}$ and $\boldsymbol{\mathcal{P}}_\alpha$ is a function of precision in a current. This works particularly well for the bosonic case, where we can estimate the single-particle transfer rates from the particle current noise $S_{\alpha\alpha}^{(N)} \geq \mathcal{K}_\alpha^{\text{cross}}$

$$\sum_\alpha \mathcal{P}_\alpha^{(\nu)} \leq \sum_\alpha \frac{1}{2} \ln \left[\frac{\sqrt{S_{\alpha\alpha}^{(N)}} + \sqrt{\mathcal{P}_\alpha^{(\nu)}}}{\sqrt{S_{\alpha\alpha}^{(N)}} - \sqrt{\mathcal{P}_\alpha^{(\nu)}}} \right] \sqrt{S_{\alpha\alpha}^{(N)} \mathcal{P}_\alpha^{(\nu)}} \leq \frac{\lambda \sigma}{k_{\text{B}}}. \tag{4.20}$$

Therefore, by measuring, for instance, the particle current and its noise, we obtain a more accurate estimate of σ by inserting the values into the logarithm, compared to using the TUR, which relies on precisely the same quantities. Moreover, by taking into account the effects of bunching in the estimate of $\mathcal{K}_\alpha^{\text{cross}}$ via (4.1.1), the

[4] A key difference between the bosonic and fermionic cases is the fact that the fermionic average occupations are upper bounded by 1 while the bosonic ones can become arbitrarily large.

inference bound (4.20) is improved.

By focusing on the semi-classical limit, we can make an interpretation of the TKUR and the inference bound (4.19). Using the precision of the particle current, the inference bound is simplified as

$$\sum_{\alpha} \frac{1}{2} \ln \left[\frac{\sqrt{S^{(N)\mathrm{cl}}_{\alpha\alpha}} + \sqrt{\mathcal{P}^{(N)\mathrm{cl}}_{\alpha}}}{\sqrt{S^{(N)\mathrm{cl}}_{\alpha\alpha}} - \sqrt{\mathcal{P}^{(N)\mathrm{cl}}_{\alpha}}} \right] \sqrt{S^{(N)\mathrm{cl}}_{\alpha\alpha} \mathcal{P}^{(N)\mathrm{cl}}_{\alpha}} = \sum_{\alpha} \frac{1}{2} \ln \left[\frac{\Gamma^{\leftarrow}_{\alpha}}{\Gamma^{\rightarrow}_{\alpha}} \right] (\Gamma^{\leftarrow}_{\alpha} - \Gamma^{\rightarrow}_{\alpha}) \leq \frac{\lambda \sigma}{k_{\mathrm{B}}}. \tag{4.21}$$

This highlights that TKUR (4.16) and the inference bound (4.19) are closely related to coarse-grainings of the expression of the entropy production in a system with time reversal symmetry [Eq. (2.43) [42]]. We note that the results of Paper B were derived without assuming that the average occupations are thermal. This means that, for instance, one could use the inference bounds to estimate entropy production of a non-thermal reservoir, something which would be difficult to measure directly.

4.3 Precision of an autonomous demon exploiting nonthermal resources and information

Paper C investigates an autonomous electronic device, based on capacitively coupled quantum dots acting as a demon. This system was previously studied in Ref. [155, 156], where two distinct regimes, (I) and (II), were identified. In regime (I), the device utilizes information and acts as a Maxwell demon [157–167], while in regime (II), the device is exploiting a nonthermal resource and acts as a so called N-demon [74, 168–171]. The goal of the device is refrigeration, and while this is achieved in both regimes, the cooling power displays much higher precision in (II) compared to (I). The main goal of paper C is to explain the difference in the precision of the cooling power between the two regimes.

The device, which consists of three coupled quantum dots, is divided into a resource region and a working substance. The working substance contains a quantum dot coupled to two electronic reservoirs L and R, with temperatures $T_{\mathrm{L}} \geq T_{\mathrm{R}}$. The resource region consists of a hot bath with temperature T_{H} and a cold bath at temperature T_{C}, simulating a nonthermal resource. Each resource reservoir is connected to one of two quantum dots. The capacitive coupling between the three quantum dots allows them to exchange energy and information by correlating their states, but not particles. In both regimes (I) and (II), there is an average heat flow out of R into L without there being an average flow of energy between the working substance and the resource region. Under the assumption of weak dot-reservoir coupling and Coulomb blockade, the dynamics are modelled as a continuous-time Markov process. Moreover, stochastic trajectories and full counting statistics were

utilized.

To characterize the performance in situations (I) and (II), the tightness of the TUR, the KUR, and a local KUR inspired by the results of Paper A are tested for the precision in the cooling power. It is found that all of the bounds are closer to being saturated in the more precise situation (II) compared to (I). Interestingly, the TUR performs better than the KUR, indicating that despite the rather large temperature differences present, the device is effectively operating close to equilibrium. The local KUR reaches comparable saturation as the TUR, but it should be noted that the local KUR is not expected to be a valid bound for the system, as the capacitive coupling causes the transfers of electrons to become correlated. The bound is, however, not found to be violated while the device operates as a demon. This analysis makes the difference in performance of the two regimes apparent but does not yet explain its origin.

The fundamental explanation is obtained by carrying out a more detailed analysis based on the stochastic trajectory analysis of Ref. [156], the framework of stochastic excursions introduced in Refs. [172, 173], and current cross-correlations. By studying the device at this level, we understand how the noise and correlations are induced, making the differences between regimes (I) and (II) clear. In Regime (II), all the dominant cycles contribute to cooling down R, while in regime (I), this is not the case: some dominant cycles are counterproductive and heat R. By suppressing the counterproductive cycles on a fluctuating level, the N-demon achieves a much higher precision than the information-based regime.

This analysis showcases how we can gain a fundamental understanding of a device's working principle by going beyond average quantities and studying cross-correlations and noise on the fluctuating level of single cycles.

CHAPTER 5

Conclusions

5.1 Summary

This thesis and the appended papers have investigated how fluctuations affect the thermodynamic performance of quantum systems with a focus on thermodynamic and kinetic uncertainty relations. In Papers A and B, bounds on current noise were derived in the spirit of thermodynamic and kinetic uncertainty relations for coherent transport out of equilibrium. By estimating transfer rates from particle current noise, we have shown one way to establish bounds on precision. This idea was further applied in Paper B to formulate bounds for thermodynamic inference based on current and noise measurements, thereby avoiding the introduction of additional, difficult-to-measure notions of dynamical activity. In Paper C, the thermodynamic and Kinetic uncertainty relations were applied to quantify the performance of an autonomous demon performing refrigeration. Furthermore, by studying the distinct operating regimes through stochastic cycles and current correlations, we explained the difference in performance as originating from their detailed operating principles.

A key issue when extending the kinetic uncertainty relation to quantum systems is the definition of dynamical activity. This is not only a technical issue but also a conceptual one. While the notion of dynamical activity in classical stochastic dynamics is intuitive, the counterpart in quantum systems is more subtle. Hence, a substantial part of this thesis has been devoted to comparing different notions of quantum dynamical activity. In Sec. 3.2.3.2, we introduced a *partial dynamical activity* based on information geometry, which helps us to put the correlator-

based definition (3.2.2.2) [44] in relation with the quantum Fisher-based definitions used in [46, 50]. In Secs. 3.2.4.2 and 3.2.4.3, the conceptual difficulties associated with defining dynamical activity in closed quantum systems with time-dependent Hamiltonians were discussed, together with the introduction of a notion based on the speed of a protocol. Finally, Sec. 3.2.5 highlighted a complementary pragmatic viewpoint, where in suitable regimes, useful parts of "activity", namely single-particle transfer rates, can be estimated from particle-current noise.

5.2 Outlook

Several questions remain unanswered. As discussed in Sec. 3.2, there are multiple inequivalent notions of dynamical activity for quantum systems. Identifying a notion of quantum dynamical activity that is both conceptually well motivated and operationally useful for precision bounds remains an open problem. If we wish to use the partial dynamical activity (3.62) to formulate bounds on precision, we would like to connect the memory term of (3.102) to measurable quantities. Moreover, we would like to do the same for the partial dynamical activity away from thermal equilibrium. Whether this is possible in specific out-of-equilibrium situations remains to be seen.

From a practical standpoint, it would be interesting to apply the idea of estimating transfer rates from particle-current noise to the jump unravelling of the GKSL master equation, as this might result in precision bounds in terms of measurable quantities in a regime that is highly relevant for quantum technologies.

As shown in Papers A and B in noninteracting or linear bosonic transport, precision is reduced due to bunching. How nonlinearities can be used to increase precision in bosonic transport is currently being investigated.

APPENDIX A

Correlator-based activity for linear bosonic transport

In this section, we calculate the correlator-based definition of the dynamical activity (3.42) for bosonic linear transport using the NEGF method, as introduced in Sec. 2.4. For simplicity of notation, we show the calculation for a central system C connected to two reservoirs L and R. The extension to the multiterminal case is analogous.

We consider a harmonic network [83] and let a column vector $\hat{u}$ contain all (rescaled) positions, and write the total Hamiltonian by partitioning the network into a left, center, and right part

$$\hat{H} = \sum_{\alpha=\mathrm{L,C,R}} \hat{H}_\alpha + \hat{V}_\mathrm{L} + \hat{V}_\mathrm{R}, \tag{A.1}$$

where $\hat{H}_\alpha = (1/2)(\dot{\hat{u}}^\alpha)^T \dot{\hat{u}}^\alpha + (1/2)(\hat{u}^\alpha)^T \mathbf{K}^\alpha \hat{u}^\alpha$, $\hat{V}_\mathrm{L} = (\hat{u}^\mathrm{L})^T \mathbf{V}^{\mathrm{LC}} \hat{u}^\mathrm{C}$ and $\hat{V}_\mathrm{R} = (\hat{u}^\mathrm{C})^T \mathbf{V}^{\mathrm{CR}} \hat{u}^\mathrm{R}$. Here $\hat{u}^\alpha$ is a column vector containing all positions of the α section of the network, such that $\hat{u} = (\hat{u}^\mathrm{L}, \hat{u}^\mathrm{C}, \hat{u}^\mathrm{R})^T$. We have the following property $\mathbf{V}^{\mathrm{LC}} = (\mathbf{V}^{\mathrm{CL}})^T$ and

$$\mathbf{K} = \begin{pmatrix} \mathbf{K}^\mathrm{L} & \mathbf{V}^{\mathrm{LC}} & 0 \\ \mathbf{V}^{\mathrm{CL}} & \mathbf{K}^\mathrm{C} & \mathbf{V}^{\mathrm{CR}} \\ 0 & \mathbf{V}^{\mathrm{RC}} & \mathbf{K}^\mathrm{R} \end{pmatrix} = \mathbf{k} + \mathbf{V}, \tag{A.2}$$

where $\mathbf{k} = \mathrm{diag}\{\mathbf{K}^{\mathrm{L}}, \mathbf{K}^{\mathrm{C}}, \mathbf{K}^{\mathrm{R}}\}$. We define a contour-ordered Green's function

$$G(\tau, \tau') = -\frac{i}{\hbar} \left\langle \mathbf{T}_{\mathcal{C}} \hat{u}(\tau) \hat{u}(\tau')^T \right\rangle, \tag{A.3}$$

which obeys the equation of motion [83]

$$\frac{\partial^2 G(\tau, \tau')}{\partial^2 \tau} = -\mathbf{K} G(\tau, \tau') - \delta(\tau, \tau') I, \tag{A.4}$$

and the following Dyson equation

$$G(\tau, \tau') = g(\tau, \tau') + \int_{\mathcal{C}} d\tau'' g(\tau, \tau'') \mathbf{V} G(\tau'', \tau'), \tag{A.5}$$

where $g(\tau, \tau')$ are the uncoupled Green's functions. Next, we calculate the correlator used to define activity (3.42) [44],

$$\mathcal{K}_\alpha(t) = \frac{1}{2\hbar^2} \int_{-t}^{t} dt' \langle\langle \{V_\alpha(t), V_\alpha(t+t')\} \rangle\rangle = \frac{1}{\hbar^2} \mathrm{Re} \int_{-t}^{t} dt' \langle\langle V_\alpha(t) V_\alpha(t+t') \rangle\rangle. \tag{A.6}$$

Focusing on the left section, and applying Wick's theorem we find

$$\begin{aligned} \mathcal{K}_{\mathrm{L}}(t) &= \frac{1}{\hbar^2} \mathrm{Re} \int_{-t}^{t} dt' \left\langle \left\langle (\hat{u}^{\mathrm{L}}(t))^T \mathbf{V}^{\mathrm{LC}} \hat{u}^{\mathrm{C}}(t) (\hat{u}^{\mathrm{L}}(t+t'))^T \mathbf{V}^{\mathrm{LC}} \hat{u}^{\mathrm{C}}(t+t') \right\rangle \right\rangle \\ &= \frac{1}{\hbar^2} \mathrm{Re} \int_{-t}^{t} dt' \mathbf{V}^{\mathrm{LC}}_{ij} \mathbf{V}^{\mathrm{LC}}_{kl} \big\{ \left\langle \hat{u}^{\mathrm{L}}_i(t) \hat{u}^{\mathrm{L}}_k(t+t') \right\rangle \left\langle \hat{u}^{\mathrm{C}}_j(t) \hat{u}^{\mathrm{C}}_l(t+t') \right\rangle + \\ &\qquad + \left\langle \hat{u}^{\mathrm{L}}_i(t) \hat{u}^{\mathrm{C}}_l(t+t') \right\rangle \left\langle \hat{u}^{\mathrm{C}}_j(t) \hat{u}^{\mathrm{L}}_k(t+t') \right\rangle \big\}. \end{aligned} \tag{A.7}$$

Here, repetition of the indices implies summation (except L,C,R). Defining the greater Green's function $G^{>}_{j,k}(t,t') = -i\langle \hat{u}_j(t) \hat{u}_k(t') \rangle / \hbar$ and using $G^{<}_{j,k}(t,t') = G^{>}_{k,j}(t',t)$ along with time translation invariance in the long time limit, such that $G^{>}_{j,k}(t,t') = G^{>}_{j,k}(t-t')$, we calculate $\lim_{t\to\infty} \mathcal{K}_{\mathrm{L}}(t) = \mathcal{K}_{\mathrm{L}}$,

$$\begin{aligned} \mathcal{K}_{\mathrm{L}} &= -\mathrm{Re} \int_{-\infty}^{\infty} dt' \mathbf{V}^{\mathrm{LC}}_{ij} \mathbf{V}^{\mathrm{LC}}_{kl} \Big\{ G^{>}_{\mathrm{L}i,\mathrm{L}k}(t, t+t') G^{>}_{\mathrm{C}j,\mathrm{C}l}(t, t+t') + \\ &\qquad + G^{>}_{\mathrm{L}i,\mathrm{C}l}(t, t+t') G^{>}_{\mathrm{C}j,\mathrm{L}k}(t, t+t') \Big\} \\ &= -\mathrm{Re} \int \frac{d\omega}{2\pi} \mathrm{tr}\big\{ \mathbf{V}^{\mathrm{CL}} G^{<}_{\mathrm{LL}}(\omega) \mathbf{V}^{\mathrm{LC}} G^{>}_{\mathrm{CC}}(\omega) \big\} + \mathrm{tr}\big\{ \mathbf{V}^{\mathrm{LC}} G^{<}_{\mathrm{CL}}(\omega) \mathbf{V}^{\mathrm{LC}} G^{>}_{\mathrm{CL}}(\omega) \big\}. \end{aligned} \tag{A.8}$$

To proceed, we need to express $\mathcal{K}_{\mathrm{L}}$ in terms of Green's functions of the central region. Both $G = g + g\mathbf{V}G$ and $G = g + G\mathbf{V}g$ are valid Dyson equations Ref. [83]. Note that these are symbolic expressions for the convolutions. By using both

versions of the Dyson equation, we can avoid calculating some additional Green's functions, e.g., $G_{\mathrm{LC}}(\omega)$. Using the Dyson equation $G = g + G\mathbf{V}g$ and Langreth's theorem [83], it follows that

$$G^{<,>}_{\mathrm{CL}}(t,t') = \int dt'' G^{r}_{\mathrm{CC}}(t,t'')\mathbf{V}^{\mathrm{CL}} g^{<,>}_{\mathrm{L}}(t'',t') + G^{<,>}_{\mathrm{CC}}(t,t'')\mathbf{V}^{\mathrm{CL}} g^{a}_{\mathrm{L}}(t'',t'), \quad \text{(A.9)}$$

which, for the steady state, gives

$$G^{<,>}_{\mathrm{CL}}(\omega) = G^{r}_{\mathrm{CC}}(\omega)\mathbf{V}^{\mathrm{CL}} g^{<,>}_{\mathrm{L}}(\omega) + G^{<,>}_{\mathrm{CC}}(\omega)\mathbf{V}^{\mathrm{CL}} g^{a}_{\mathrm{L}}(\omega). \quad \text{(A.10)}$$

If we use $G = g + g\mathbf{V}G$ instead, we find

$$G^{<,>}_{\mathrm{LL}}(t,t') = g^{<,>}_{\mathrm{L}}(t,t') + \int dt'' g^{r}_{\mathrm{L}}(t,t'')\mathbf{V}^{\mathrm{LC}} G^{<,>}_{\mathrm{CL}}(t'',t') + g^{<,>}_{\mathrm{L}}(t,t'')\mathbf{V}^{\mathrm{LC}} G^{a}_{\mathrm{CL}}(t'',t'), \quad \text{(A.11)}$$

and

$$G^{<,>}_{\mathrm{LL}}(\omega) = g^{<,>}_{\mathrm{L}}(\omega) + g^{r}_{\mathrm{L}}(\omega)\mathbf{V}^{\mathrm{LC}} G^{<,>}_{\mathrm{CL}}(\omega) + g^{<,>}_{\mathrm{L}}(\omega)\mathbf{V}^{\mathrm{LC}} G^{a}_{\mathrm{CL}}(\omega), \quad \text{(A.12)}$$

in the frequency domain. Next using the Langreth rule $G^{r,a}_{\mathrm{CL}}(\omega) = G^{r,a}_{\mathrm{CC}}(\omega)\mathbf{V}^{\mathrm{CL}} g^{r,a}_{\mathrm{L}}(\omega)$ [83] we arrive at

$$\begin{aligned} G^{<,>}_{\mathrm{LL}}(\omega) =& g^{<,>}_{\mathrm{L}}(\omega) + g^{r}_{\mathrm{L}}(\omega)\mathbf{V}^{\mathrm{LC}}\left[G^{r}_{\mathrm{CC}}(\omega)\mathbf{V}^{\mathrm{CL}} g^{<,>}_{\mathrm{L}}(\omega) + G^{<,>}_{\mathrm{CC}}(\omega)\mathbf{V}^{\mathrm{CL}} g^{a}_{\mathrm{L}}(\omega)\right] + \\ &+ g^{<,>}_{\mathrm{L}}(\omega)\mathbf{V}^{\mathrm{LC}} G^{a}_{\mathrm{CC}}(\omega)\mathbf{V}^{\mathrm{CL}} g^{a}_{\mathrm{L}}(\omega). \end{aligned} \quad \text{(A.13)}$$

We have now expressed everything in terms of the unperturbed and central Green's functions; what remains is to simplify the expression for the activity. Using the cyclicity of the trace and supressing the frequency arguments, we start with

$$\begin{aligned} \mathrm{tr}\{\mathbf{V}^{\mathrm{LC}} G^{<}_{\mathrm{CL}}\mathbf{V}^{\mathrm{LC}} G^{>}_{\mathrm{CL}}\} &= \mathrm{tr}\{[G^{r}_{\mathrm{CC}}\Sigma^{<}_{\mathrm{L}} + G^{<}_{\mathrm{CC}}\Sigma^{a}_{\mathrm{L}}][G^{r}_{\mathrm{CC}}\Sigma^{>}_{\mathrm{L}} + G^{>}_{\mathrm{CC}}\Sigma^{a}_{\mathrm{L}}]\} \\ &= \mathrm{tr}\{G^{r}_{\mathrm{CC}}\Sigma^{<}_{\mathrm{L}} G^{r}_{\mathrm{CC}}\Sigma^{>}_{\mathrm{L}} + G^{r}_{\mathrm{CC}}\Sigma^{<}_{\mathrm{L}} G^{>}_{\mathrm{CC}}\Sigma^{a}_{\mathrm{L}}\} + \\ &\quad + \mathrm{tr}\{G^{<}_{\mathrm{CC}}\Sigma^{a}_{\mathrm{L}} G^{r}_{\mathrm{CC}}\Sigma^{>}_{\mathrm{L}} + G^{<}_{\mathrm{CC}}\Sigma^{a}_{\mathrm{L}} G^{>}_{\mathrm{CC}}\Sigma^{a}_{\mathrm{L}}\}. \end{aligned} \quad \text{(A.14)}$$

Here we used the self energies defined by $\Sigma^{\bullet}_{\alpha} = \mathbf{V}^{\mathrm{C}\alpha} g^{\bullet}_{\alpha}\mathbf{V}^{\alpha\mathrm{C}}$. Next we assume that the retarded and advanced bath self energies are purely imaginary and use

$$\begin{aligned} \Sigma^{r}_{\alpha} &= -i\Gamma_{\alpha}/2, \quad \Sigma^{a}_{\alpha} = i\Gamma_{\alpha}/2, \\ \Sigma^{<}_{\alpha} &= -if_{\alpha}\Gamma_{\alpha}, \quad \Sigma^{>}_{\alpha} = -i(1+f_{\alpha})\Gamma_{\alpha}, \end{aligned} \quad \text{(A.15)}$$

where the spectral function is given by $\Gamma_{\alpha} = i(\Sigma^{r}_{\alpha} - \Sigma^{a}_{\alpha})$. For this form of lesser and greater self-energies, we need to assume that the reservoirs are in internal thermal equilibrium, such that the fluctuation-dissipation relation holds. Using

$F^{+}_{\alpha\beta} = f_\alpha(1+f_\beta)$ and $\mathbf{T}_{\alpha\beta} = \Gamma_\alpha G^r_{\mathrm{CC}} \Gamma_\beta G^a_{\mathrm{CC}}$ and from now on dropping the indices of the central Green's functions, we can rewrite the terms. We start with

$$\mathrm{tr}\big\{G^r \Sigma^<_{\mathrm{L}} G^r \Sigma^>_{\mathrm{L}}\big\} = -\,\mathrm{tr}\{G^r \Gamma_{\mathrm{L}} G^r \Gamma_{\mathrm{L}}\} F^{+}_{\mathrm{LL}}. \tag{A.16}$$

It is the real part of this term which will appear in the expression for $\mathcal{K}_{\mathrm{L}}$. Thus, by using $i\sum_\beta G^r \Gamma_\beta G^a = G^a - G^r$ (follows from Dyson equation for the center [83]), we find

$$\mathrm{tr}\big\{G^r \Sigma^<_{\mathrm{L}} G^r \Sigma^>_{\mathrm{L}}\big\} + \mathrm{tr}\big\{G^r \Sigma^<_{\mathrm{L}} G^r \Sigma^>_{\mathrm{L}}\big\}^\dagger = -2\,\mathrm{tr}\{\mathbf{T}_{\mathrm{LL}}\} F^{+}_{\mathrm{LL}} + \sum_{\beta\gamma} \mathrm{tr}\{\mathbf{T}_{\mathrm{L}\beta}\mathbf{T}_{\mathrm{L}\gamma}\} F^{+}_{\mathrm{LL}}. \tag{A.17}$$

Next, by using $G^{<,>} = \sum_{\beta=\mathrm{L,R}} G^r \Sigma^{<,>}_\beta G^a$ (following from the Dyson equation for the center [83]) we find

$$\begin{aligned} &\mathrm{tr}\big\{G^r \Sigma^<_{\mathrm{L}} G^> \Sigma^a_{\mathrm{L}}\big\} = -i \sum_\beta \mathrm{tr}\{\Gamma_{\mathrm{L}} G^r \mathbf{T}_{\mathrm{L}\beta}\} F^{+}_{\mathrm{L}\beta}/2, \\ &\mathrm{tr}\big\{G^r \Sigma^<_{\mathrm{L}} G^> \Sigma^a_{\mathrm{L}}\big\} + \mathrm{tr}\big\{G^r \Sigma^<_{\mathrm{L}} G^> \Sigma^a_{\mathrm{L}}\big\}^\dagger = -\sum_{\beta\gamma} \mathrm{tr}\{\mathbf{T}_{\mathrm{L}\gamma}\mathbf{T}_{\mathrm{L}\beta}\} F^{+}_{\mathrm{L}\beta}/2. \end{aligned} \tag{A.18}$$

The next term is

$$\begin{aligned} &\mathrm{tr}\big\{G^< \Sigma^a_{\mathrm{L}} G^r \Sigma^>_{\mathrm{L}}\big\} = -i \sum_\beta \mathrm{tr}\{\mathbf{T}_{\mathrm{L}\beta}\Gamma_{\mathrm{L}} G^r\} F^{+}_{\beta\mathrm{L}}/2, \\ &\mathrm{tr}\big\{G^< \Sigma^a_{\mathrm{L}} G^r \Sigma^>_{\mathrm{L}}\big\} + \mathrm{tr}\big\{G^< \Sigma^a_{\mathrm{L}} G^r \Sigma^>_{\mathrm{L}}\big\}^\dagger = -\sum_{\beta\gamma} \mathrm{tr}\{\mathbf{T}_{\mathrm{L}\gamma}\mathbf{T}_{\mathrm{L}\beta}\} F^{+}_{\beta\mathrm{L}}/2. \end{aligned} \tag{A.19}$$

Moreover we have

$$\mathrm{tr}\big\{G^< \Sigma^a_{\mathrm{L}} G^> \Sigma^a_{\mathrm{L}}\big\} = \sum_{\beta\gamma} \mathrm{tr}\{\mathbf{T}_{\mathrm{L}\beta}\mathbf{T}_{\mathrm{L}\gamma}\} F^{+}_{\beta\gamma}/4. \tag{A.20}$$

For the second term in $\mathcal{K}_{\mathrm{L}}$, we have

$$\begin{aligned} \mathrm{tr}\big\{\mathbf{V}^{\mathrm{CL}} G^<_{\mathrm{LL}} \mathbf{V}^{\mathrm{LC}} G^>_{\mathrm{CC}}\big\} = \mathrm{tr}\big\{&\Sigma^<_{\mathrm{L}} G^>_{\mathrm{CC}} + \Sigma^r_{\mathrm{L}} G^r_{\mathrm{CC}} \Sigma^<_{\mathrm{L}} G^>_{\mathrm{CC}}\big\} + \\ &+ \mathrm{tr}\big\{\Sigma^r_{\mathrm{L}} G^<_{\mathrm{CC}} \Sigma^a_{\mathrm{L}} G^>_{\mathrm{CC}} + \Sigma^<_{\mathrm{L}} G^a_{\mathrm{CC}} \Sigma^a_{\mathrm{L}} G^>_{\mathrm{CC}}\big\}. \end{aligned} \tag{A.21}$$

Simplifying the terms yields

$$\mathrm{tr}\big\{\Sigma^<_{\mathrm{L}} G^>\big\} = -\sum_\beta \mathrm{tr}\{\mathbf{T}_{\mathrm{L}\beta}\} F^{+}_{\mathrm{L}\beta}, \tag{A.22}$$

and

$$\mathrm{tr}\big\{\Sigma^r_{\mathrm{L}} G^r \Sigma^<_{\mathrm{L}} G^>\big\} = i \sum_\beta \mathrm{tr}\{\Gamma_{\mathrm{L}} G^r \mathbf{T}_{\mathrm{L}\beta}\} F^{+}_{\mathrm{L}\beta}/2. \tag{A.23}$$

Next we find

$$\mathrm{tr}\big\{\Sigma^r_{\rm L} G^< \Sigma^a_{\rm L} G^>\big\} = -\sum_{\beta\gamma} \mathrm{tr}\{\mathbf{T}_{{\rm L}\beta}\mathbf{T}_{{\rm L}\gamma}\} F^+_{\beta\gamma}/4, \tag{A.24}$$

and lastly

$$\mathrm{tr}\big\{\Sigma^<_{\rm L} G^a \Sigma^a_{\rm L} G^>\big\} = -i\sum_{\beta} \mathrm{tr}\{\Gamma_{\rm L} G^a \Gamma_{\rm L} G^r \Gamma_\beta G^a\} F^+_{{\rm L}\beta}/2 = -i\sum_{\beta} \mathrm{tr}\{\Gamma_{\rm L} G^a \mathbf{T}_{{\rm L}\beta}\} F^+_{{\rm L}\beta}/2. \tag{A.25}$$

By combining terms we get

$$\mathrm{tr}\big\{\Sigma^r_{\rm L} G^< \Sigma^a_{\rm L} G^>\big\} + \mathrm{tr}\big\{G^< \Sigma^a_{\rm L} G^> \Sigma^a_{\rm L}\big\} = 0 \tag{A.26}$$

and

$$\mathrm{tr}\big\{\Sigma^r_{\rm L} G^r \Sigma^<_{\rm L} G^>\big\} + \mathrm{tr}\big\{\Sigma^<_{\rm L} G^a \Sigma^a_{\rm L} G^>\big\} = \sum_{\beta\gamma} \mathrm{tr}\{\mathbf{T}_{{\rm L}\beta}\mathbf{T}_{{\rm L}\gamma}\} F^+_{{\rm L}\beta}/2, \tag{A.27}$$

where we used $G^a - G^r = i\sum_\beta G^r \Gamma_\beta G^a$.

In order to obtain an expression for $\mathcal{K}_{\rm L}$ which is symmetric in β and L it is useful to write $\mathcal{K}_{\rm L}$ in a different but equivalent way and average the expressions. In particular

$$\begin{aligned}
\mathcal{K}_{\rm L} &= -\,\mathrm{Re}\int_{-\infty}^{\infty} dt' \mathbf{V}^{\rm LC}_{ij}\mathbf{V}^{\rm LC}_{kl}\Big\{G^>_{{\rm L}i,{\rm L}k}(t,t+t')G^>_{{\rm C}j,{\rm C}l}(t,t+t') \\
&\qquad\qquad + G^>_{{\rm L}i,{\rm C}l}(t,t+t')G^>_{{\rm C}j,{\rm L}k}(t,t+t')\Big\} \\
&= -\,\mathrm{Re}\int \frac{d\omega}{2\pi}\,\mathrm{tr}\big\{\mathbf{V}^{\rm CL} G^>_{\rm LL}(\omega)\mathbf{V}^{\rm LC} G^<_{\rm CC}(\omega)\big\} + \mathrm{tr}\big\{\mathbf{V}^{\rm CL} G^>_{\rm LC}(\omega)\mathbf{V}^{\rm CL} G^<_{\rm LC}(\omega)\big\}.
\end{aligned} \tag{A.28}$$

We note that $\mathrm{tr}\big\{\mathbf{V}^{\rm CL} G^>_{\rm LL}(\omega)\mathbf{V}^{\rm LC} G^<_{\rm CC}(\omega)\big\}$ and $\mathrm{tr}\big\{\mathbf{V}^{\rm CL} G^<_{\rm LL}(\omega)\mathbf{V}^{\rm LC} G^>_{\rm CC}(\omega)\big\}$ give the same contribution to $\mathcal{K}_{\rm L}$ after taking the real part and integrating over frequency. This is follows from $G^<_{j,k}(t,t') = G^>_{k,j}(t',t)$ and stationarity. Expanding this term we have

$$\mathrm{tr}\big\{\mathbf{V}^{\rm CL} G^>_{\rm LL}\mathbf{V}^{\rm LC} G^<_{\rm CC}\big\} = \mathrm{tr}\big\{\Sigma^>_{\rm L} G^< + \Sigma^r_{\rm L} G^r \Sigma^>_{\rm L} G^< + \Sigma^r_{\rm L} G^> \Sigma^a_{\rm L} G^< + \Sigma^>_{\rm L} G^a \Sigma^a_{\rm L} G^<\big\}. \tag{A.29}$$

Simplyfying the expression we find

$$\mathrm{tr}\big\{\Sigma^>_{\rm L} G^<\big\} = -\sum_{\beta} \mathrm{tr}\{\mathbf{T}_{{\rm L}\beta}\} F^+_{\beta{\rm L}}, \tag{A.30}$$

and

$$\mathrm{tr}\big\{\Sigma^r_{\rm L} G^r \Sigma^>_{\rm L} G^<\big\} = i\sum_{\beta} \mathrm{tr}\{\Gamma_{\rm L} G^r \mathbf{T}_{{\rm L}\beta}\} F^+_{\beta{\rm L}}/2. \tag{A.31}$$

Furthermore we find

$$\mathrm{tr}\{\Sigma_{\mathrm{L}}^{r} G^{>} \Sigma_{\mathrm{L}}^{a} G^{<}\} = -\,\mathrm{tr}\{\mathbf{T}_{\mathrm{L}\beta}\mathbf{T}_{\mathrm{L}\gamma}\} F^{+}_{\beta\gamma}/4, \tag{A.32}$$

and finally

$$\mathrm{tr}\{\Sigma_{\mathrm{L}}^{>} G^{a} \Sigma_{\mathrm{L}}^{a} G^{<}\} = -i \sum_{\beta} \mathrm{tr}\{\Gamma_{\mathrm{L}} G^{a} \mathbf{T}_{\mathrm{L}\beta}\} F^{+}_{\beta\mathrm{L}}/2. \tag{A.33}$$

Combining terms we find

$$\mathrm{tr}\{\Sigma_{\mathrm{L}}^{r} G^{r} \Sigma_{\mathrm{L}}^{>} G^{<}\} + \mathrm{tr}\{\Sigma_{\mathrm{L}}^{>} G^{a} \Sigma_{\mathrm{L}}^{a} G^{<}\} = \sum_{\beta\gamma} \mathrm{tr}\{\mathbf{T}_{\mathrm{L}\gamma}\mathbf{T}_{\mathrm{L}\beta}\} F^{+}_{\beta\mathrm{L}}/2. \tag{A.34}$$

Averaging the two equivalent expressions for the term, yields

$$\begin{aligned}
&\frac{1}{2}\left(\mathrm{tr}\{\mathbf{V}^{\mathrm{CL}} G^{>}_{\mathrm{LL}}(\omega)\mathbf{V}^{\mathrm{LC}} G^{<}_{\mathrm{CC}}(\omega)\} + \mathrm{tr}\{\mathbf{V}^{\mathrm{CL}} G^{<}_{\mathrm{LL}}(\omega)\mathbf{V}^{\mathrm{LC}} G^{>}_{\mathrm{CC}}(\omega)\}\right) \\
&= -\sum_{\beta} \mathrm{tr}\{\mathbf{T}_{\mathrm{L}\beta}\}(F^{+}_{\mathrm{L}\beta} + F^{+}_{\beta\mathrm{L}})/2 - \sum_{\beta\gamma} \mathrm{tr}\{\mathbf{T}_{\mathrm{L}\beta}\mathbf{T}_{\mathrm{L}\gamma}\} F^{+}_{\beta\gamma}/4 + \\
&\quad + \sum_{\beta\gamma} \mathrm{tr}\{\mathbf{T}_{\mathrm{L}\gamma}\mathbf{T}_{\mathrm{L}\beta}\}(F^{+}_{\mathrm{L}\beta} + F^{+}_{\beta\mathrm{L}})/4.
\end{aligned} \tag{A.35}$$

Using this symmetrized expression in the activity results in

$$\begin{aligned}
\mathcal{K}_{\mathrm{L}} &= \int_{-\infty}^{\infty} \frac{d\omega}{2\pi} \frac{1}{2} \Big(\mathrm{tr}\Big\{ 4\mathbf{T}_{\mathrm{LL}}(\omega) - \Big(\sum_{\beta} \mathbf{T}_{\mathrm{L}\beta}(\omega) \Big)^{2} \Big\} F^{+}_{\mathrm{LL}}(\omega) + \\
&\qquad + \sum_{\beta \neq \mathrm{L}} \mathrm{tr}\{\mathbf{T}_{\mathrm{L}\beta}(\omega)\}(F^{+}_{\mathrm{L}\beta}(\omega) + F^{+}_{\beta\mathrm{L}}(\omega)) \Big) \\
&= \int_{0}^{\infty} \frac{d\omega}{2\pi} \Big(\mathrm{tr}\Big\{ 4\mathbf{T}_{\mathrm{LL}}(\omega) - \Big(\sum_{\beta} \mathbf{T}_{\mathrm{L}\beta}(\omega) \Big)^{2} \Big\} F^{+}_{\mathrm{LL}}(\omega) + \\
&\qquad + \sum_{\beta \neq \mathrm{L}} \mathrm{tr}\{\mathbf{T}_{\mathrm{L}\beta}(\omega)\}(F^{+}_{\mathrm{L}\beta}(\omega) + F^{+}_{\beta\mathrm{L}}(\omega)) \Big).
\end{aligned} \tag{A.36}$$

This is analogous to fermionic result presented in Ref. [44] with appropriate replacement of $F^{+}_{\alpha\beta}(\omega) \mapsto F^{-}_{\alpha\beta}(\omega)$ and fermionic average occupations. Moreover, the generalization to multiple terminals is analogous to the result presented in the main text (3.43).

Next, we point out that for both the fermionic and bosonic cases, the steady state partial dynamical activity (3.62) scales at most linearly with time. This is concluded from Eq. (3.43) and the corresponding fermionic expression of Ref. [44] having no time dependence and the bound (3.76).

APPENDIX B

Weak coupling limit of correlator-based activity

In Ref. [44], where the correlator-based definition of dynamical activity (3.42) was introduced, it was shown that the definition recovered the standard rate of jumps (3.26) for a quadratic Hamiltonian. Here, we follow a different approach by applying the Born, Markov, and secular approximations to show that Eq. (3.42) recovers the standard GKSL definition also for Hamiltonians which are not quadratic. We consider the Hamiltonian of a system coupled to baths labelled by $\alpha, \beta, \ldots$

$$\hat{H} = \hat{H}_{\mathrm{S}} + \sum_{\alpha} (\hat{H}_{\alpha} + \hat{V}_{\alpha}), \tag{B.1}$$

where the interaction between bath α and the central system is given by

$$\hat{V}_{\alpha} = \sum_{k} \hat{A}_{\alpha k} \otimes \hat{B}_{\alpha k} = \hat{A}_{\alpha k}^{\dagger} \otimes \hat{B}_{\alpha k}^{\dagger}. \tag{B.2}$$

Here $\hat{A}_{\alpha k}$ is an operator of the system and $\hat{B}_{\alpha k}$ is an operator of bath α. Furthermore, we define $\hat{H}_0 = \hat{H}_{\mathrm{S}} + \sum_{\alpha} \hat{H}_{\alpha}$ and $\hat{V} = \sum_{\alpha} \hat{V}_{\alpha}$ with the aim of switching to the interaction picture. We define the time evolution operators

$$\begin{aligned} \hat{U}_0(t,0) &= T_+ \exp\left\{ -\frac{i}{\hbar} \int_0^t d\tau \hat{H}_0(\tau) \right\}, \\ \hat{U}_{\mathrm{I}}(t,0) &= T_+ \exp\left\{ -\frac{i}{\hbar} \int_0^t d\tau \hat{V}^{\mathrm{I}}(\tau) \right\}, \end{aligned} \tag{B.3}$$

where $\hat{V}^{\mathrm{I}}(t) = \hat{U}_0^\dagger(t,0)\hat{V}\hat{U}_0(t,0)$. The density operator in the interaction picture at time t is given by $\hat{\rho}^{\mathrm{I}}(t) = \hat{U}_{\mathrm{I}}(t,0)\hat{\rho}(0)\hat{U}_{\mathrm{I}}^\dagger(t,0)$. Starting from the Heisenberg picture, we rewrite the correlator in the interaction picture

$$\mathrm{tr}\Big\{\hat{V}(t+t')\hat{V}(t)\rho(0)\Big\} = \mathrm{tr}\Big\{\hat{U}_{\mathrm{I}}^\dagger(t+t',t)\hat{V}^{\mathrm{I}}(t+t')\hat{U}_{\mathrm{I}}(t+t',t)\hat{V}^{\mathrm{I}}(t)\hat{\rho}^{\mathrm{I}}(t)\Big\}. \quad \text{(B.4)}$$

We note that the expression for the activity used for GKSL dynamics is second order in the interaction and linear in the density matrix. Since the correlation-based activity (3.42) is second order in $\hat{V}_\alpha^{\mathrm{H}}(t)$ we expand $\hat{U}_{\mathrm{I}}^\dagger(t+t',t)$ and $\hat{U}_{\mathrm{I}}(t+t',t)$ to zeroth order, since the rest of the term would only contribute to higher order. Keeping terms which are maximum second order in $\hat{V}^{\mathrm{I}}$ we get

$$\mathrm{tr}\Big\{\hat{V}(t+t')\hat{V}(t)\hat{\rho}(0)\Big\} \approx \mathrm{tr}\Big\{\hat{V}^{\mathrm{I}}(t+t')\hat{V}^{\mathrm{I}}(t)\hat{\rho}^{\mathrm{I}}(t)\Big\}. \quad \text{(B.5)}$$

Next, we assume that the spectrum of $\hat{H}_{\mathrm{S}}$ is discrete and denote the eigenvalues of the system Hamiltonian as ϵ with the projector onto the eigenspace of ϵ as $\hat{\Pi}(\epsilon)$. We define

$$\hat{A}_{\alpha k}(\omega) = \sum_{\epsilon'-\epsilon=\omega} \hat{\Pi}(\epsilon)\hat{A}_{\alpha k}\hat{\Pi}(\epsilon'), \quad \text{(B.6)}$$

with the properties [96]

$$[\hat{H}_{\mathrm{S}}, \hat{A}_{\alpha k}(\omega)] = -\hbar\omega\hat{A}_{\alpha k}(\omega), \quad \hat{A}_{\alpha k}^\dagger(\omega) = \hat{A}_{\alpha k}(-\omega). \quad \text{(B.7)}$$

Under the assumption of there being no explicit time dependence, the operators in the interaction picture evolve as

$$\hat{A}_{\alpha k}^{\mathrm{I}}(\omega;t) = e^{i\hat{H}_{\mathrm{S}}t/\hbar}\hat{A}_{\alpha k}(\omega)e^{-i\hat{H}_{\mathrm{S}}t/\hbar} = e^{-i\omega t}\hat{A}_{\alpha k}(\omega), \quad \text{(B.8)}$$

$$\hat{B}_{\alpha k}^{\mathrm{I}}(t) = e^{i\hat{H}_\alpha t/\hbar}\hat{B}_{\alpha k}e^{-i\hat{H}_\alpha t/\hbar}. \quad \text{(B.9)}$$

Moreover, we assume $\langle\hat{B}_\alpha^{\mathrm{I}}(t)\rangle = 0$ and weak coupling, such that we can use the Born approximation $\hat{\rho}^{\mathrm{I}}(t) \approx \hat{\rho}_{\mathrm{S}}^{\mathrm{I}}(t)\bigotimes_\alpha \hat{\rho}_\alpha$, where $\hat{\rho}_\alpha$ are density matrices of the baths. This means that the correlator of the full interaction Hamiltonian decomposes into a sum

$$\mathrm{tr}\Big\{\hat{V}^{\mathrm{I}}(t+t')\hat{V}^{\mathrm{I}}(t)\hat{\rho}^{\mathrm{I}}(t)\Big\} = \sum_\alpha \mathrm{tr}\Big\{\hat{V}_\alpha^{\mathrm{I}}(t+t')\hat{V}_\alpha^{\mathrm{I}}(t)\hat{\rho}^{\mathrm{I}}(t)\Big\}. \quad \text{(B.10)}$$

Thus, we focus on the generalised activity for a single reservoir and approximate

$$\begin{aligned}\mathcal{K}_\alpha(t) &\approx \mathrm{Re}\sum_{kk'}\int_{-t}^{t}\frac{dt'}{\hbar^2}\,\mathrm{tr}\Big\{\hat{A}^{\mathrm{I}}_{\alpha k'}(t+t')\hat{A}^{\mathrm{I}}_{\alpha k}(t)\hat{\rho}^{\mathrm{I}}_{\mathrm{S}}(t)\Big\}\,\mathrm{tr}\Big\{\hat{B}^{\mathrm{I}}_{\alpha k'}(t+t')\hat{B}^{\mathrm{I}}_{\alpha k}(t)\hat{\rho}_\alpha\Big\}\\ &= \mathrm{Re}\sum_{kk'}\sum_{\omega,\omega'}e^{-i(\omega+\omega')t}\,\mathrm{tr}\Big\{\hat{A}_{\alpha k'}(\omega')\hat{A}_{\alpha k}(\omega)\hat{\rho}^{\mathrm{I}}_{\mathrm{S}}(t)\Big\}\times\\ &\qquad\times\int_{-t}^{t}\frac{dt'}{\hbar^2}e^{-i\omega' t'}\,\mathrm{tr}\Big\{\hat{B}^{\mathrm{I}\dagger}_{\alpha k'}(t+t')\hat{B}^{\mathrm{I}}_{\alpha k}(t)\rho_\alpha\Big\}.\end{aligned} \tag{B.11}$$

As a first step, we investigate the steady state limit and use the secular approximation, together with assuming that the bath state is stationary, which results in

$$\mathcal{K}_\alpha = \mathrm{Re}\sum_{kk'}\sum_{\omega}\mathrm{tr}\Big\{\hat{A}_{\alpha k'}(-\omega)\hat{A}_{\alpha k}(\omega)\hat{\rho}^{\mathrm{I}}_{\mathrm{S}}(t)\Big\}\int_{-\infty}^{\infty}\frac{dt'}{\hbar^2}e^{i\omega t'}\,\mathrm{tr}\Big\{\hat{B}^{\mathrm{I}\dagger}_{\alpha k'}(t')\hat{B}^{\mathrm{I}}_{\alpha k}(0)\hat{\rho}_\alpha\Big\}. \tag{B.12}$$

We should note that to get the total number of interactions observed $\mathcal{A}_\alpha(t_{\mathrm{M}})$ during a measurement time t_{M}, one integrates $\mathcal{A}_\alpha(t_{\mathrm{M}}) = \int_0^{t_{\mathrm{M}}} dt\mathcal{K}_\alpha(t)$, which is why we neglect the rotating terms. Defining

$$\gamma^\alpha_{k'k}(\omega) = \mathrm{Re}\int_{-\infty}^{\infty}dt' e^{i\omega t'}\,\mathrm{tr}\Big\{\hat{B}^{\mathrm{I}}_{\alpha k'}(t')\hat{B}^{\mathrm{I}}_{\alpha k}(0)\hat{\rho}_\alpha\Big\}, \tag{B.13}$$

we find

$$\begin{aligned}\mathcal{K}_\alpha &= \sum_{kk'}\sum_{\omega}\frac{\gamma^\alpha_{k'k}(\omega)}{\hbar^2}\,\mathrm{tr}\Big\{\hat{A}_{\alpha k}(\omega)\rho_{\mathrm{S}}(\infty)\hat{A}^\dagger_{\alpha k'}(\omega)\Big\}\\ &= \sum_{\omega}\sum_{j}\mathrm{tr}\Big\{\hat{L}^\dagger_{\alpha j}(\omega)\hat{L}_{\alpha j}(\omega)\rho_{\mathrm{S}}(\infty)\Big\}.\end{aligned} \tag{B.14}$$

In the last step, we diagonalised $\gamma^\alpha_{k'k}(\omega)$ and identified the standard Lindblad form for the jump operators, see Eq. (2.101). The total dynamical activity rate is obtained by summing the local rates $\mathcal{K}_\alpha = \sum_\alpha \mathcal{K}_\alpha$.

To investigate activity outside the steady-state regime, we employ the Markov approximation and assume that the bath correlations decay quickly relative to the system dynamics, allowing us to extend the integrals. Furthermore, we perform a rotating wave approximation and neglect any terms where $\omega \neq -\omega'$. Under these

assumptions, the time-dependent correlator follows as

$$\begin{aligned}\mathcal{K}_\alpha(t) &= \mathrm{Re}\sum_{kk'}\int_{-t}^{t}\frac{dt'}{\hbar^2}\,\mathrm{tr}\Big\{\hat{A}^{\mathrm{I}}_{\alpha k'}(t+t')\hat{A}^{\mathrm{I}}_{\alpha k}(t)\hat{\rho}^{\mathrm{I}}_S(t)\Big\}\,\mathrm{tr}\Big\{\hat{B}^{\mathrm{I}}_{\alpha k'}(t+t')\hat{B}^{\mathrm{I}}_{\alpha k}(t)\hat{\rho}_\alpha\Big\}\\ &= \mathrm{Re}\sum_{kk'}\sum_{\omega\omega'}e^{-i(\omega+\omega')t}\,\mathrm{tr}\Big\{\hat{A}_{\alpha k'}(\omega')\hat{A}_{\alpha k}(\omega)\hat{\rho}^{\mathrm{I}}_{\mathrm{S}}(t)\Big\}\times\\ &\times\int_{-\infty}^{\infty}\frac{dt'}{\hbar^2}e^{-i\omega' t'}\,\mathrm{tr}\Big\{\hat{B}^{\mathrm{I}\dagger}_{\alpha k'}(t+t')\hat{B}^{\mathrm{I}}_{\alpha k}(t)\hat{\rho}_\alpha\Big\}\\ &\approx\sum_{\omega}\sum_{j}\mathrm{tr}\Big\{\hat{L}^{\dagger}_{\alpha j}(\omega)\hat{L}_{\alpha j}(\omega)\hat{\rho}^{\mathrm{I}}_S(t)\Big\},\end{aligned}\tag{B.15}$$

where we made the same identification of the standard GKSL jump operators as for the steady state case. Thus, we see that the correlation-based activity (3.42) recovers the time-dependent activity of the GKSL dynamics of Eq. (3.26). This calculation shows that the generalized activity, defined as the symmetrised autocorrelator of the interaction Hamiltonian in general, recovers the standard activity defined as the number of jumps induced by the bath on the system used for GKSL dynamics. Furthermore, this would also recover the activity of a classical continuous-time Markov process, since these dynamics can also be modelled by a GKSL equation.

APPENDIX C

Partial dynamical activity at thermal equilibrium

Here we provide a derivation of a formula for the partial dynamical activity (3.62) for a system at thermal equilibrium as presented in Eq. (3.78). At thermal equilibrium, with inverse temperature $\beta = 1/k_{\mathrm{B}}T$ for a Hamiltonian $\hat{H} = \hat{H}_0 + \hat{V} = \sum_i \epsilon_i |\epsilon_i\rangle \langle\epsilon_i|$ the density matrix is expressed as

$$\hat{\rho} = \sum_i p_i |\epsilon_i\rangle \langle\epsilon_i|, \quad p_i = e^{-\epsilon_i\beta}/Z, \quad Z = \sum_i e^{-\epsilon_i\beta}. \tag{C.1}$$

The expression for the PDA with respect to $\hat{V}$ is given by

$$\mathscr{A}(t) = \frac{1}{2\hbar^2} \sum_{ij} \frac{(p_i - p_j)^2}{p_i + p_j} |\langle\epsilon_i| \int_0^t d\tau \hat{V}^{\mathrm{H}}(\tau) |\epsilon_j\rangle|^2. \tag{C.2}$$

By introducing $\omega_{ij} = (\epsilon_i - \epsilon_j)/\hbar$ and using the Boltzmann factors [134] we expand the integrands inside the square modulus and obtain

$$\begin{aligned} &\sum_{ij} \frac{(p_i - p_j)^2}{p_i + p_j} \langle\epsilon_i| \hat{V}^{\mathrm{H}}(t) |\epsilon_j\rangle \langle\epsilon_j| \hat{V}^{\mathrm{H}}(t') |\epsilon_i\rangle = \\ &\quad = \sum_{ij} \tanh^2[\hbar\omega_{ij}\beta/2] \frac{1}{Z} \left(e^{-\epsilon_i\beta} + e^{-\epsilon_j\beta}\right) V_{ij} V_{ji} e^{i\omega_{ij}t} e^{-i\omega_{ij}t'}, \end{aligned} \tag{C.3}$$

where we defined $V_{ij} = \langle \epsilon_i | \hat{V} | \epsilon_j \rangle$. Moreover,

$$R_{VV}(t,t') = \langle \{ \hat{V}^{\mathrm{H}}(t), \hat{V}^{\mathrm{H}}(t') \} \rangle = \sum_{ij} \frac{1}{Z} \left(e^{-\epsilon_i \beta} + e^{-\epsilon_j \beta} \right) V_{ij} V_{ji} e^{i\omega_{ij} t} e^{-i\omega_{ij} t'}. \tag{C.4}$$

Now, using $2\pi\delta(\omega + \omega_{ij}) = \int_{-\infty}^{\infty} dt e^{i(\omega+\omega_{ij})t}$, we find

$$\begin{aligned} R_{VV}(\omega,\omega') &= \int_{-\infty}^{\infty} dt \int_{-\infty}^{\infty} dt' \langle \{ \hat{V}^{\mathrm{H}}(t), \hat{V}^{\mathrm{H}}(t') \} \rangle e^{-i\omega t} e^{-i\omega' t'} \\ &= 4\pi^2 \sum_{ij} \frac{1}{Z} (e^{-\epsilon_i \beta} + e^{-\epsilon_j \beta}) V_{ij} V_{ji} \delta(\omega - \omega_{ij}) \delta(\omega' + \omega_{ij}). \end{aligned} \tag{C.5}$$

We are thus able to express

$$\begin{aligned} &\frac{1}{4\pi^2} \int_{-\infty}^{\infty} d\omega \int_{-\infty}^{\infty} d\omega' R_{VV}(\omega,\omega') e^{i\omega t} e^{i\omega' t'} \tanh[\hbar\omega\beta/2] \tanh[-\hbar\omega'\beta/2] = \\ &= \sum_{ij} \tanh^2[\hbar\omega_{ij}\beta/2] \frac{1}{Z} \left(e^{-\epsilon_i \beta} + e^{-\epsilon_j \beta} \right) V_{ij} V_{ji} e^{i\omega_{ij} t} e^{-i\omega_{ij} t'}. \end{aligned} \tag{C.6}$$

Using this representation, the PDA can be written as

$$\begin{aligned} \mathscr{A}(t) = \int_0^t d\tau \int_0^t d\tau' \int_{-\infty}^{\infty} d\omega \int_{-\infty}^{\infty} d\omega' \frac{1}{2\hbar^2} \Big(\\ \tanh \left[\frac{\hbar\omega}{2k_{\mathrm{B}}T} \right] e^{i\omega\tau} \tanh \left[\frac{\hbar\omega'}{2k_{\mathrm{B}}T} \right] e^{-i\omega'\tau'} \frac{R_{VV}(\omega,-\omega')}{4\pi^2} \Big). \end{aligned} \tag{C.7}$$

Furthermore, since $R_{VV}(t,t') = R_{VV}(t-t')$ we have $R_{VV}(\omega,\omega') = 2\pi\delta(\omega + \omega') R_{VV}(\omega)$ where

$$R_{VV}(\omega) = \int_{-\infty}^{\infty} dt \langle \{ \hat{V}^{\mathrm{H}}(t), \hat{V}^{\mathrm{H}}(0) \} \rangle e^{-i\omega t}. \tag{C.8}$$

This allows us to perform one of the frequency integrals and simplify the PDA as

$$\begin{aligned} \mathscr{A}(t) &= \int_0^t d\tau \int_0^t d\tau' \int_{-\infty}^{\infty} d\omega \frac{1}{4\pi\hbar^2} \Big(\tanh^2 \left[\frac{\hbar\omega}{2k_{\mathrm{B}}T} \right] e^{i\omega(\tau-\tau')} R_{VV}(\omega) \Big) \\ &= \frac{1}{\pi\hbar^2} \int_{-\infty}^{\infty} d\omega \tanh^2 \left[\frac{\hbar\omega}{2k_{\mathrm{B}}T} \right] \frac{\sin^2[\omega t/2]}{\omega^2} R_{VV}(\omega). \end{aligned} \tag{C.9}$$

This is Eq. (3.78) from the main text.

References

[1] Martin Josefsson et al. “A quantum-dot heat engine operating close to the thermodynamic efficiency limits”. In: *Nat. Nanotechnol.* 13 (Oct. 2018), pp. 920–924. ISSN: 1748-3395.

[2] Mohammed Ali Aamir et al. “Thermally driven quantum refrigerator autonomously resets a superconducting qubit”. In: *Nat. Phys.* 21 (Feb. 2025), pp. 318–323. ISSN: 1745-2481.

[3] Simon Sundelin et al. “Quantum refrigeration powered by noise in a superconducting circuit”. In: *Nat. Commun.* 17.359 (Jan. 2026), p. 359. ISSN: 2041-1723.

[4] Florian Meier et al. “Precision is not limited by the second law of thermodynamics”. In: *Nat. Phys.* 21 (July 2025), pp. 1147–1152. ISSN: 1745-2481.

[5] Steve Campbell et al. “Roadmap on quantum thermodynamics”. In: *Quantum Sci. Technol.* 11.1 (Jan. 2026), p. 012501. ISSN: 2058-9565.

[6] A. Einstein. “Über die von der molekularkinetischen Theorie der Wärme geforderte Bewegung von in ruhenden Flüssigkeiten suspendierten Teilchen”. In: *Ann. Phys.* 322.8 (Jan. 1905), pp. 549–560. ISSN: 0003-3804.

[7] R. De-Picciotto et al. “Direct observation of a fractional charge”. In: *Nature* 389.6647 (Sept. 1997), pp. 162–164. ISSN: 0028-0836.

[8] L. Saminadayar et al. “Observation of the $e/3$ Fractionally Charged Laughlin Quasiparticle”. In: *Phys. Rev. Lett.* 79.13 (Sept. 1997), pp. 2526–2529.

[9] Herbert B. Callen and Theodore A. Welton. “Irreversibility and Generalized Noise”. In: *Phys. Rev.* 83.1 (July 1951), pp. 34–40. ISSN: 1536-6065.

[10] Ryogo Kubo. “Statistical-Mechanical Theory of Irreversible Processes. I. General Theory and Simple Applications to Magnetic and Conduction Problems”. In: *J. Phys. Soc. Jpn.* 12.6 (June 1957), pp. 570–586. ISSN: 0031-9015.

[11] R. Kubo. “The fluctuation-dissipation theorem”. In: *Rep. Prog. Phys.* 29.1 (Jan. 1966), p. 255. ISSN: 0034-4885.

[12] J. B. Johnson. “Thermal Agitation of Electricity in Conductors”. In: *Nature* 119 (Jan. 1927), pp. 50–51. ISSN: 1476-4687.

[13] H. Nyquist. “Thermal Agitation of Electric Charge in Conductors”. In: *Phys. Rev.* 32.1 (July 1928), pp. 110–113.

[14] Bernhard Altaner, Matteo Polettini, and Massimiliano Esposito. “Fluctuation-Dissipation Relations Far from Equilibrium”. In: *Phys. Rev. Lett.* 117.18 (Oct. 2016), p. 180601. ISSN: 1079-7114.

[15] Andreas Dechant and Shin-ichi Sasa. “Fluctuation–response inequality out of equilibrium”. In: *Proc. Natl. Acad. Sci. U.S.A.* 117.12 (Mar. 2020), pp. 6430–6436.

[16] G. Gallavotti and E. G. D. Cohen. “Dynamical Ensembles in Nonequilibrium Statistical Mechanics”. In: *Phys. Rev. Lett.* 74.14 (Apr. 1995), pp. 2694–2697.

[17] Denis J. Evans, E. G. D. Cohen, and G. P. Morriss. “Probability of second law violations in shearing steady states”. In: *Phys. Rev. Lett.* 71.15 (Oct. 1993), pp. 2401–2404.

[18] Jorge Kurchan. “Fluctuation theorem for stochastic dynamics”. In: *J. Phys. A: Math. Gen.* 31.16 (Apr. 1998), p. 3719. ISSN: 0305-4470.

[19] Joel L. Lebowitz and Herbert Spohn. “A Gallavotti–Cohen-Type Symmetry in the Large Deviation Functional for Stochastic Dynamics”. In: *J. Stat. Phys.* 95.1 (Apr. 1999), pp. 333–365. ISSN: 1572-9613.

[20] C. Jarzynski. “Nonequilibrium Equality for Free Energy Differences”. In: *Phys. Rev. Lett.* 78.14 (Apr. 1997), pp. 2690–2693.

[21] C. Jarzynski. “Equilibrium free-energy differences from nonequilibrium measurements: A master-equation approach”. In: *Phys. Rev. E* 56.5 (Nov. 1997), pp. 5018–5035.

[22] Gavin E. Crooks. “Entropy production fluctuation theorem and the nonequilibrium work relation for free energy differences”. In: *Phys. Rev. E* 60.3 (Sept. 1999), pp. 2721–2726.

[23] Gavin E. Crooks. “Path-ensemble averages in systems driven far from equilibrium”. In: *Phys. Rev. E* 61.3 (Mar. 2000), pp. 2361–2366.

[24] Udo Seifert. “Stochastic thermodynamics, fluctuation theorems and molecular machines”. In: *Rep. Prog. Phys.* 75.12 (Nov. 2012), p. 126001. ISSN: 0034-4885.

[25] Andre C. Barato and Udo Seifert. “Thermodynamic Uncertainty Relation for Biomolecular Processes”. In: *Phys. Rev. Lett.* 114.15 (Apr. 2015), p. 158101.

[26] Todd R. Gingrich et al. “Dissipation Bounds All Steady-State Current Fluctuations”. In: *Phys. Rev. Lett.* 116.12 (Mar. 2016), p. 120601.

[27] Jordan M. Horowitz and Todd R. Gingrich. “Thermodynamic uncertainty relations constrain non-equilibrium fluctuations”. In: *Nat. Phys.* 16 (Jan. 2020), pp. 15–20. ISSN: 1745-2481.

[28] Timur Koyuk and Udo Seifert. “Thermodynamic Uncertainty Relation for Time-Dependent Driving”. In: *Phys. Rev. Lett.* 125.26 (Dec. 2020), p. 260604.

[29] Juan P. Garrahan. “Simple bounds on fluctuations and uncertainty relations for first-passage times of counting observables”. In: *Phys. Rev. E* 95.3 (Mar. 2017), p. 032134.

[30] Ivan Di Terlizzi and Marco Baiesi. “Kinetic uncertainty relation”. In: *J. Phys. A: Math. Theor.* 52.2 (Dec. 2018), 02LT03. ISSN: 1751-8121.

[31] Jiawei Yan et al. “Kinetic Uncertainty Relations for the Control of Stochastic Reaction Networks”. In: *Phys. Rev. Lett.* 123.10 (Sept. 2019), p. 108101. ISSN: 1079-7114.

[32] Ken Hiura and Shin-ichi Sasa. “Kinetic uncertainty relation on first-passage time for accumulated current”. In: *Phys. Rev. E* 103.5 (May 2021), p. L050103. ISSN: 2470-0053.

[33] Kangqiao Liu and Jie Gu. “Dynamical activity universally bounds precision of response in Markovian nonequilibrium systems”. In: *Commun. Phys.* 8.62 (Feb. 2025), pp. 1–9. ISSN: 2399-3650.

[34] Van Tuan Vo, Tan Van Vu, and Yoshihiko Hasegawa. “Unified thermodynamic–kinetic uncertainty relation”. In: *J. Phys. A: Math. Theor.* 55.40 (Sept. 2022), p. 405004. ISSN: 1751-8121.

[35] Yoshihiko Hasegawa and Tomohiro Nishiyama. “Thermodynamic Concentration Inequalities and Trade-Off Relations”. In: *Phys. Rev. Lett.* 133.24 (Dec. 2024), p. 247101.

[36] Kay Brandner, Taro Hanazato, and Keiji Saito. “Thermodynamic Bounds on Precision in Ballistic Multiterminal Transport”. en. In: *Physical Review Letters* 120.9 (Mar. 2018), p. 090601. ISSN: 0031-9007, 1079-7114.

[37] Bijay Kumar Agarwalla and Dvira Segal. “Assessing the validity of the thermodynamic uncertainty relation in quantum systems”. In: *Phys. Rev. B* 98.15 (Oct. 2018), p. 155438.

[38] Sushant Saryal et al. “Thermodynamic uncertainty relation in thermal transport”. In: *Phys. Rev. E* 100.4 (Oct. 2019), p. 042101.

[39] Kacper Prech et al. “Entanglement and thermokinetic uncertainty relations in coherent mesoscopic transport”. In: *Phys. Rev. Res.* 5.2 (June 2023), p. 023155.

[40] Kacper Prech, Patrick P. Potts, and Gabriel T. Landi. "Role of Quantum Coherence in Kinetic Uncertainty Relations". In: *Phys. Rev. Lett.* 134.2 (Jan. 2025), p. 020401.

[41] Elina Potanina et al. "Thermodynamic bounds on coherent transport in periodically driven conductors". In: *Physical Review X* 11.2 (Apr. 2021), p. 021013.

[42] Kay Brandner and Keiji Saito. "Thermodynamic Uncertainty Relations for Coherent Transport". In: *arXiv* (Feb. 2025).

[43] Kay Brandner and Keiji Saito. "Thermodynamic bound on current fluctuations in coherent conductors". In: *J. Phys. A: Math. Theor.* 58.43 (Oct. 2025), p. 435002. ISSN: 1751-8121.

[44] Gianmichele Blasi et al. "Quantum Kinetic Uncertainty Relations in Mesoscopic Conductors at Strong Coupling". In: *arXiv* (2025).

[45] Yoshihiko Hasegawa. "Quantum Thermodynamic Uncertainty Relation for Continuous Measurement". In: *Phys. Rev. Lett.* 125.5 (July 2020), p. 050601.

[46] Yoshihiko Hasegawa. "Unifying speed limit, thermodynamic uncertainty relation and Heisenberg principle via bulk-boundary correspondence". In: *Nat. Commun.* 14.2828 (May 2023), p. 2828. ISSN: 2041-1723.

[47] Yoshihiko Hasegawa. "Fundamental Precision Limits in Finite-Dimensional Quantum Thermal Machines". In: *Phys. Rev. Lett.* 135.20 (Nov. 2025), p. 200404.

[48] Tan Van Vu. "Fundamental Bounds on Precision and Response for Quantum Trajectory Observables". In: *PRX Quantum* 6.1 (Mar. 2025), p. 010343.

[49] Tan Van Vu, Ryotaro Honma, and Keiji Saito. "Universal Precision Limits in General Open Quantum Systems". In: *arXiv* (Aug. 2025).

[50] Tomohiro Nishiyama and Yoshihiko Hasegawa. "Exact solution to quantum dynamical activity". In: *Phys. Rev. E* 109.4 (Apr. 2024), p. 044114.

[51] Philipp Strasberg. *Quantum stochastic thermodynamics: Foundations and Selected Applications*. Oxford University Press, 2022.

[52] Patrick P. Potts. "Quantum Thermodynamics". In: *arXiv* (June 2024).

[53] Massimiliano Esposito, Katja Lindenberg, and Christian Van den Broeck. "Entropy production as correlation between system and reservoir". In: *New J. Phys.* 12.1 (Jan. 2010), p. 013013. ISSN: 1367-2630.

[54] Krzysztof Ptaszyński and Massimiliano Esposito. "Entropy Production in Open Systems: The Predominant Role of Intraenvironment Correlations". In: *Phys. Rev. Lett.* 123.20 (Nov. 2019), p. 200603.

[55] Philipp Strasberg and Massimiliano Esposito. "Stochastic thermodynamics in the strong coupling regime: An unambiguous approach based on coarse graining". In: *Phys. Rev. E* 95.6 (June 2017), p. 062101.

[56] Ángel Rivas. "Strong Coupling Thermodynamics of Open Quantum Systems". In: *Phys. Rev. Lett.* 124.16 (Apr. 2020), p. 160601.

[57] Peter Talkner and Peter Hänggi. "Colloquium: Statistical mechanics and thermodynamics at strong coupling: Quantum and classical". In: *Rev. Mod. Phys.* 92.4 (Oct. 2020), p. 041002.

[58] Yu V. Nazarov and M. Kindermann. "Full counting statistics of a general quantum mechanical variable". In: *Eur. Phys. J. B* 35.3 (Oct. 2003), pp. 413–420. ISSN: 1434-6036.

[59] Ludovico Tesser et al. "Stochastic entropy production in scattering theory". In: *arXiv* (Apr. 2026).

[60] M. Büttiker. "Scattering theory of current and intensity noise correlations in conductors and wave guides". In: *Phys. Rev. B* 46.19 (Nov. 1992), pp. 12485–12507.

[61] Ya. M. Blanter and M. Büttiker. "Shot noise in mesoscopic conductors". In: *Physics Reports* 336.1 (Sept. 2000), pp. 1–166. ISSN: 0370-1573.

[62] Yuli V. Nazarov and Yaroslav M. Blanter. *Quantum Transport: Introduction to Nanoscience*. Cambridge, England, UK: Cambridge University Press, May 2009. ISBN: 978-0-52183246-5.

[63] Michael V. Moskalets. *Scattering matrix approach to non-stationary quantum transport*. OCLC: ocn730403761. London : Singapore ; Hackensack N.J: Imperial College Press ; World Scientific Publishing [distributor], 2012. ISBN: 9781848168343.

[64] Christophe Texier and Markus Büttiker. "Effect of incoherent scattering on shot noise correlations in the quantum Hall regime". In: *Phys. Rev. B* 62.11 (Sept. 2000), pp. 7454–7458.

[65] G. B. Lesovik and Ivan Aleksandrovich Sadovskyy. "Scattering matrix approach to the description of quantum electron transport". In: *Phys.-Usp.* 54.10 (Oct. 2011), pp. 1007–1059. ISSN: 1063-7869.

[66] C. Altimiras et al. "Tuning Energy Relaxation along Quantum Hall Channels". In: *Phys. Rev. Lett.* 105.22 (Nov. 2010), p. 226804.

[67] Giuliano Benenti et al. "Fundamental aspects of steady-state conversion of heat to work at the nanoscale". In: *Phys. Rep.* 694 (June 2017), pp. 1–124. ISSN: 0370-1573.

[68] Ludovico Tesser, Robert S. Whitney, and Janine Splettstoesser. "Thermodynamic Performance of Hot-Carrier Solar Cells: A Quantum Transport Model". In: *Phys. Rev. Appl.* 19.4 (Apr. 2023), p. 044038.

[69] Margherita Maiuri, Marco Garavelli, and Giulio Cerullo. "Ultrafast Spectroscopy: State of the Art and Open Challenges". In: *J. Am. Chem. Soc.* 142.1 (Jan. 2020), pp. 3–15. ISSN: 0002-7863.

[70] M. Uehlein et al. "Capturing non-equilibrium electron dynamics in metals accurately and efficiently". In: *J. Appl. Phys.* 138.6 (Aug. 2025). ISSN: 0021-8979.

[71] Ya. M. Blanter and M. Büttiker. "Shot noise in mesoscopic conductors". In: *Phys. Rep.* 336.1 (Sept. 2000), pp. 1–166. ISSN: 0370-1573.

[72] Michael V. Moskalets. *Scattering Matrix Approach to Non-Stationary Quantum Transport*. London, England, UK: World Scientific Publishing Company, Sept. 2011. ISBN: 978-1-84816-834-3.

[73] Federica Haupt, Tomáš Novotný, and Wolfgang Belzig. "Current noise in molecular junctions: Effects of the electron-phonon interaction". In: *Phys. Rev. B* 82.16 (Oct. 2010), p. 165441.

[74] Sebastian E. Deghi and Raúl A. Bustos-Marún. "Entropy current and efficiency of quantum machines driven by nonequilibrium incoherent reservoirs". In: *Phys. Rev. B* 102.4 (July 2020), p. 045415.

[75] Matteo Acciai et al. "Constraints between entropy production and its fluctuations in nonthermal engines". In: *Phys. Rev. B* 109.7 (Feb. 2024), p. 075405. ISSN: 2469-9969.

[76] Ludovico Tesser. "Thermodynamic constraints on noise". PhD thesis. Sweden: Chalmers University of Technology, 2025. ISBN: 978-91-8103-141-6.

[77] Gheorghe Nenciu. "Independent electron model for open quantum systems: Landauer-Büttiker formula and strict positivity of the entropy production". In: *J. Math. Phys.* 48.3 (Mar. 2007), p. 033302. ISSN: 0022-2488.

[78] Didrik Palmqvist, Ludovico Tesser, and Janine Splettstoesser. "Combining kinetic and thermodynamic uncertainty relations in quantum transport". In: *Quantum Sci. Technol.* 10.3 (July 2025), p. 035059. ISSN: 2058-9565.

[79] Ludovico Tesser. "Fluctuations and nonequilibrium thermodynamics in electronic nanosystems". In: *Chalmers University of Technology* ().

[80] Daniel S. Fisher and Patrick A. Lee. "Relation between conductivity and transmission matrix". In: *Phys. Rev. B* 23.12 (June 1981), pp. 6851–6854.

[81] Supriyo Datta. *Electronic Transport in Mesoscopic Systems*. Cambridge, England, UK: Cambridge University Press, Sept. 1995. ISBN: 978-0-52141604-7.

[82] Hocine Boumrar et al. “Equivalence of wave function matching and Green’s functions methods for quantum transport: generalized Fisher–Lee relation”. In: *J. Phys.: Condens. Matter* 32.35 (June 2020), p. 355302. ISSN: 0953-8984.

[83] Jian-Sheng Wang et al. “Nonequilibrium Green’s function method for quantum thermal transport”. In: *Front. Phys.* 9.6 (Dec. 2014), pp. 673–697. ISSN: 2095-0470.

[84] Bijay Kumar Agarwalla. *Study of full-counting statistics in heat transport in transient and steady state and quantum fluctuation theorems*. [Online; accessed 16. Apr. 2026]. Jan. 2013.

[85] Yigal Meir and Ned S. Wingreen. “Landauer formula for the current through an interacting electron region”. In: *Phys. Rev. Lett.* 68.16 (Apr. 1992), pp. 2512–2515.

[86] Antti-Pekka Jauho, Ned S. Wingreen, and Yigal Meir. “Time-dependent transport in interacting and noninteracting resonant-tunneling systems”. In: *Phys. Rev. B* 50.8 (Aug. 1994), pp. 5528–5544.

[87] C. Caroli et al. “Direct calculation of the tunneling current”. In: *J. Phys. C: Solid State Phys.* 4.8 (June 1971), p. 916. ISSN: 0022-3719.

[88] Bijay Kumar Agarwalla and Dvira Segal. “Energy current and its statistics in the nonequilibrium spin-boson model: Majorana fermion representation”. In: *New J. Phys.* 19.4 (Apr. 2017), p. 043030. ISSN: 1367-2630.

[89] Nicolai Friis. “Reasonable fermionic quantum information theories require relativity”. In: *New J. Phys.* 18.3 (Mar. 2016), p. 033014. ISSN: 1367-2630.

[90] Nicetu Tibau Vidal et al. “Quantum operations in an information theory for fermions”. In: *Phys. Rev. A* 104.3 (Sept. 2021), p. 032411.

[91] Mauro Cirio et al. “Canonical derivation of the fermionic influence superoperator”. In: *Phys. Rev. B* 105.3 (Jan. 2022), p. 035121.

[92] Sadao Nakajima. “On Quantum Theory of Transport Phenomena: Steady Diffusion”. In: *Prog. Theor. Phys.* 20.6 (Dec. 1958), pp. 948–959. ISSN: 0033-068X.

[93] Robert Zwanzig. “Ensemble Method in the Theory of Irreversibility”. In: *J. Chem. Phys.* 33.5 (Nov. 1960), pp. 1338–1341. ISSN: 0021-9606.

[94] Ángel Rivas et al. “Markovian master equations: a critical study”. In: *New J. Phys.* 12.11 (Nov. 2010), p. 113032. ISSN: 1367-2630.

[95] Andrea Donarini and Milena Grifoni. “Density Matrix Methods for Quantum Transport”. In: *Quantum Transport in Interacting Nanojunctions*. Cham, Switzerland: Springer, Feb. 2024, pp. 123–149. ISBN: 978-3-031-55619-7.

[96] Heinz-Peter Breuer and Francesco Petruccione. *The Theory of Open Quantum Systems*. Oxford University PressOxford, Jan. 2007. ISBN: 9780191706349.

[97] Makoto Yamaguchi, Tatsuro Yuge, and Tetsuo Ogawa. “Markovian quantum master equation beyond adiabatic regime”. In: *Phys. Rev. E* 95.1 (Jan. 2017), p. 012136.

[98] Gabriel T. Landi et al. “Current Fluctuations in Open Quantum Systems: Bridging the Gap Between Quantum Continuous Measurements and Full Counting Statistics”. In: *PRX Quantum* 5.2 (Apr. 2024), p. 020201.

[99] L. S. Levitov and G. B. Lesovik. “Charge distribution in quantum shot noise”. In: Письма в ЖЭТФ 58 (3 1993), p. 225.

[100] Leonid S. Levitov, Hyunwoo Lee, and Gordey B. Lesovik. “Electron counting statistics and coherent states of electric current”. In: *J. Math. Phys.* 37.10 (Oct. 1996), pp. 4845–4866. ISSN: 0022-2488.

[101] P. Solinas and S. Gasparinetti. “Full distribution of work done on a quantum system for arbitrary initial states”. In: *Phys. Rev. E* 92.4 (Oct. 2015), p. 042150.

[102] Massimiliano Esposito, Upendra Harbola, and Shaul Mukamel. “Nonequilibrium fluctuations, fluctuation theorems, and counting statistics in quantum systems”. In: *Rev. Mod. Phys.* 81.4 (Dec. 2009), pp. 1665–1702.

[103] I. Klich. “An Elementary Derivation of Levitov’s Formula”. In: *Quantum Noise in Mesoscopic Physics*. Dordrecht, The Netherlands: Springer, 2003, pp. 397–402. ISBN: 978-94-010-0089-5.

[104] Bijay Kumar Agarwalla, Baowen Li, and Jian-Sheng Wang. “Full-counting statistics of heat transport in harmonic junctions: Transient, steady states, and fluctuation theorems”. In: *Phys. Rev. E* 85.5 (May 2012), p. 051142.

[105] Fei Zhan, Sergey Denisov, and Peter Hänggi. “Electronic heat transport across a molecular wire: Power spectrum of heat fluctuations”. In: *Phys. Rev. B* 84.19 (Nov. 2011), p. 195117.

[106] Huanan Li et al. “Cumulants of heat transfer across nonlinear quantum systems”. In: *Eur. Phys. J. B* 86.12 (Dec. 2013), p. 500. ISSN: 1434-6036.

[107] Gernot Schaller. *Open Quantum Systems Far from Equilibrium*. Cham, Switzerland: Springer International Publishing, 2014. ISBN: 978-3-319-03877-3.

[108] Yoshihiko Hasegawa. “Thermodynamic Uncertainty Relation for General Open Quantum Systems”. In: *Phys. Rev. Lett.* 126.1 (Jan. 2021), p. 010602.

[109] Abhaya S. Hegde, André M. Timpanaro, and Gabriel T. Landi. “Tightening the thermodynamic uncertainty relations with null-entropy events: What we learn when nothing happens”. In: *Phys. Rev. E* 113.3 (Mar. 2026), p. 034111.

[110] Tomohiro Nishiyama and Yoshihiko Hasegawa. “Unified speed limits in classical and quantum dynamics via temporal Fisher information”. In: *arXiv* (Apr. 2025).

[111] Hayato Yunoki and Yoshihiko Hasegawa. "Kinetic Uncertainty Relation in Collective Dissipative Quantum Many-Body Systems". In: *arXiv* (Apr. 2026).

[112] Sekimoto. *Stochastic energetics, vol. 799*. Springer Berlin Heidelberg, 2010.

[113] Chapin S. Korosec et al. "Motility of an autonomous protein-based artificial motor that operates via a burnt-bridge principle". In: *Nat. Commun.* 15.1511 (Feb. 2024), p. 1511. ISSN: 2041-1723.

[114] N.G. van Kampen. *Stochastic processes in physics and chemistry N.G. van Kampen Aut*. Elsevier, 2008.

[115] Peter G. Bergmann and Joel L. Lebowitz. "New Approach to Nonequilibrium Processes". In: *Phys. Rev.* 99.2 (July 1955), pp. 578–587.

[116] Christian Maes and Karel Netočný. "Time-Reversal and Entropy". In: *J. Stat. Phys.* 110.1 (Jan. 2003), pp. 269–310. ISSN: 1572-9613.

[117] Bernard Derrida. "Non-equilibrium steady states: fluctuations and large deviations of the density and of thecurrent". In: *J. Stat. Mech.: Theory Exp.* 2007.07 (July 2007), P07023. ISSN: 1742-5468.

[118] Christian Maes. "Frenesy: Time-symmetric dynamical activity in nonequilibria". In: *Phys. Rep.* 850 (Mar. 2020), pp. 1–33. ISSN: 0370-1573.

[119] Jordan M. Horowitz and Todd R. Gingrich. "Proof of the finite-time thermodynamic uncertainty relation for steady-state currents". In: *Phys. Rev. E* 96.2 (Aug. 2017), p. 020103.

[120] Udo Seifert. "From Stochastic Thermodynamics to Thermodynamic Inference". In: *Annu. Rev. Condens. Matter Phys.* Volume 10, 2019 (Mar. 2019), pp. 171–192.

[121] Patrick Pietzonka. "Classical Pendulum Clocks Break the Thermodynamic Uncertainty Relation". In: *Phys. Rev. Lett.* 128.13 (Apr. 2022), p. 130606.

[122] Hyun-Myung Chun, Lukas P. Fischer, and Udo Seifert. "Effect of a magnetic field on the thermodynamic uncertainty relation". In: *Phys. Rev. E* 99.4 (Apr. 2019), p. 042128.

[123] Rolf Landauer. "Inadequacy of entropy and entropy derivatives in characterizing the steady state". In: *Phys. Rev. A* 12.2 (Aug. 1975), pp. 636–638.

[124] Christian Maes and Karel Netočný. "Heat Bounds and the Blowtorch Theorem". In: *Ann. Henri Poincaré* 14.5 (July 2013), pp. 1193–1202. ISSN: 1424-0661.

[125] Moupriya Das et al. "Landauer's blowtorch effect as a thermodynamic cross process: Brownian cooling". In: *Phys. Rev. E* 92.5 (Nov. 2015), p. 052102.

[126] Riley J. Preston and Daniel S. Kosov. "A physically realizable molecular motor driven by the Landauer blowtorch effect". In: *J. Chem. Phys.* 158.22 (June 2023). ISSN: 0021-9606.

[127] Katarzyna Macieszczak. "Ultimate Kinetic Uncertainty Relation and Optimal Performance of Stochastic Clocks". In: *arXiv* (July 2024).

[128] Kacper Prech et al. "Optimal Time Estimation and the Clock Uncertainty Relation for Stochastic Processes". In: *Phys. Rev. X* 15.3 (Sept. 2025), p. 031068.

[129] Tan Van Vu and Keiji Saito. "Thermodynamic Unification of Optimal Transport: Thermodynamic Uncertainty Relation, Minimum Dissipation, and Thermodynamic Speed Limits". In: *Phys. Rev. X* 13.1 (Feb. 2023), p. 011013.

[130] A. A. Clerk et al. "Introduction to quantum noise, measurement, and amplification". In: *Rev. Mod. Phys.* 82.2 (Apr. 2010), p. 1155.

[131] Samuel L. Braunstein and Carlton M. Caves. "Statistical distance and the geometry of quantum states". In: *Phys. Rev. Lett.* 72.22 (May 1994), pp. 3439–3443.

[132] Carl W. Helstrom. "Quantum detection and estimation theory". In: *J. Stat. Phys.* 1.2 (June 1969), pp. 231–252. ISSN: 0022-4715.

[133] Alexander Holevo. *Probabilistic and Statistical Aspects of Quantum Theory.* Italy: Scuola Normale Superiore, 1982. ISBN: 978-88-7642-378-9.

[134] Jing Liu et al. "Quantum Fisher information matrix and multiparameter estimation". In: *J. Phys. A: Math. Theor.* 53.2 (Dec. 2019), p. 023001. ISSN: 1751-8121.

[135] Shi-Jian Gu. "FIDELITY APPROACH TO QUANTUM PHASE TRANSITIONS". In: *Int. J. Mod. Phys B* 24.23 (Sept. 2010), pp. 4371–4458. ISSN: 0217-9792.

[136] Paolo Zanardi, Lorenzo Campos Venuti, and Paolo Giorda. "Bures metric over thermal state manifolds and quantum criticality". In: *Phys. Rev. A* 76.6 (Dec. 2007), p. 062318.

[137] Ugo Marzolino and Daniel Braun. "Precision measurements of temperature and chemical potential of quantum gases". In: *Phys. Rev. A* 88.6 (Dec. 2013), p. 063609.

[138] Matteo G. A. Paris. "Achieving the Landau bound to precision of quantum thermometry in systems with vanishing gap". In: *J. Phys. A: Math. Theor.* 49.3 (Dec. 2015), 03LT02. ISSN: 1751-8121.

[139] Patrick P. Potts, Jonatan Bohr Brask, and Nicolas Brunner. "Fundamental limits on low-temperature quantum thermometry with finite resolution". In: *Quantum* 3 (July 2019), p. 161.

[140] Paolo Zanardi, Paolo Giorda, and Marco Cozzini. "Information-Theoretic Differential Geometry of Quantum Phase Transitions". In: *Phys. Rev. Lett.* 99.10 (Sept. 2007), p. 100603.

[141] Antonella De Pasquale et al. "Local quantum thermal susceptibility". In: *Nat. Commun.* 7.12782 (Sept. 2016), p. 12782. ISSN: 2041-1723.

[142] F. Pennini and A. Plastino. "Fisher information and fluctuations in quantum gas systems". In: *Physica A* 675 (Oct. 2025), p. 130779. ISSN: 0378-4371.

[143] Jing Liu, Xiao-Xing Jing, and Xiaoguang Wang. "Quantum metrology with unitary parametrization processes". In: *Sci. Rep.* 5.8565 (Feb. 2015), p. 8565. ISSN: 2045-2322.

[144] Samuel L. Braunstein, Carlton M. Caves, and G. J. Milburn. "Generalized Uncertainty Relations: Theory, Examples, and Lorentz Invariance". In: *Ann. Phys.* 247.1 (Apr. 1996), pp. 135–173. ISSN: 0003-4916.

[145] Sergio Boixo et al. "Generalized Limits for Single-Parameter Quantum Estimation". In: *Phys. Rev. Lett.* 98.9 (Feb. 2007), p. 090401.

[146] Søren Gammelmark and Klaus Mølmer. "Fisher Information and the Quantum Cram\'er-Rao Sensitivity Limit of Continuous Measurements". In: *Phys. Rev. Lett.* 112.17 (Apr. 2014), p. 170401.

[147] L. Mandelstam and Tamm I. "The uncertainty relation between energy and time in nonrelativistic quantum mechanics". In: *J. Phys. (USSR)* 9 (1945), p. 249.

[148] Sebastian Deffner and Steve Campbell. "Quantum speed limits: from Heisenberg's uncertainty principle to optimal quantum control". In: *J. Phys. A: Math. Theor.* 50.45 (Oct. 2017), p. 453001. ISSN: 1751-8121.

[149] J. Anandan and Y. Aharonov. "Geometry of quantum evolution". In: *Phys. Rev. Lett.* 65.14 (Oct. 1990), pp. 1697–1700.

[150] Jos Uffink. "The rate of evolution of a quantum state". In: *Am. J. Phys.* 61.10 (Oct. 1993), pp. 935–936. ISSN: 0002-9505.

[151] Van Tuan Vo, Tan Van Vu, and Yoshihiko Hasegawa. "Unified thermodynamic-kinetic uncertainty relation". In: *Journal of Physics A: Mathematical and Theoretical* 55.40 (Oct. 2022). arXiv:2203.11501 [cond-mat, physics:quant-ph], p. 405004. ISSN: 1751-8113, 1751-8121.

[152] J. G. Skellam. "The Frequency Distribution of the Difference Between Two Poisson Variates Belonging to Different Populations". In: *Journal of the Royal Statistical Society* 109.3 (1946), pp. 296–296. ISSN: 09528385, 23972335.

[153] M. Reznikov et al. "Temporal Correlation of Electrons: Suppression of Shot Noise in a Ballistic Quantum Point Contact". In: *Phys. Rev. Lett.* 75.18 (Oct. 1995), pp. 3340–3343.

[154] A. Kumar et al. “Experimental Test of the Quantum Shot Noise Reduction Theory”. In: *Phys. Rev. Lett.* 76.15 (Apr. 1996), pp. 2778–2781.

[155] Robert S. Whitney et al. “Thermoelectricity without absorbing energy from the heat sources”. In: *Physica E* 75 (Jan. 2016), pp. 257–265. ISSN: 1386-9477.

[156] Juliette Monsel et al. “Autonomous demon exploiting heat and information at the trajectory level”. In: *Phys. Rev. B* 111.4 (Jan. 2025), p. 045419.

[157] Gernot Schaller et al. “Probing the power of an electronic Maxwell’s demon: Single-electron transistor monitored by a quantum point contact”. In: *Phys. Rev. B* 84.8 (Aug. 2011), p. 085418.

[158] Dmitri V. Averin, Mikko Möttönen, and Jukka P. Pekola. “Maxwell’s demon based on a single-electron pump”. In: *Phys. Rev. B* 84.24 (Dec. 2011), p. 245448.

[159] Massimiliano Esposito and Gernot Schaller. “Stochastic thermodynamics for “Maxwell demon” feedbacks”. In: *Europhys. Lett.* 99.3 (Aug. 2012), p. 30003. ISSN: 0295-5075.

[160] Jonne V. Koski et al. “Experimental realization of a Szilard engine with a single electron”. In: *Proc. Natl. Acad. Sci. U.S.A.* 111.38 (Sept. 2014), pp. 13786–13789.

[161] Gernot Schaller et al. “Electronic Maxwell demon in the coherent strong-coupling regime”. In: *Phys. Rev. B* 97.19 (May 2018), p. 195104.

[162] Björn Annby-Andersson et al. “Maxwell’s demon in a double quantum dot with continuous charge detection”. In: *Phys. Rev. B* 101.16 (Apr. 2020), p. 165404.

[163] Björn Annby-Andersson et al. “Maxwell’s demon across the quantum-to-classical transition”. In: *Phys. Rev. Res.* 6.4 (Nov. 2024), p. 043216.

[164] Kensaku Chida et al. “Power generator driven by Maxwell’s demon”. In: *Nat. Commun.* 8.15301 (May 2017), p. 15301. ISSN: 2041-1723.

[165] Nathanaël Cottet et al. “Observing a quantum Maxwell demon at work”. In: *Proc. Natl. Acad. Sci. U.S.A.* 114.29 (July 2017), pp. 7561–7564.

[166] Philipp Strasberg et al. “Fermionic reaction coordinates and their application to an autonomous Maxwell demon in the strong-coupling regime”. In: *Phys. Rev. B* 97.20 (May 2018), p. 205405.

[167] J. V. Koski et al. “On-Chip Maxwell’s Demon as an Information-Powered Refrigerator”. In: *Phys. Rev. Lett.* 115.26 (Dec. 2015), p. 260602.

[168] Rafael Sánchez, Janine Splettstoesser, and Robert S. Whitney. “Nonequilibrium System as a Demon”. In: *Phys. Rev. Lett.* 123.21 (Nov. 2019), p. 216801.

[169] Sergio Ciliberto. “Autonomous out-of-equilibrium Maxwell’s demon for controlling the energy fluxes produced by thermal fluctuations”. In: *Phys. Rev. E* 102.5 (Nov. 2020), p. 050103.

[170] Fatemeh Hajiloo et al. “Quantifying nonequilibrium thermodynamic operations in a multiterminal mesoscopic system”. In: *Phys. Rev. B* 102.15 (Oct. 2020), p. 155405.

[171] Jincheng Lu, Jian-Hua Jiang, and Yoseph Imry. “Unconventional four-terminal thermoelectric transport due to inelastic transport: Cooling by transverse heat current, transverse thermoelectric effect, and Maxwell demon”. In: *Phys. Rev. B* 103.8 (Feb. 2021), p. 085429.

[172] Guilherme Fiusa et al. “Counting observables in stochastic excursions”. In: *arXiv* (May 2025).

[173] Guilherme Fiusa et al. “A framework for fluctuating times and counting observables in stochastic excursions”. In: *arXiv* (June 2025).